ISSN 1881-7831 Online ISSN 1881-784X

# DD&T

## Drug Discoveries & Therapeutics

Volume 19, Number 4
August 2025

IRCA BSSA

IACMHR

www.ddtjournal.com

DD&T
Drug Discoveries & Therapeutics

**ISSN:** 1881-7831
**Online ISSN:** 1881-784X
**CODEN:** DDTRBX
**Issues/Year:** 6
**Language:** English
**Publisher:** IACMHR Co., Ltd.

**Drug Discoveries & Therapeutics** is one of a series of peer-reviewed journals of the International Research and Cooperation Association for Bio & Socio-Sciences Advancement (IRCA-BSSA) Group. It is published bimonthly by the International Advancement Center for Medicine & Health Research Co., Ltd. (IACMHR Co., Ltd.) and supported by the IRCA-BSSA.

**Drug Discoveries & Therapeutics** publishes contributions in all fields of pharmaceutical and therapeutic research such as medicinal chemistry, pharmacology, pharmaceutical analysis, pharmaceutics, pharmaceutical administration, and experimental and clinical studies of effects, mechanisms, or uses of various treatments. Studies in drug-related fields such as biology, biochemistry, physiology, microbiology, and immunology are also within the scope of this journal.

**Drug Discoveries & Therapeutics** publishes Original Articles, Brief Reports, Reviews, Policy Forum articles, Case Reports, Communications, Editorials, News, and Letters on all aspects of the field of pharmaceutical research. All contributions should seek to promote international collaboration in pharmaceutical science.

# Editorial Board



## Editorial and Head Office:

Pearl City Koishikawa 603,
2-4-5 Kasuga, Bunkyo-ku,
Tokyo 112-0003, Japan
E-mail: office@ddtjournal.com

# Drug Discoveries & Therapeutics

## Editorial and Head Office

Pearl City Koishikawa 603, 2-4-5 Kasuga, Bunkyo-ku,
Tokyo 112-0003, Japan

E-mail: office@ddtjournal.com
URL: www.ddtjournal.com

# CONTENTS

*Volume 19, Number 4, 2025*

## Policy Forum



## Review



## Original Article



## Brief Report

## Correspondence

***Policy Forum***

DOI: 10.5582/ddt.2025.01056

# Revitalizing Japan's biomedical ecosystem: Policy initiatives, challenges, and future directions

**Ryo Okuyama***

College of International Management, Ritsumeikan Asia Pacific University, Beppu, Oita, Japan.

**SUMMARY**: Japan's international competitiveness in biomedical innovation is declining, as evidenced by its expanding trade deficit in pharmaceuticals. One reason for this is that the ecosystem connecting academic research outcomes to startups and new businesses, and promoting commercialization and industrial applications is not functioning adequately. Recently, the Japanese government has implemented policy measures to revitalize biomedical ecosystems. This study reviews the current state and characteristics of the biomedical ecosystems in Japan. Several biomedical ecosystems, both with and without geographic concentration, have been established and operated over the past 25 years, most of which are relatively small-scale and driven by governments. Recently, the Japanese government has aimed to form larger biocommunities, including biomedical innovations, to expand the bioeconomy. This study discusses these policy initiatives and their associated challenges. Furthermore, it outlines recent government initiatives to strengthen the drug discovery ecosystem, which focuses on attracting talent, companies, and new drug developers from overseas. Based on these analyses, this study addresses the challenges faced by Japan's biomedical ecosystem and discusses future directions.

***Keywords***: Bio-cluster, policy measure, biocommunity, Japanese government, drug discovery

## 1. Introduction

Japan's international competitiveness in biomedical innovation remains low. Particularly in pharmaceuticals, the trade deficit reached 4.6 trillion yen in 2022, highlighting the strong need to enhance drug discovery capabilities (*1*). One reason for this is the limited number of promising biomedical startups in Japan (*2*). Biomedical innovation relies heavily on basic academic research (*3*). Furthermore, this requires considerable time and costs, as evidenced by the development of new drugs (*4,5*). Consequently, startups, primarily university spin-offs that employ academic research achievements and investment money to support long-term risky research and development (R&D), have significantly contributed to biomedical innovations (*6*). However, Japan's startups are relatively inactive, which is believed to have contributed to the country's international lag in the biomedical field, particularly in pharmaceuticals (*2*). Recently, the number of startups involved in drug discovery has increased globally (*7,8*), making the maturation of the startup ecosystem and the nurturing of promising startups an urgent issue for Japan. It is well known that scientific and technological innovations often emerge from geographically proximate clusters of stakeholders, including research institutions, startups, existing companies, manufacturing companies, and venture capitalists (*9*). In the U.S., biomedical clusters such as those in Boston and the Bay Area have significantly contributed to innovations in the life sciences sector (*3*). Therefore, enhancing the biomedical ecosystem is crucial to strengthen Japan's competitiveness in this sector. This review summarizes current examples and the status of Japan's biomedical ecosystems. Moreover, it outlines the recent government measures aimed at cluster formation to strengthen the ecosystem. Particularly regarding drug discovery, the government has recently introduced policy measures to enhance the ecosystem, which this literature also summarizes. Based on these insights, the literature aims to provide an overview of the current status and challenges of Japan's biomedical ecosystems and discuss future directions.

## 2. Biomedical ecosystem in Japan

In Japan, clusters of concentrated biotechnology-related institutions and companies have been established since the birth of the KOBE Biomedical Innovation Cluster in 1998. Representative Japanese bio-clusters are presented

in Table 1. The size of each cluster is smaller than those of Boston and the Bay Area. In the life science cluster in Boston, 116,000 people are employed, and over 1,700 companies and organizations are concentrated (*10*). In comparison, Japan's largest bio-cluster, the KOBE Biomedical Innovation Cluster, has 12,700 employees from 363 companies and organizations, whereas KING SKYFRONT employs 5,200 people from 70 companies and organizations (Table 1). Most of these clusters were created under the leadership of national and local governments, with Shonan Health Innovation Park being the only one established by private-sector initiatives. In contrast, ecosystems were autonomously formed in Boston and the Bay Area, with universities, private venture capital, and pharmaceutical companies playing central roles (*11*). Even if the framework of an ecosystem is publicly established by the governments, it will not be effective unless stakeholders such as universities and research institutions, entrepreneurs and startups, incumbent companies, venture capitalists, and supporting institutions develop spontaneous incentives and motivation. In this context, market-oriented clusters, such as those in the U.S., demonstrate particular strengths when compared to government-led clusters — especially in terms of decision-making speed and clarity of profit distribution. For example, in Boston, venture capitalists with deep expertise in cutting-edge biotechnology have been investing in biotech startups from their early stages, leveraging their ability to assess technological potential (*12*). In some cases, they even take the lead in

**Table 1. Representative biomedical ecosystems in Japan**

| Name | Promoter | Year established | Summary |
|---|---|---|---|
| Geographically clustered ecosystem | | | |
| KOBE Biomedical Innovation Cluster | Kobe City | 1998 | Japan's largest biomedical cluster where universities, research institutes, companies, and specialized hospitals are concentrated. They pursue innovative collaboration and groundbreaking discoveries in medical, pharmaceutical, and biomedical fields, where 12700 people and 363 member and partner companies/institutions are working (*24*). |
| Tsuruoka Science Park | Yamagata Prefecture, Tsuruoka City | 1999 | Established through alliance between Keio University's Institute of Advanced Biosciences and cities in Yamagata prefecture. Advanced biotechnology research has been conducted, resulting in the birth of startups. Twenty-two organizations including research institutes, large companies, startups and related companies are working (*25*). |
| KING SKYFRONT | MEXT*, Kawasaki City | 2011 | Created as an open innovation hub that creates new industry from the world's highest standard R&D in life science and environment fields, where 5200 people and 70 institutions are working (*26*). |
| Shonan Health Innovation Park | Takeda Pharmaceutical | 2018 | Established by Takeda Pharmaceutical company to open its then in-house research center to outside organizations. It aims at the place where industry, government, and academia gather and accelerate health innovation. In all, 2500 people and 150 companies including pharmaceutical companies, next-generation medicine, cell agriculture, AI, government, and other fields are working (*27*). |
| Nakanoshima Qross | Osaka Prefecture, Osaka City | 2019 | Established by 21 private companies and Osaka prefecture as the international center for future medicine. They aim to create, practice, and share future medicines such as regenerative medicines. The main building was opened in June, 2024 (*28*). |
| Ecosystems without geographical concentration | | | |
| DSANJ** | Osaka Chamber Commerce and Industry | 2005 | A program that collects research seeds for drug discovery and related technologies, biomarkers, diagnostic agents and reagents from Japanese academic scholars and matches them with pharmaceutical companies (*29*). |
| LINK-J | Mitsui Fudosan | 2016 | Established to create platforms where people and information are exchanged and promote new life science industries (*30*). |
| The iD3 Booster | AMED*** | 2017 | A program for accelerating the translation of promising basic research into innovative new medicines. It aims at providing drug discovery knowledge, resource for necessary experiments, and funds to basic research scientists who aim at drug discovery (*31*). |

*MEXT: Ministry of Education, Culture, Sports, Science and Technology; **DSANJ: Drug Seeds Alliance Network Japan; ***AMED: Japan Agency for Medical Research and Development.

founding new ventures based on promising technologies (*13*). Established pharmaceutical companies also make substantial early investments in high-potential startups to secure future profits (*14*). In contrast, clusters led by governments or local authorities tend to be slower in making investment decisions. They also often lack strong intermediary functions that connect startups with private venture capital or pharmaceutical firms, and the distribution of potential profits tends to be more ambiguous. While public-sector initiatives have helped build the foundational structures of regional clusters, fostering dynamic and self-sustaining collaboration among diverse stakeholders remains a critical hurdle. Strengthening these organic linkages — particularly those that bridge academia, startups, and industry — will be essential for Japan to fully realize the potential of its biomedical innovation ecosystem.

The scope of business areas varies depending on each Japanese bio-cluster. The KOBE Biomedical Innovation Cluster targets a wide range of life science businesses, including healthcare delivery, the development of new treatments, disease prediction and prevention, and the creation of new industries in the medical and health fields. Although the Shonan Health Innovation Park primarily focuses on R&D in pharmaceuticals and advanced medical care, it also hosts companies and organizations related to research equipment, medical devices, and non-medical fields, such as agriculture, artificial intelligence (AI), Internet of Things, and robotics. KING SKYFRONT in Kawasaki covers a broad range of business areas, including health, medical care, welfare, and the environment. However, during the nine years from 2013, the Center of Open Innovation Network for Smart health (COINS) project was conducted in KING SKYFRONT and it focused on six research themes under the concept of "In-Body Hospitals" (*15*). This project led to the creation of nine startups and received the highest ratings of S+ in the government's post-project evaluation (*16*). Nakanoshima Qross focuses on regenerative medicines. A focused approach that leverages the research strengths of institutions and companies concentrated within a cluster, as observed in the example of the COINS project, appears effective. However, when exploring business opportunities, it is also necessary to pursue the potential across a wide range of fields. An approach that effectively enhances the productivity of these bio-clusters should be closely monitored.

Efforts have also been made to form ecosystems without geographic concentrations (Table 1). A pioneering initiative by DSANJ that primarily aimed to connect academia and pharmaceutical companies for drug discovery was later taken over by The Japan Agency for Medical Research and Development (AMED) and evolved into the Innovative Drug Discovery and Development (iD3) Booster program, which not only facilitates connections but also promotes practical academia-driven drug discovery in collaboration with the private sector (*17*). The iD3 Booster program is a unique initiative that provides knowledge and strategies to academic scholars aiming at drug discovery and makes actual research resources available to academic scholars by linking public research institutions and private companies under the government's leadership. This program is expected to contribute to uncovering drug discovery seeds at universities and promote their applied development.

### 3. Government-certified biocommunity

Recently, the Japanese government has promoted the formation of larger-scale biocommunities. The Japanese government developed and implemented Bio-strategy in 2020, followed by the amendment as Bioeconomy Strategy in 2024 (*18,19*). This strategy aims to resolve environmental, food, health and other issues and achieve a circular economy and sustainable economic growth by using biotechnology and biomass, covering various biotechnology fields, including biomedical innovations such as biopharmaceuticals, regenerative medicine, cell therapy, gene therapy, and digital health (*19*). In this strategy, the importance of establishing bio-research and technology hubs and stakeholder networks has been discussed with reference to the examples in Boston and London, concluding with the promotion of community formation aimed at expanding the bioeconomy (*20*). The envisioned biocommunity in the strategy aims to function as a hub for bio-innovation, with R&D institutions, startups, incumbent companies, incubation facilities, investment funds, core hospitals, and biomanufacturing organizations concentrated and networked together (*20*). With this direction, a public call for biocommunity was launched in 2021. Consequently, the Cabinet Office certified two global biocommunities and six local biocommunities, and registered two incubating biocommunities for further development (Table 2). Global biocommunities are expected to function as catalysts by promoting collaboration between state-of-the-art R&D organizations and related companies and institutions, thereby enhancing access to global data, human resources, investment, and research. Their goal is to become the world's most advanced developmental base in the field of biotechnology. Local biocommunities aim to expand collaboration among local companies, business entities, and universities; lead forays into the global market; and stimulate the revitalization of the regional economy (*18*).

These approaches are not efforts to create entirely new biocommunities but rather initiatives to strengthen collaboration between existing organizations. Greater Tokyo Biocommunity connects eight areas around Tokyo (Tsukuba, Kashiwanoha, Hongo/Ochanomizu/ Tokyo Station, Nihonbashi, Kawasaki, Yokohama, Shonan, Chiba/Kazusa) as a bio-innovation hub and

**Table 2. Biocommunities certified and registered by the Cabinet Office of Japan**

| |
|---|
| **Global Biocommunities (certified)** |
| Greater Tokyo Biocommunity |
| Bio Community Kansai |
| **Regional Biotech Communities (certified)** |
| Hokkaido Prime Bio Community |
| Tsuruoka Bio Community |
| Nagaoka Bio Community |
| Hiroshima Bio DX Community |
| Fukuoka Bio Community |
| Okinawa Bio Community |
| **Incubating Biocommunities (registered)** |
| Tokai Biocommunity |
| Gunma Green Innovation Platform |

Extracted from Reference (*32*).

aims at becoming the world's premier innovation center by strengthening research collaboration, startup development, investment in manufacturing facilities, infrastructure, international recognition, and foreign investment. In these eight areas, various institutions are involved in biotechnology-related research, development, manufacturing, and supporting functions. Biocommunity Kansai aims to realize a cutting-edge bioeconomy society by forming an open network among biotechnology-related companies, research institutes, banks, funds, academia, public administrations, and business associations in the Kansai area. This biocommunity leverages existing clusters, such as Doshomachi in Osaka, which thrived as a "town of medicine"; Kyoto, a world leader in induced pluripotent stem cells and cancer immunotherapy; Kobe, known for its base in advanced medical technology; and Nada and Fushimi, which have flourished through fermentation.

Enhancing communication among geographically close R&D institutions is important to generate further synergy. However, the extent of impact that can be expected from promoting collaborations through policies among institutions that have already been operating in proximity is unclear. If sufficient synergy has not yet been achieved despite geographical proximity, it is crucial to thoroughly examine the causes of the lack of collaborations and implement effective solutions to achieve meaningful results.

## 4. Recent policy initiative to facilitate drug discovery ecosystem

The Cabinet Secretariat decided to establish the "Council of the Concept for Early Prevalence of the Novel Drugs to Patients by Improving Drug Discovery Capabilities" (hereinafter, the Council) on December 26, 2023. The Council aims to ensure access to pharmaceuticals and strengthen drug discovery capabilities (*21*). The Council was held five times between December 27, 2023, and May 22, 2024, resulting in an interim report. Strategic goals and action plans were established to implement the recommendations from an interim report. The action plans included timelines and key performance indicators (KPIs). On July 30, 2024, the government hosted the Drug Discovery Ecosystem Summit, inviting approximately 20 pharmaceutical companies and related organizations from Japan and abroad to present this strategic goals and action plans (*21*).

The interim report decided three strategic goals, such as "Prompt delivery of novel drugs to patients," "Become one of the world's leading drug discovery sites," and "Cyclically develop investment and innovation," and measures to achieve these goals. The measures were categorized as follows; 1. Strengthen Japan's Drug Discovery Capabilities; 2. Prompt Delivery of Novel Drugs to Patients; and 3. Construction of a Social System that Allows Continued Cyclical Development of Investment and Innovation. Four, three, and three policy measures were proposed for each category, respectively, and further detailed items were included in each policy measure. Timelines and KPIs up to the year 2028 were set for each measure (*22*). The strategic goals, categories, and policy measures are summarized in Table 3.

Initiatives of the Japanese government have focused on ecosystem development. As reported in Section 2, regional cluster development and network formation for biomedical innovation have been conducted over the past 25 years in Japan. Nevertheless, biomedical startups have not been sufficiently nurtured and international competitiveness in pharmaceuticals has decreased in Japan (*2*). Considering this, the government's efforts to strengthen the drug discovery ecosystem through specific measures are commendable. Not only creating clusters and forming networks, but also effectively functioning the ecosystem has become important. This initiative is expected to have a positive impact. In Boston and San Francisco Bay Area, several factors contribute to the success of their biomedical clusters. One key element is the robust framework for industry-academia collaboration. For example, institutions like Massachusetts Institute of Technology and Stanford University have dedicated offices and funding programs to support technology transfer and commercialization (*23*). Furthermore, the presence of a mature venture capital ecosystem, with well-established exit channels through initial public offerings and merger & acquisition, creates strong incentives for innovation and entrepreneurship. The flexibility of the U.S. patent system, particularly under the Bayh-Dole Act, also enables universities to retain intellectual property rights and license them effectively, facilitating knowledge spillover and commercialization (*23*). These insights highlight the importance for Japan to pursue a more holistic strategy, fostering dynamic interactions between universities, startups, investors, and public agencies to ensure its ecosystems function effectively.

**Table 3. Three strategic goals and policy measures proposed by the Council**

| |
|---|
| **Strategic goals** |
| Prompt delivery of novel drugs to patients |
| Become one of the world's leading drug discovery sites |
| Cyclically develop investment and innovation |
| |
| **Policy measures** |
| 1. *Strengthen Japan's Drug Discovery Capabilities* |
| Proactively recruit and utilize human resources with foreign experience and commercialization know-how, together with funding, chiefly through the public-private council |
| System for conducting international-level clinical trials and studies |
| Domestic manufacturing system for new modality drugs |
| Continuous generation and development of drug discovery seeds in academia and startups |
| 2. *Prompt Delivery of Novel Drugs to Patients* |
| Review of pharmaceutical regulations, *etc*. |
| Promotion of the development of drugs for children, intractable diseases, and rare diseases |
| PMDA's consultation/review system |
| 3. *Construction of a Social System that Allows Continued Cyclical Development of Investment and Innovation* |
| Appropriate evaluation of the value of innovative drugs, departure from dependence on long-listed products, *etc*. |
| Promotion of self-care and self-medication by supporting the switch to over-the-counter (OTC) drugs, *etc*. |
| Promote the use of biosimilars and utilize private insurance in addition to public insurance for new technologies |

Extracted from Reference (*22*).

In this initiative, not only are the strategic goals clearly outlined, but concrete action plans have also been presented with timelines and KPIs to achieve these goals. This bold proposal demonstrates a serious commitment toward realizing it. A future challenge will be to determine the effectiveness of this method. The timeline of the action plans spans five years, ending in 2028; however, it is essential to monitor KPI achievements along the way and adjust the plan as required. Careful and responsive action is crucial to ensure success.

The unique aspect of this initiative is its ambitious focus on attracting accelerator talent, companies, and new drug development projects from overseas. The challenge in this proposal is to secure talent from abroad. It would be difficult for someone with limited Japanese proficiency to make efforts to understand Japanese pharmaceutical regulations and interact with the authorities. Moreover, understanding and practicing Japan's unique business customs, such as an emphasis on teamwork and high-context communication, are essential. Considering the language, compensation, and cultural barriers, it is questionable how many overseas professionals are willing to relocate to Japan to serve as accelerators. Instead, the development of domestic talent should be emphasized. Japan has traditionally relied on large pharmaceutical companies to lead drug discovery and development, and it is likely that many individuals with extensive R&D experience in these companies possess the potential to serve as accelerator talent in startups. In addition, enhancing the attractiveness of the Japanese pharmaceutical market and increasing incentives for foreign companies to develop new drugs in Japan are crucial. Thus, efforts to attract foreign talent should be considered alongside measures such as fair drug pricing systems and the simplification and acceleration of approval processes.

## 5. Conclusions

In Japan, the establishment of bio-clusters has been driven primarily by the government over the past 25 years. Efforts have also been made to form networks without geographic concentration and support academic drug discovery. However, it is difficult to ascertain whether these ecosystems have successfully nurtured startups and generated significant bio-innovations. Recently, the Japanese government has aimed to form larger-scale biocommunities by connecting existing research, development, and manufacturing institutions. Specific policies have been introduced to build drug discovery ecosystems that focus on attracting foreign talent and capital. Building an ecosystem requires time and an alignment with the interests of all stakeholders, necessitating long-term efforts. For the Japanese biomedical ecosystem to generate sufficient achievements, a self-sustaining and positive cycle within the ecosystem must be established. The steady achievement of the action plans set by the government and ongoing efforts to strengthen the ecosystem are highly anticipated.

*Funding*: None.

*Conflict of Interest*: Ryo Okuyama is an advisor of The Japan Agency for Medical Research and Development (AMED), Academic Research and Industrial Collaboration Management Office of Kyushu University, and Graduate School of Science and Engineering of Kagoshima University.

## References

1. Mano H. Sekai to nihon no souyaku no genjyo. *https://*

*www.cas.go.jp/jp/seisaku/souyakuryoku/dai1/siryou5.pdf* (accessed September 18, 2024). (in Japanese)
2. Okuyama R. Strengthening the Competitiveness of Japan's Pharmaceutical Industry: Analysis of Country Differences in the Origin of New Drugs and Japan's Highly Productive Firm. Biol Pharm Bull. 2023; 46:718-724.
3. Pisano GP. Science Business: The Promise, the Reality and the Future of Biotech. Harvard Business School Press, Boston, MA, 2006.
4. Shareef U, Altaf A, Ahmed M, Akhtar N, Almuhayawi MS, Al Jaouni SK, Selim S, Abdelgawad MA, Nagshabandi MK. A comprehensive review of discovery and development of drugs discovered from 2020-2022. Saudi Pharm J. 2024; 32:101913.
5. Wouters OJ, McKee M, Luyten J. Estimated Research and Development Investment Needed to Bring a New Medicine to Market, 2009-2018. JAMA. 2020; 323:844-853.
6. Kneller R. The importance of new companies for drug discovery: origins of a decade of new drugs. Nat Rev Drug Discov. 2010; 9:867-882.
7. Okuyama R. Chronological analysis of first-in-class drugs approved from 2011 to 2022: their technological trend and origin. Pharmaceutics. 2023; 15:1794.
8. Okuyama R. Increased contribution of small companies to late-entry drugs: a changing trend in FDA-approved drugs during the 2020s. Drug Discov Today. 2024; 29:103866.
9. Porter ME. Clusters and the New Economics of Competition. Harv Bus Rev. 1998; 76:77-90.
10. MassBio. 2024 Industry Snapshot. *https://www.massbio.org/wp-content/uploads/2024/08/2024_IndustrySnapshot.pdf* (accessed September 18, 2024).
11. Nishino F, Hanzawa S. Innovation Ecosystem and Regional/Professional Labor Market: A Case Study of Boston. Hitotsubashi Bull Soc Sci. 2020; 12:1-26. (in Japanese)
12. Ledford H. Biotechnology: The start-up engine. Nature. 2013; 501:476-478.
13. Hong L, Pisano GP, Yu H. Institutionalized Entrepreneurship: Flagship Pioneering. Harv Bus School Case. 2018; 718:484.
14. Okuyama R. mRNA and Adenoviral Vector Vaccine Platforms Utilized in COVID-19 Vaccines: Technologies, Ecosystem, and Future Directions. Vaccines. 2023; 11:1737.
15. COINS. Research. *https://coins.kawasaki-net.ne.jp/en/research/index.html* (accessed September 18, 2024). (in Japanese)
16. Japan Science and Technology Agency. Center of Innovation Program: After-Action report. 2022; 28-31. *https://www.jst.go.jp/coi/hyoka/data/jigohyoka.pdf* (accessed September 18, 2024). (in Japanese)
17. Sakurai T. Nihon ni okeru souyaku ecosystem no genjyo to kadai. Shodai Bus Rev. 2020; 10:81-100. (in Japanese)
18. Integrated Innovation Strategy Promotion Council. Bio-Strategy 2020. *https://www8.cao.go.jp/cstp/bio/bio2020_honbun.pdf* (accessed September 18, 2024). (in Japanese)
19. Integrated Innovation Strategy Promotion Council. Bioeconomy Strategy. *https://www8.cao.go.jp/cstp/bio/bio_economy_en.pdf* (accessed September 18, 2024).
20. The Cabinet Office. Biocommunity formation related policies in Bio-strategy. *https://www.meti.go.jp/shingikai/sankoshin/shomu_ryutsu/bio/pdf/010_02_00.pdf* (accessed September 18, 2024). (in Japanese)
21. The Cabinet Secretariat. Council of the Concept for Early Prevalence of the Novel Drugs to Patients by Improving Drug Discovery Capabilities. *https://www.cas.go.jp/jp/seisaku/souyakuryoku/index.html* (accessed September 18, 2024). (in Japanese)
22. National Healthcare Policy Secretariat. Strategic Goal and Action Plan for Improving Drug Discovery Capabilities to Support Early Availability of Innovative Drug -Toward Implementation of the Interim Report-. *https://www.cas.go.jp/jp/seisaku/souyakuryoku/pdf/toward_implementation_of_the_interim_report.pdf* (accessed September 18, 2024). (in Japanese)
23. Mowery DC, Nelson RR, Sampat BN, Ziedonis AA. Ivory tower and industrial innovation: University-industry technology transfer before and after the Bayh-Dole Act. Stanford Business Books, Stanford, CA, 2004.
24. KOBE Biomedical Innovation Cluster. Homepage. *https://www.fbri-kobe.org/kbic/english/* (accessed September 18, 2024).
25. Tsuruoka Science Park. Homepage. *https://tsuruoka-sp.jp/en/* (accessed September 18, 2024).
26. KING SKYFRONT. Homepage. *https://www.king-skyfront.jp/en/* (accessed September 18, 2024).
27. Shonan iPark. Homepage. *https://www.shonan-ipark.com/en/* (accessed September 18, 2024).
28. Nakanoshima Qross. Homepage. *https://www.nakanoshima-qross.jp/* (accessed September 18, 2024). (in Japanese)
29. DSANJ. Homepage. *https://www.dsanj.jp/index_en.html* (accessed September 18, 2024).
30. LINK-J. Homepage. *https://www.link-j.org/en/* (accessed September 18, 2024).
31. AMED iD3 Catalyst Unit. Homepage. *https://id3catalyst.jp/e/booster.html* (accessed September 18, 2024).
32. The Cabinet Office. Bioeconomy Strategy. *https://www8.cao.go.jp/cstp/bio/index.html* (accessed September 18, 2024). (in Japanese)

Received June 16, 2025; Revised August 6, 2025; Accepted August 20, 2025.

**Address correspondence to:*
Ryo Okuyama, College of International Management, Ritsumeikan Asia Pacific University, 1-1 Jyumonjibaru, Beppu, Oita 874-8577, Japan.
E-mail: ryooku@apu.ac.jp; ryooku93125@yahoo.co.jp

Released online in J-STAGE as advance publication August 23, 2025.

***Review***

DOI: 10.5582/ddt.2025.01067

# Serum lipid levels serve as predictors for osteoporosis or osteopenia in postmenopausal women: A meta-analysis of observational studies

**Feijun Ye[1,§], Yanlin Zhang[2,§], Ziqin Chen[3], Jing Zhou[4], Jing Wang[5,6], Xiayan Fu[1], Qing Qi[7,*], Ling Wang[8,9,*]**

[1] Reproductive Medicine Center, Zhoushan Maternal and Child Health Care Hospital, Zhoushan, Zhejiang, China;
[2] College of Acupuncture-Moxibustion and Orthopedics, Hubei University of Chinese Medicine, Wuhan, Hubei, China;
[3] College of Chinese Medicine, Hubei University of Chinese Medicine, Wuhan, Hubei, China;
[4] Department of Obstetrics and Gynecology, Southern Medical University Nanfang Hospital, Guangzhou, Guangdong, China;
[5] Hainan Women and Children's Medical Center, Haikou, Hainan, China;
[6] Guizhou University of Traditional Chinese Medicine, Guiyang, Guizhou, China;
[7] School of Physical Education, Wuhan Business University, Wuhan, Hubei, China;
[8] Department of Obstetrics and Reproductive Immunology, Shanghai East Hospital, Tongji University School of Medicine, Shanghai, China;
[9] Department of Obstetrics, The First Affiliated Hospital, Guizhou University of Traditional Chinese Medicine, Guiyang, China.

**SUMMARY**: This meta-analysis summarizes the differences in serum lipid levels among postmenopausal women with osteopenia, osteoporosis, and normal bone mass, aiming to establish reliable lipid markers for predicting bone loss in postmenopausal women. Relevant literature published up to March 21, 2024, was sourced from databases including PubMed, Embase, Web of Science, and the Cochrane Library. Following a thorough evaluation in accordance with established inclusion and exclusion criteria, the meta-analysis incorporated 14 studies, involving a total of 12,974 postmenopausal women. The weighted mean deviation (WMD) and 95% confidence intervals (CIs) were conducted by RevMan 5.4 software. The findings indicated that serum triglyceride (TG) concentrations were significantly lower in osteopenia (WMD = -6.82, 95% CI: -9.80 to -3.83, $P = 0.05$, $I^2 = 42\%$) and osteoporosis (WMD = -10.28, 95% CI: -14.51 to -6.04, $P < 0.001$, $I^2 = 45\%$) women compared to their normal counterparts. In addition, serum high-density lipoprotein cholesterol (HDL-C) levels were notably elevated in osteoporosis women (WMD = 1.66, 95% CI: 0.75 to 2.57, $P = 0.0004$, $I^2 = 43\%$). However, no significant discrepancies were found in total cholesterol and low-density lipoprotein cholesterol levels among postmenopausal women with bone loss. Sensitivity analysis showed that the results of the meta-analysis were reliable. Egger's test showed no publication bias in the included studies. Consequently, our meta-analysis shows that low serum TG levels predict the onset of osteopenia in postmenopausal women, while high serum HDL-C levels suggest a potential risk for osteoporosis.

***Keywords***: perimenopausal women, osteopenia, serum lipid levels, meta-analysis

## 1. Introduction

Postmenopausal osteoporosis represents the predominant type of osteoporosis among women. Epidemiological studies indicate that more than 50% of individuals aged over 50 are affected by osteoporosis, with approximately 70% of these cases occurring in postmenopausal women (*1*), which is responsible for a globally higher incidence of vertebral fractures in women over 50 than in men of the same age (*2*). The higher prevalence of osteoporosis in postmenopausal women is mainly attributed to an increase in bone turnover rate caused by elevated follicle-stimulating hormone, estrogen deficiency, elevated osteocalcin levels, and disorders in lipid metabolism (*3-6*). Osteoporotic vertebral fractures bring high societal costs and mortality; however, currently, available therapeutic options are primarily confined to either suppressing bone resorption or enhancing bone formation, with both strategies being associated with specific side effects (*7,8*). Therefore, the prevention of postmenopausal osteoporosis and osteoporotic fractures remains promising approaches for reducing both incidence and morbidity.

It is well known that bone metabolic balance is the relative balance between osteoclast-mediated bone resorption and osteoblast-mediated bone formation

(*9*). Lipid utilization of osteoblast is necessary for normal skeletal homeostasis. However, dyslipidemia may impair osteoblast function and contribute to bone remodeling imbalances, particularly postmenopausal osteoporosis (*10*). This condition is characterized by an exaggerated rate of bone resorption and a predominant loss of trabecular bone compared to cortical bone (*8*). The change in lipid metabolism may be a key initiating factor of osteoporosis and play a double-edged role. For example, low-density lipoprotein (LDL) can significantly improve the viability of osteoclasts by inducing cholesterol delivery. In contrast, high-density lipoprotein (HDL) can suppress the fusion and survival of osteoclasts by promoting cholesterol efflux (*11,12*). Research has indicated that cholesterol metabolism, adipocytokine, and sphingolipid signaling pathways were significantly enriched on the fifth day following surgery in a murine model of postmenopausal osteoporosis (*13*). These findings further underscore the critical role of lipid metabolism during the early stages of osteoporosis.

Compared to bone mineral density (BMD) values, serum lipid levels are more accessible health information for most postmenopausal women. However, how serum lipid levels affect bone loss in postmenopausal women has not been determined. Gu *et al.* (*14*) found no notable connection between BMD and lipid levels in postmenopausal women. Alfahal *et al*. (*15*) reported postmenopausal women with osteoporosis tend to perform higher total cholesterol (TC), triglyceride (TG), and serum LDL cholesterol (LDL-C) than those with normal bone mass. In contrast, Li *et al.* (*16*) concluded that postmenopausal women with high serum HDL cholesterol (HDL-C) levels were more likely to develop osteoporosis in China. Consequently, the present study summarizes the differences in lipid levels among postmenopausal women with osteopenia, osteoporosis, and normal bone mass, aiming to establish reliable lipid markers for predicting bone loss in postmenopausal women.

## 2. Materials and Methods

### 2.1. Search strategy

A comprehensive literature search of the databases PubMed, Embase, Web of Science, and the Cochrane Library was conducted from their inception until March 21, 2024. The search utilized the keywords "Osteoporosis, Postmenopausal" AND ["Lipoproteins" OR "Cholesterol" OR "Triglycerides" OR "Lipoproteins, HDL" OR "Lipoproteins, LDL"] AND ["Case-Control Studies" OR "Cohort Studies" OR "Cross-Sectional Studies"]. The search strategies for each database are detailed in Table S1 (*https://www.ddtjournal.com/action/getSupplementalData.php?ID=270*).

### 2.2. Inclusion criteria

Inclusion criteria include: (a) Participants were required to be postmenopausal women; (b) all included studies were observational, comprising case-control, cohort, or cross-sectional designs; (c) studies need to provide bone T-value and corresponding lipid data; (d) studies need to be classified strictly according to the criteria set by the World Health Organization (WHO) (*17*): Women with a T-value ≥ -1 of BMD were classified as normal controls; those with -1 > T-value > -2.5 were categorized as having osteopenia; those with T-value ≤ -2.5 were identified as having osteoporosis.

Exclusion criteria include: (a) Subjects were not postmenopausal women; (b) data failed to present the relationship between serum lipid levels and bone T scores; (c) studies did not conform to the established inclusion criteria; (d) participants accepted treatment with bone-active medications, lipid-lowering agents, or corticosteroids; (e) participants underwent severe metabolic disorders or unexplained osteoporosis; (f) research was not published in English; (g) duplicate publications; (h) articles were not classified as observational studies; (i) Studies lacked original text or complete data.

### 2.3. Data extraction

The evaluation process was conducted using EndNote software. Citations obtained from various database searches were consolidated, and duplicates were eliminated. Two reviewers independently evaluated the literature abstract to determine adherence to the inclusion criteria. Review the full text of studies deemed potentially relevant. Any disagreements were resolved through joint deliberation, with the participation of a third reviewer as necessary. The following items were extracted from all, including research: author, publication date, research type, country, basis for grouping, sample size, age, body mass index (BMI), and BMD evaluation.

### 2.4. Quality assessment of studies

The Newcastle-Ottawa Quality Assessment Scale (NOS) was employed to evaluate the quality of included studies (*18*). Scores ranging from 0 to 3, 4 to 6, and 7 to 9 correspond to low, medium, and high quality of included studies, respectively. Any disagreements between the two reviewers, Chen ZQ and Zhou J, were addressed through discussion.

### 2.5. Statistical analysis

#### 2.5.1. Meta-analysis statistics

The weighted mean deviation (WMD) and 95% confidence intervals (CIs) were conducted by RevMan 5.4 software. A significance level of $P$-value < 0.05 was predetermined. The heterogeneity of studies was evaluated using $I^2$ statistics. A fixed-effects model

was used if heterogeneity was slight ($I^2$ < 40%), and a random-effects model was used otherwise. Sensitivity analyses and Egger's tests were performed by Stata 16.0 software. Additionally, if more than 10 articles were pooled for analysis, funnel plots were conducted to assess potential publication bias.

2.5.2. Subgroup analyses

We performed a subgroup analysis of the high heterogeneity results based on the following factors: The level of country development (developed *vs.* developing), dietary pattern of residents (mediterranean *vs.* western *vs.* eastern), BMD evaluation methods (lumbar spine *vs.* lumbar spine and others), sample size (≥ 200 *vs.* < 200), literature quality (high *vs.* median), and mean age of patients (≤ 55 *vs.* > 55). Instances where data were not reported in the studies were noted as "not provided." A *P*-value < 0.05 was set as statistically significant.

## 3. Results

3.1. Study selection

The initial search identified 276 potentially relevant studies. Sixty-one duplicate studies were removed. Following the predetermined inclusion and exclusion criteria, 179 studies were excluded based on an evaluation of their abstracts, while 22 studies were excluded after a thorough review of their full texts. Ultimately, 14 studies (*14,19-31*) were deemed suitable for inclusion in this meta-analysis. The flowchart of this study is shown in Figure 1.

3.2. Study characteristics

The studies included in this analysis were sourced from four databases and published prior to March 21, 2024. Table 1 provides a comprehensive overview of the characteristics of all included studies, which comprises 8 studies that adopted a case-control design, a cohort study design, and 5 cross-sectional studies. Our meta-analysis involved 12,974 postmenopausal women from 9 countries, including 2,772 osteoporosis patients, 4,552 osteopenia patients, and 5,650 women with normal bone mass. The NOS was adopted to assess the non-randomized studies' methodological quality. All studies were assessed as having median or high quality, as shown in Table 2.

3.3. Pooled findings

Initially, we compared the serum lipid concentrations in postmenopausal women with osteopenia versus those with normal bone mass. Utilizing a random-effects model, we found a significant reduction in TG levels (WMD = -6.82, 95% CI: -9.80 to -3.83, $P$ = 0.05, $I^2$ = 42%) in osteopenia women. No significant differences were noted in TC ($P$ = 0.91, $I^2$ = 24%), HDL-C ($P$ = 0.43, $I^2$ = 82%), and LDL-C ($P$ = 0.81, $I^2$ = 0%) between the two groups (Figures 2A-2D).

To further investigate the differences in serum

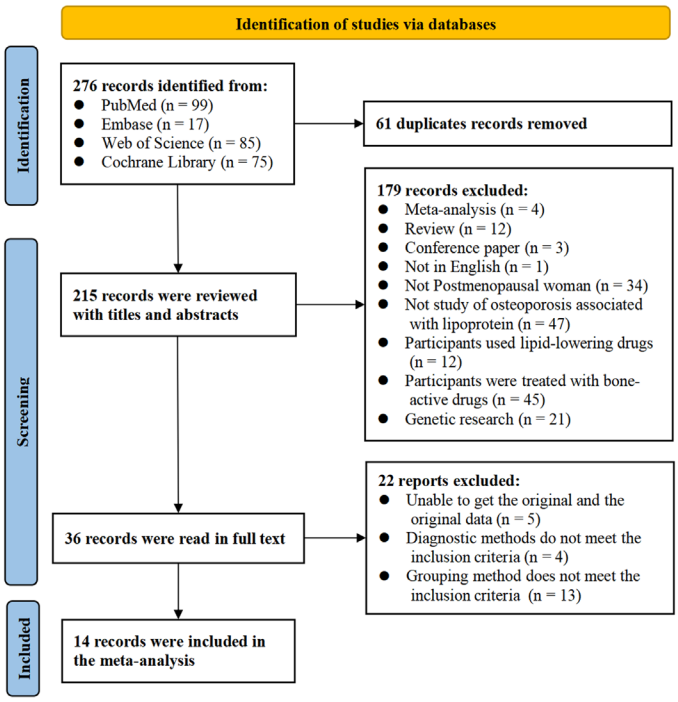


**Figure 1. A flowchart of the study.**

**Table 1. Main characteristics of included studies**

| Author, year (reference) | Country | Study design | Groups | Grouping standard | Participant | BMD test site (instrument) | Age (years)[a] | BMI (kg/m$^2$)[a] |
|---|---|---|---|---|---|---|---|---|
| Abbasi M 2016 (*24*) | Iran | Cross-sectional | Osteoporosis | T ≤ -2.5 | 80 | Lumbar spine and femoral neck (DEXA) | 60.03 ± 8.21 | 33.64 ± 9.22 |
| | | | Normal | T ≥ -1 | 63 | | 53.47 ± 7.33 | 31.61 ± 7.95 |
| Alay I 2020 (*22*) | Turkey | Case-control | Osteoporosis | T ≤ -2.5 | 176 | Lumbar spine (L1-L4) and the femoral neck (DEXA) | 54.54 ± 7.37 | 28.02 ± 4.58 |
| | | | Osteopenia | -2.5 < T < -1 | 179 | | 54.43 ± 6.22 | 29.42 ± 4.87 |
| | | | Normal | T ≥ -1 | 97 | | 51.67 ± 6.06 | 29.56 ± 5.01 |
| Cui R 2016 (*26*) | Germany | Case-control | Osteoporosis | T ≤ -2.5 | 253 | Lumbar spine (L1-L4) (DEXA) | 65.00 ± 9.63 | 24.09 ± 3.70 |
| | | | Osteopenia | -2.5 < T < -1 | 1602 | | 60.00 ± 7.41 | 25.15 ± 3.30 |
| | | | Normal | T ≥ -1 | 2098 | | 57.00 ± 5.93 | 25.80 ± 3.43 |
| D'Amelio P 2001 (*19*) | Italy | Case-control | Osteoporosis | T ≤ -2.5 | 37 | Lumbar spine (DEXA) | 53.40 ± 3.10 | Not provided |
| | | | Normal | T ≥ -1 | 43 | | 61.00 ± 6.80 | Not provided |
| Demir B 2008 (*20*) | Turkey | Case-control | Osteoporosis | T ≤ -2.5 | 1085 | Lumbar spine (L1-L4) (DEXA) | 47.70 ± 4.80 | 27.60 ± 4.30 |
| | | | Osteopenia | -2.5 < T < -1 | 449 | | 48.30 ± 4.40 | 28.40 ± 4.50 |
| | | | Normal | T ≥ -1 | 1235 | | 48.60 ± 4.10 | 29.80 ± 4.80 |
| Erden E 2023 (*23*) | Turkey | Cross-sectional | Osteoporosis | T ≤ -2.5 | 60 | Lumbar spine (L1-L4) and femur neck (DEXA) | 56.50 ± 3.70 | 28.55 ± 5.04 |
| | | | Osteopenia | -2.5 < T < -1 | 60 | | 56.00 ± 5.78 | 29.7 ± 4.52 |
| | | | Normal | T ≥ -1 | 60 | | 56.00 ± 5.19 | 29.45 ± 2.15 |
| Gu LJ 2019 (*14*) | China | Case-control | Osteoporosis | T ≤ -2.5 | 529 | Left calcaneus (ultrasound BMD analyzer) | 65.49 ± 8.18 | 23.54 ± 3.20 |
| | | | Osteopenia | -2.5 < T < -1 | 1616 | | 59.64 ± 7.28 | 23.67 ± 3.16 |
| | | | Normal | T ≥ -1 | 1400 | | 57.15 ± 7.19 | 23.63 ± 3.28 |
| Naguib M 2022 (*29*) | Egypt | Cross-sectional | Osteoporosis | T ≤ -2.5 | 25 | Lumbar spine and the total hip (DEXA) | 56.00 ± 5.45 | 34.09 ± 3.85 |
| | | | Osteopenia | -2.5 < T < -1 | 25 | | 56.75 ± 6.29 | 31.42 ± 3.43 |
| | | | Normal | T ≥ -1 | 25 | | 52.77 ± 3.55 | 33.18 ± 6.02 |
| Pliatsika P 2012 (*25*) | Greece | Cross-sectional | Osteoporosis | T ≤ -2.5 | 71 | Lumbar spine (L2-L4) (DEXA) | Not provided | Not provided |
| | | | Osteopenia | -2.5 < T < -1 | 248 | | Not provided | Not provided |
| | | | Normal | T ≥ -1 | 272 | | Not provided | Not provided |
| Pontes TA 2019 (*30*) | Brazil | Case-control | Osteoporosis | T ≤ -2.5 | 24 | Lumbar spine (L1-L4), femoral neck, and total femur (Hologic Bone | 60.80 ± 6.00 | 25.58 ± 4.80 |
| | | | Osteopenia | -2.5 < T < -1 | 26 | Densitometer Discovery Ci) | 61.88 ± 7.90 | 27.20 ± 5.20 |
| | | | Normal | T ≥ -1 | 28 | | 60.38 ± 6.20 | 25.35 ± 3.40 |
| Safari A 2019 (*27*) | Iran | Case-control | Osteoporosis | T ≤ -2.5 | 44 | Lumbar spine and hip (DEXA) | 64.22 ± 13.85 | 30.47 ± 5.77 |
| | | | Normal | T ≥ -1 | 44 | | 63.67 ± 6.40 | 27.52 ± 4.75 |
| Tamaki J 2009 (*21*) | Japan | Cohort studies | Osteoporosis | T ≤ -2.5 | 78 | Lumbar spine (L2-L4), total hip, and the distal forearm (DEXA) | 65.91 ± 7.36 | 23.40 ± 3.55 |
| | | | Osteopenia | -2.5 < T < -1 | 133 | | 61.34 ± 6.83 | 23.35 ± 2.55 |
| | | | Normal | T ≥ -1 | 92 | | 55.98 ± 5.59 | 25.40 ± 3.36 |
| Yaprak EÜ 2016 (*31*) | Turkey | Cross-sectional | Osteoporosis | T ≤ -2.5 | 88 | Lumbar spine (L1-L4) and hip (femoral neck) (DEXA) | 55.00 ± 10.25 | 31.00 ± 4.40 |
| | | | Normal | T ≥ -1 | 88 | | 56.00 ± 9.50 | 31.40 ± 4.80 |
| Zhao X 2023 (*28*) | China | Case-control | Osteoporosis | T ≤ -2.5 | 222 | Lumbar spine (L1-L4) and the bilateral hip (DEXA) | 68.09 ± 7.32 | 24.60 ± 3.47 |
| | | | Osteopenia | -2.5 < T < -1 | 214 | | 62.87 ± 7.44 | 25.47 ± 3.17 |
| | | | Normal | T ≥ -1 | 105 | | 60.37 ± 6.51 | 26.49 ± 3.80 |

*Note:* BMD: bone mineral density; BMI: body mass index; DEXA: dual-energy X-ray absorptiometry. [a]Data are shown as mean ± SD.

lipid levels among postmenopausal women with varying degrees of bone loss, we compared the lipid concentrations of osteoporosis and normal women. Our study revealed a significant decrease in TG (WMD = -10.28, 95% CI: -14.51 to -6.04, $P < 0.001$, $I^2 = 45\%$) and an increase in HDL-C (WMD = 1.66, 95% CI: 0.75 to 2.57, $P = 0.0004$, $I^2 = 43\%$) levels in osteoporosis women. No significant differences were found in TC ($P = 0.84$, $I^2 = 9\%$) and LDL-C ($P = 0.59$, $I^2 = 18\%$) levels between the two groups (Figures 3A-3D).

### 3.4. Subgroup analyses

Focusing on various study characteristics, we conducted a subgroup analysis of research on HDL-C levels in osteopenia and normal women to uncover potential sources of heterogeneity (Figures 4A-4F). The findings remained consistent regardless of the BMD evaluation ($P = 0.15$), sample size ($P = 0.51$), quality of the literature ($P = 0.67$), and mean age of patients ($P = 0.80$). Among postmenopausal women in developed nations, levels of HDL-C are significantly elevated in those with osteopenia (WMD = 2.24, 95% CI: 1.56 to 2.93, $P < 0.001$, $I^2 = 0\%$). Conversely, this disparity is not observed in developing countries (WMD = -0.11, 95% CI: -1.29 to 1.07, $P = 0.83$, $I^2 = 62\%$) (Figure 4A). Stratification analysis based on the national development level markedly reduced heterogeneity within each subgroup, and the difference in effect size between the two subgroups was statistically significant ($P < 0.001$).

To rule out the possibility of chance, we performed subgroup analyses based on the dietary patterns of postmenopausal women. The results showed that across all three dietary pattern subgroups, there were no statistically significant differences in HDL-C levels between women with osteopenia and normal bone mass ($P > 0.05$) (Figure 4B). Nonetheless, the effect size differences among the three dietary subgroups were statistically significant ($P = 0.001$). These findings suggest that national development level and dietary structure may contribute to the high heterogeneity observed in HDL-C comparisons between postmenopausal women with osteopenia and normal bone mass. However, these factors did not affect the

**Table 2. Quality evaluation of included studies**

| Reference | Selection | Comparability | Exposure/Outcome | Core | Quality |
|---|---|---|---|---|---|
| Abbasi M 2016 (*24*) | ** | * | *** | 6 | Median |
| Alay I 2020 (*22*) | **** | ** | ** | 8 | High |
| Cui R 2016 (*26*) | **** | * | ** | 7 | High |
| D'Amelio P 2001 (*19*) | *** | * | ** | 6 | Median |
| Demir B 2008 (*20*) | *** | * | ** | 6 | Median |
| Erden E 2023 (*23*) | ** | * | ** | 5 | Median |
| Gu L.J. 2019 (*14*) | *** | * | ** | 6 | Median |
| Naguib M 2022 (*29*) | *** | ** | ** | 7 | High |
| Pliatsika P 2012 (*25*) | ** | * | ** | 5 | Median |
| Pontes T.A. 2019 (*30*) | ** | * | ** | 5 | Median |
| Safari A 2019 (*27*) | **** | ** | ** | 8 | High |
| Tamaki J 2009 (*21*) | *** | ** | ** | 7 | High |
| Yaprak E.Ü. 2016 (*31*) | ** | ** | ** | 6 | Median |
| Zhao X 2023 (*28*) | *** | ** | ** | 7 | High |

*Note:* The number of stars indicates the score of the item.

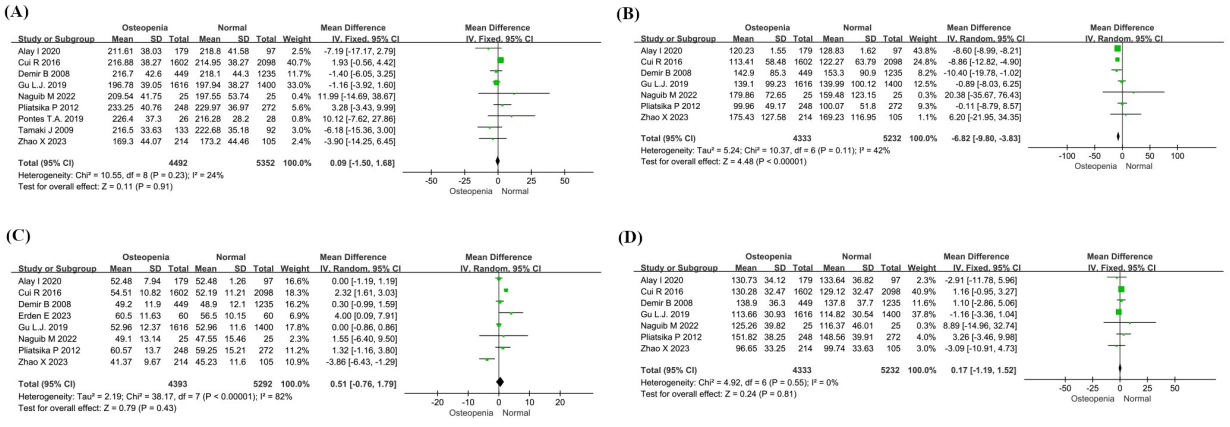


**Figure 2. Forest plots of the comparison of serum lipid levels in postmenopausal women with osteopenia and normal bone mass.** TC **(A)**, TG **(B)**, HDL-C **(C)**, and LDL-C **(D)**. Abbreviations: SD: standard deviation; 95% CI: 95% confidence interval.

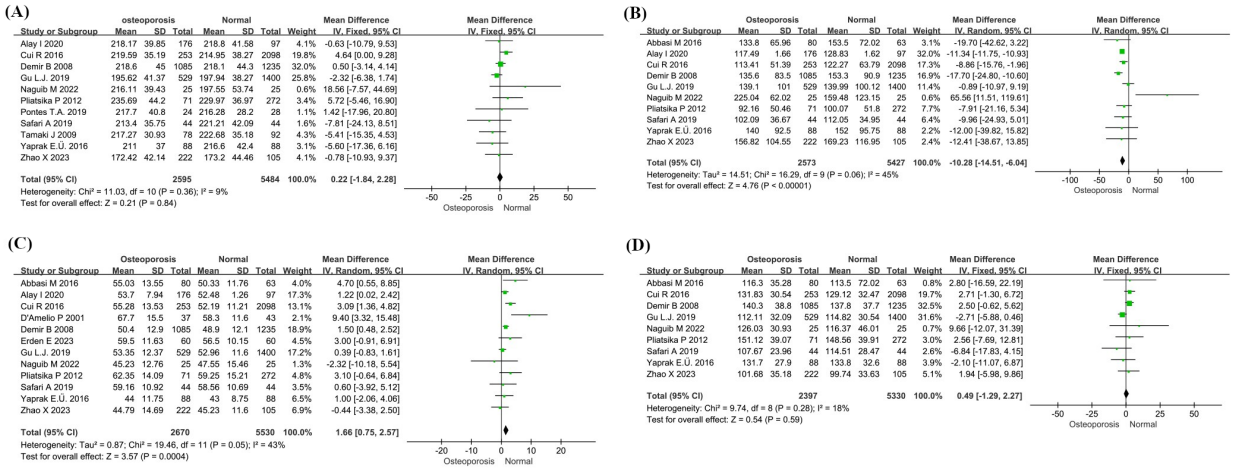


**Figure 3. Forest plots of the comparison of serum lipid levels in postmenopausal women with osteoporosis and normal bone mass.** TC **(A)**, TG **(B)**, HDL-C **(C)**, and LDL-C **(D)**. Abbreviations: SD: standard deviation; 95% CI: 95% confidence interval.

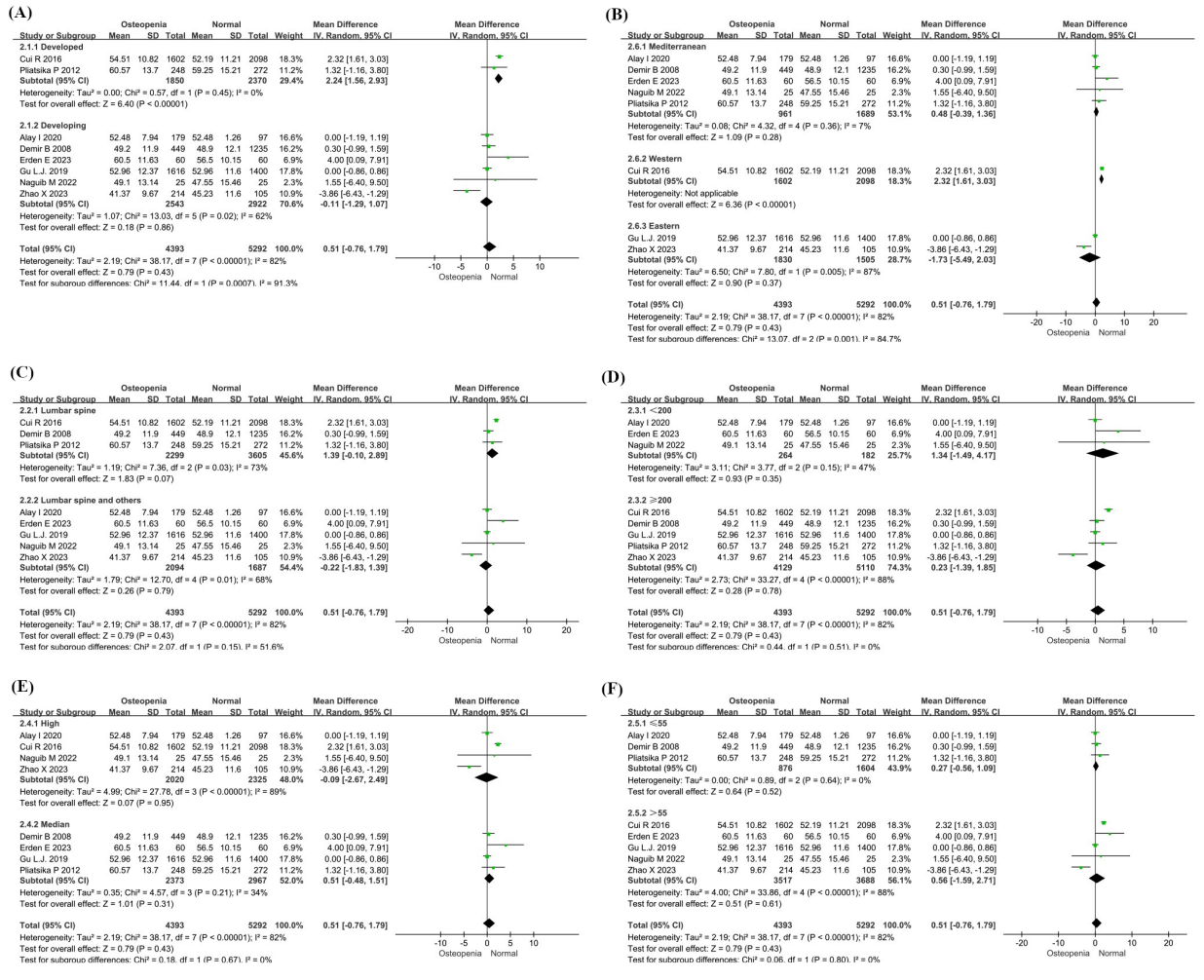


**Figure 4. Forest plots of the subgroup analysis of the serum HDL-C levels in postmenopausal women with osteopenia and normal bone mass based on different study characteristics.** Country development level **(A)**, dietary pattern of residents**(B)**, BMD evaluation **(C)**, sample size **(D)**, literature quality **(E)**, and mean age of patients **(F)**. Abbreviations: SD: standard deviation; 95% CI: 95% confidence interval.

main analysis results.

3.5. Sensitivity analysis

We found no significant discrepancies between pre-sensitivity and post-sensitivity pooled effect sizes when systematically removing individual studies related to serum lipid concentration—regardless of bone loss severity among postmenopausal women (Figure S1, *https://www.ddtjournal.com/action/getSupplementalData.php?ID=270*). Therefore, the results of our meta-analysis are reliable.

3.6. Publication bias

A funnel plot (applicable if ≥ 10 studies were included) and Egger's test were implemented using Stata software to assess potential publication bias for included studies. The Egger's test indicated that our research showed no signs of publication bias, both in postmenopausal women with osteopenia ($P$ = 0.78 for TC, $P$ = 0.49 for TG, $P$ = 0.53 for HDL-C, and $P$ = 0.95 for LDL-C) and in those with osteoporosis ($P$ = 0.95 for TC, $P$ = 0.62 for TG, $P$ = 0.35 for HDL-C, and $P$ = 0.91 for LDL-C). In addition, the funnel plot of the study on the connection between serum lipid concentration and bone T score in osteoporosis women showed symmetry (Figure S2, *https://www.ddtjournal.com/action/getSupplementalData.php?ID=270*).

**4. Discussion**

4.1. Main findings

This meta-analysis aimed to explore the relationship between bone health and lipid levels in postmenopausal women. It examined three bone conditions (normal, osteopenia, and osteoporosis) and four lipid parameters (TC, TG, HDL-C, and LDL-C), incorporating data from 14 studies involving 12,974 participants. The findings indicated that TG levels in postmenopausal women with osteopenia and osteoporosis are significantly lower than those in women with normal bone mass, suggesting that low serum TG levels may be indicative of bone loss in the population. Additionally, serum HDL-C concentrations were found to be significantly greater in osteoporosis women, implying that elevated HDL-C may serve as an indicator of osteoporosis in postmenopausal women. However, our analysis indicated that variations in TC and LDL-C did not correlate with bone mass in postmenopausal women. This implies that TC and LDL-C might not be reliable serological markers for forecasting bone loss in this population. Our subgroup analysis determined that national development level and dietary structure may contribute to the high heterogeneity observed in HDL-C comparisons between postmenopausal women with osteopenia and normal bone mass. However, these factors did not affect the main analysis results.

4.2. Implications

The level of bone mass in mammals relies on a delicate balance between bone formation and resorption—two critical processes carried out by osteoblasts and osteoclasts, respectively. Continuous communication between these two cell types is meticulously coordinated through bone remodeling, which is essential for maintaining bone homeostasis. Disruption in this coupling can lead to significant issues related to various bone diseases, including osteoporosis (*32*). Indeed, it has been demonstrated that disturbances within lipid metabolic pathways can differentially impact bone cells, contributing to the development of skeletal pathologies.

The association between serum TG levels and osteoporosis has been a contentious topic in the literature. For instance, while some studies have established a strong association between fasting serum TG concentrations and lumbar bone density (*33*), others have found no relationship (*34*). In our investigation, low serum TG levels indicated diminished bone mass, aligning with previous findings that suggest elevated TG levels may reflect a favorable nutritional status for bone health (*35*). Serum TG levels are intricately linked to BMD. For instance, adipocytes and osteoblasts originate from pluripotent mesenchymal stem cells, and a range of cytokines released by adipose tissue can influence bone remodeling *via* the central nervous system and autonomic innervation (*36,37*). Furthermore, research indicates that TG can create a protective barrier between collagen fibers and mineral crystals, which facilitates the adhesion of the protein matrix and contributes to the stability of bone (*38*). In summary, serum TG levels serve as reliable indicators of early bone loss, and low serum TG concentrations should prompt postmenopausal women to be vigilant regarding their bone health.

Apolipoprotein E (ApoE) and apolipoprotein A1 (ApoA1), two key molecules that regulate HDL biogenesis, are related to protect against atherosclerosis and maintain plasma lipid homeostasis (*39*). Studies have shown that a lack of ApoE may prevent bone marrow mesenchymal stem cells from maturing at an early stage, thereby affecting lipoblast and osteoblast lineages through unknown mechanisms (*40*). Alterations in ApoA1 may contribute to the pathogenesis of bone metastases by affecting signaling cascades and molecular pathways (*32*). In essence, disturbances in HDL metabolic pathways seem to encourage the transformation of cells into fat-storing adipocytes and hinder the development of bone-forming osteoblasts. Changes influence the intriguing interplay in certain bone-related chemokines and signaling routes. Our meta-analysis indicates that elevated HDL-C levels may be linked to severe bone loss, known as osteoporosis in

postmenopausal women. Additionally, high HDL-C levels in healthy older adults also predict an increased fracture risk (*41*). Consequently, elevated serum HDL-C levels warrant significant attention in postmenopausal women.

The enzymes and molecules that govern cholesterol balance are intricately intertwined with the process of bone formation. When TC levels soar, they may pave the way for osteoporosis, as cholesterol and its byproducts play a pivotal role in maintaining bone health by modulating the growth and function of osteoblasts and osteoclasts (*42*). LDL-C-induced cholesterol delivery can significantly increase osteoclast activity, while LDL-C consumption can inhibit osteoclast formation (*43,44*). However, our study did not find elevated TC and LDL-C levels in postmenopausal women with osteopenia and osteoporosis. In line with our discoveries, a comprehensive study involving 667 postmenopausal women revealed no noteworthy link between TC and LDL-C concentration and BMD in the spine and femoral neck, as determined through multifactor analysis (*45*). In addition, studies have shown that compared with natural menopause, the variety of TC, TG, and other lipid markers in women undergoing surgical menopause are more significant (*46*). However, our study could not determine the cause of menopause in our subjects. Further observational studies are needed to determine the predictive power of TC and LDL-C on bone status in postmenopausal women.

### 4.3. Limitations

There are several limitations to this review. First, we could not stratify participants by race, diet, exercise, smoking history, *etc*., because that information was unavailable in the original literature. Second, the included literature on lipid levels in women with osteopenia is limited, comprising fewer than ten studies, several of which involved small sample sizes. This may restrict the generalizability of our findings. To mitigate potential bias, several rigorous methodologies were employed. These included an extensive literature review, the establishment of strict guidelines for data extraction, the formulation of explicit inclusion and exclusion criteria, the use of a random effects model for estimation, and the execution of subgroup analyses. Despite certain limitations, this meta-analysis provides valuable insights into the relevance of serum lipid levels and bone status in postmenopausal women.

## 5. Conclusion

This study suggests that bone loss in postmenopausal women is associated with serum lipid levels. Our meta-analysis shows that low serum TG levels predict the onset of osteopenia in postmenopausal women, while high serum HDL-C levels suggest a potential risk for osteoporosis. These findings may assist clinicians in assessing the bone health of postmenopausal women and contribute to the early prevention and diagnosis of osteopenia and osteoporosis.

*Funding*: This work was supported by grants from a project under the National Natural Science Foundation of China (grant No. 82374243 to L Wang) and a project of the Science and Technology Research Project of Hubei Provincial Education Department (grant No. B2024275 to Q Qi).

*Conflict of Interest*: The authors have no conflicts of interest to disclose.

## References

1. Ballane G, Cauley JA, Luckey MM, El-Hajj Fuleihan G. Worldwide prevalence and incidence of osteoporotic vertebral fractures. Osteoporos Int. 2017; 28:1531-1542.
2. Sözen T, Özışık L, Başaran N. An overview and management of osteoporosis. Eur J Rheumatol. 2017; 4:46-56.
3. Sun H, Qi Q, Pan X, Zhou J, Wang J, Li L, Li D, Wang L. Bu-Shen-Ning-Xin decoction inhibits macrophage activation to ameliorate premature ovarian insufficiency-related osteoimmune disorder *via* FSH/FSHR pathway. Drug Discov Ther. 2024;18:106-116.
4. During A. Osteoporosis: A role for lipids. Biochimie. 2020; 178:49-55.
5. Garnero P, Sornay-Rendu E, Chapuy MC, Delmas PD. Increased bone turnover in late postmenopausal women is a major determinant of osteoporosis. J Bone Miner Res. 1996; 11:337-349.
6. Wu SF, Du XJ. Body mass index may positively correlate with bone mineral density of lumbar vertebra and femoral neck in postmenopausal females. Med Sci Monit. 2016; 22:145-151.
7. Chai S, Yang Y, Wei L, Cao Y, Ma J, Zheng X, Teng J, Qin N. Luteolin rescues postmenopausal osteoporosis elicited by OVX through alleviating osteoblast pyroptosis *via* activating PI3K-AKT signaling. Phytomedicine. 2024; 128:155516.
8. Awasthi H, Mani D, Singh D, Gupta A. The underlying pathophysiology and therapeutic approaches for osteoporosis. Med Res Rev. 2018; 38:2024-2057.
9. Feng X, McDonald JM. Disorders of bone remodeling. Annu Rev Pathol. 2011; 6:121-145.
10. Alekos NS, Moorer MC, Riddle RC. Dual effects of lipid metabolism on osteoblast function. Front Endocrinol (Lausanne). 2020; 11:578194.
11. Sato T, Morita I, Murota S. Involvement of cholesterol in osteoclast-like cell formation *via* cellular fusion. Bone. 1998; 23:135-140.
12. Huang X, Lv Y, He P, Wang Z, Xiong F, He L, Zheng X, Zhang D, Cao Q, Tang C. HDL impairs osteoclastogenesis and induces osteoclast apoptosis *via* upregulation of ABCG1 expression. Acta Biochim Biophys Sin (Shanghai). 2018; 50:853-861.
13. Wang S, Qiu Y, Tang C, Tang H, Liu J, Chen J, Zhang L, Tang G. Early changes of bone metabolites and lymphocyte subsets may participate in osteoporosis onset:

A preliminary study of a postmenopausal osteoporosis mouse model. Front Endocrinol (Lausanne). 2024; 15:1323647.
14. Gu LJ, Lai XY, Wang YP, Zhang JM, Liu JP. A community-based study of the relationship between calcaneal bone mineral density and systemic parameters of blood glucose and lipids. Medicine (Baltimore). 2019; 98:e16096.
15. Alfahal AO, Ali AE, Modawe GO, Doush WM. Association between serum lipid profile, body mass index and osteoporosis in postmenopausal Sudanese women. Afr Health Sci. 2022; 22:399-406.
16. Li S, Guo H, Liu Y, Wu F, Zhang H, Zhang Z, Xie Z, Sheng Z, Liao E. Relationships of serum lipid profiles and bone mineral density in postmenopausal Chinese women. Clin Endocrinol (Oxf). 2015; 82:53-58.
17. Organization WH. Management of osteoporosis in postmenopausal women: the 2021 position statement of The North American Menopause Society. Menopause. 2021; 28:973-997.
18. Zhang Y, Huang L, Wang D, Ren P, Hong Q, Kang D. The ROBINS-I and the NOS had similar reliability but differed in applicability: A random sampling observational studies of systematic reviews/meta-analysis. J Evid Based Med. 2021; 14:112-122.
19. D'Amelio P, Pescarmona GP, Gariboldi A, Isaia GC. High density lipoproteins (HDL) in women with postmenopausal osteoporosis: A preliminary study. Menopause. 2001; 8:429-432.
20. Demir B, Haberal A, Geyik P, Baskan B, Ozturkoglu E, Karacay O, Deveci S. Identification of the risk factors for osteoporosis among postmenopausal women. Maturitas. 2008; 60:253-256.
21. Tamaki J, Iki M, Hirano Y, Sato Y, Kajita E, Kagamimori S, Kagawa Y, Yoneshima H. Low bone mass is associated with carotid atherosclerosis in postmenopausal women: The Japanese Population-based Osteoporosis (JPOS) Cohort Study. Osteoporos Int. 2009; 20:53-60.
22. Alay I, Kaya C, Cengiz H, Yildiz S, Ekin M, Yasar L. The relation of body mass index, menopausal symptoms, and lipid profile with bone mineral density in postmenopausal women. Taiwan J Obstet Gynecol. 2020; 59:61-66.
23. Erden E, Turk AC, Fidan N, Erden E. Relationship between blood monocyte-HDL ratio and carotid intima media thickness in with postmenopausal women. J Clin Densitom. 2023; 26:101428.
24. Abbasi M, Farzam SA, Mamaghani Z, Yazdi Z. Relationship between metabolic syndrome and its components with bone densitometry in postmenopausal women. Diabetes Metab Syndr. 2017; 11 Suppl 1:S73-S76.
25. Pliatsika P, Antoniou A, Alexandrou A, Panoulis C, Kouskouni E, Augoulea A, Dendrinos S, Aravantinos L, Creatsa M, Lambrinoudaki I. Serum lipid levels and bone mineral density in Greek postmenopausal women. Gynecol Endocrinol. 2012; 28:655-660.
26. Cui R, Zhou L, Li Z, Li Q, Qi Z, Zhang J. Assessment risk of osteoporosis in Chinese people: Relationship among body mass index, serum lipid profiles, blood glucose, and bone mineral density. Clin Interv Aging. 2016; 11:887-895.
27. Safari A, Borhani-Haghighi A, Dianatpour M, Heydari ST, Foroughinia F, Ranjbar Omrani G. Circulating serum amyloid A, hs-CRP and vitamin D levels in postmenopausal osteoporosis. Galen Med J. 2019; 8:e1548.
28. Zhao X, Sun J, Xin S, Zhang X. Correlation between blood lipid level and osteoporosis in older adults with type 2 diabetes mellitus-a retrospective study based on inpatients in Beijing, China. Biomolecules. 2023; 13:616.
29. Naguib M, Ali N, ElSaraf N, Rashed L, Azzam H. Does serum osteocalcin level affect carotid atherosclerosis in postmenopausal diabetic females? A case-control study. Int J Gen Med. 2022; 15:4513-4523.
30. Pontes TA, Barbosa AD, Silva RD, Melo-Junior MR, Silva RO. Osteopenia-osteoporosis discrimination in postmenopausal women by 1H NMR-based metabonomics. PLoS One. 2019; 14:e0217348.
31. Engin-Üstün Y, Çağlayan EK, Göçmen AY, Polat MF. Postmenopausal osteoporosis is associated with serum chemerin and irisin but not with apolipoprotein M levels. J Menopausal Med. 2016; 22:76-79.
32. Papachristou NI, Blair HC, Kypreos KE, Papachristou DJ. High-density lipoprotein (HDL) metabolism and bone mass. J Endocrinol. 2017; 233:R95-R107.
33. Dennison EM, Syddall HE, Aihie Sayer A, Martin HJ, Cooper C. Lipid profile, obesity and bone mineral density: the Hertfordshire cohort study. QJM. 2007; 100:297-303.
34. Go JH, Song YM, Park JH, Park JY, Choi YH. Association between serum cholesterol level and bone mineral density at lumbar spine and femur neck in postmenopausal Korean women. Korean J Fam Med. 2012; 33:166-173.
35. Zhao H, Zheng C, Gan K, Qi C, Ren L, Song G. High body mass index and triglycerides help protect against osteoporosis in patients with type 2 diabetes mellitus. J Diabetes Res. 2020; 2020:1517879.
36. Akune T, Ohba S, Kamekura S, Yamaguchi M, Chung U-i, Kubota N, Terauchi Y, Harada Y, Azuma Y, Nakamura K, Kadowaki T, Kawaguchi H. PPAR γ insufficiency enhances osteogenesis through osteoblast formation from bone marrow progenitors. J Clin Invest. 2004; 113:846-855.
37. Kajimura D, Lee HW, Riley KJ, Arteaga-Solis E, Ferron M, Zhou B, Clarke CJ, Hannun YA, DePinho RA, Guo XE, Mann JJ, Karsenty G. Adiponectin regulates bone mass *via* opposite central and peripheral mechanisms through FoxO1. Cell Metab. 2013; 17:901-915.
38. Xu S, Yu JJ. Beneath the minerals, a layer of round lipid particles was identified to mediate collagen calcification in compact bone formation. Biophys J. 2006; 91:4221-4229.
39. Kypreos KE, Zannis VI. Pathway of biogenesis of apolipoprotein E-containing HDL *in vivo* with the participation of ABCA1 and LCAT. Biochem J. 2007; 403:359-367.
40. Bartelt A, Beil FT, Schinke T, Roeser K, Ruether W, Heeren J, Niemeier A. Apolipoprotein E-dependent inverse regulation of vertebral bone and adipose tissue mass in C57Bl/6 mice: Modulation by diet-induced obesity. Bone. 2010; 47:736-745.
41. Hussain SM, Ebeling PR, Barker AL, Beilin LJ, Tonkin AM, McNeil JJ. Association of plasma high-density lipoprotein cholesterol level with risk of fractures in healthy older adults. JAMA Cardiol. 2023; 8:268-272.
42. Bao C, Wu T, Zhu S, Wang X, Zhang Y, Wang X, Yang L, He C. Regulation of cholesterol homeostasis in osteoporosis mechanisms and therapeutics. Clin Sci (Lond). 2023; 137:1131-1143.
43. Okayasu M, Nakayachi M, Hayashida C, Ito J, Kaneda T, Masuhara M, Suda N, Sato T, Hakeda Y. Low-density lipoprotein receptor deficiency causes impaired osteoclastogenesis and increased bone mass in mice because of defect in osteoclastic cell-cell fusion. J Biol

Chem. 2012; 287:19229-19241.
44. Luegmayr E, Glantschnig H, Wesolowski GA, Gentile MA, Fisher JE, Rodan GA, Reszka AA. Osteoclast formation, survival and morphology are highly dependent on exogenous cholesterol/lipoproteins. Cell Death Differ. 2004; 11 Suppl 1:S108-118.
45. Zolfaroli I, Ortiz E, García-Pérez M, Hidalgo-Mora JJ, Tarín JJ, Cano A. Positive association of high-density lipoprotein cholesterol with lumbar and femoral neck bone mineral density in postmenopausal women. Maturitas. 2021; 147:41-46.
46. Pavel OR, Popescu M, Novac L, Mogoantă L, Pavel LP, Vicaș RM, Trăistaru MR. Postmenopausal osteoporosis - clinical, biological and histopathological aspects. Rom J Morphol Embryol. 2016; 57:121-130.

Received July 13, 2025; Revised August 20, 2025; Accepted August 23, 2025.

[§]These authors contributed equally to this work.
**Address correspondence to:*
Ling Wang, Department of Obstetrics and Reproductive Immunology, Shanghai East Hospital, Tongji University School of Medicine, No. 1800 Yuntai Road, Shanghai 200100, China.
E-mail: dr.wangling@vip.163.com

Qing Qi, Wuhan Business University, 816 Dongfeng Avenue, Wuhan Economic and Technological Development Zone, Wuhan, Hubei 430056, China.
E-mail: qiqing007@126.com

Released online in J-STAGE as advance publication August 28, 2025.

*Original Article*

DOI: 10.5582/ddt.2025.01047

# Bovine lactoferrin intake prevents hepatic injury in a mouse model of non-alcoholic steatohepatitis induced by choline and methionine deficiency

**Ryoken Aoki[1,2,3], Kentaro Ishido[4], Megumi Furukawa[4], Yukiko Ishibashi[5], Shotaro Nozaki[4], Neon Ito[4], Masahiro Toho[4], Daichi Nagashima[6,7], Nobuo Izumo[4,7,*]**

[1] Department of Functional Brain Activities, United Graduate School of Child Development, Osaka University, Osaka, Japan;
[2] Center for Pharmaceutical Education, Yokohama University of Pharmacy, Kanagawa, Japan;
[3] Research Center for Child Mental Development, University of Fukui, Fukui, Japan;
[4] Laboratory of Pharmacotherapy, Yokohama University of Pharmacy, Kanagawa, Japan;
[5] Laboratory of Drug Analysis, Yokohama University of Pharmacy, Kanagawa, Japan;
[6] Laboratory of Clinical Pharmaceutics, Yokohama University of Pharmacy, Kanagawa, Japan;
[7] General Health Medical Research Center, Yokohama University of Pharmacy, Kanagawa, Japan.

**SUMMARY**: Lactoferrin, a multifunctional protein found in breast milk, is important for the regulation of immune function. Non-alcoholic steatohepatitis (NASH), which is characterized by hepatitis and fibrosis, has no established drug treatment. In this study, we aimed to investigate the effects of lactoferrin on hepatocyte inflammation in a mouse model of NASH induced with a choline-deficient, L-amino acid-defined, high-fat diet (CDAHFD). As a method, C57BL/6JJmsSlc mice were fed CDAHFD for 14 days and simultaneously intake lactoferrin (3.3 g/kg or 6.6 g/kg) of water. Then, plasma levels aspartate aminotransferase (ALT) and alanine aminotransferase (AST) were measured and gene expression levels of inflammatory cytokines in the liver were examined. Plasma levels of ALT and AST significantly increased in the NASH model, indicating hepatocyte inflammation, and lactoferrin intake suppressed their elevation in a dose-dependent manner. Histological analysis revealed that lactoferrin alleviated the fatty liver-associated tissue damage. Additionally, lactoferrin suppressed the gene expression of the pro-inflammatory cytokines tumor necrosis factor (TNF-α), interleukin (IL)-1β, and IL-6 and the macrophage migration factor (MCP)-1, suggesting inhibition of macrophage activation. Lactoferrin also significantly reduced the expression of apoptosis-related genes (caspase 3 and p53), indicating its anti-apoptotic effects. Furthermore, lactoferrin alleviated oxidative stress by suppressing inducible nitric oxide synthase expression. These findings suggest that lactoferrin prevented liver injury in the mouse model of NASH induced by CDAHFD feeding by inhibiting macrophage-mediated inflammation and alleviating oxidative stress caused by fat accumulation.

***Keywords***: Fat accumulation, macrophage, TNF-α, MCP-1, iNOS

## 1. Introduction

The incidence of non-alcoholic fatty liver disease (NAFLD) is increasing with the prevalence of metabolic syndrome, diabetes, and dyslipidemia (*1*). NAFLD development includes stages of non-alcoholic fatty liver (NAFL), non-alcoholic steatohepatitis (NASH), chronic inflammation, and fibrosis. Cirrhosis or hepatocellular carcinoma is the end stage of liver disease caused by NASH (*2,3*). The pathogenesis of NAFLD to NASH is considered to involve a variety of factors but is most likely due to the deposition of triglycerides and other lipids in hepatocytes as a result of long-term disordered eating habits. Consequently, increased inflammation is considered to be caused by increased oxidative stress and abnormal immune function following endotoxin exposure (*4*). This progression induces irreversible liver damage in patients with cirrhosis and hepatocellular carcinoma, which are also the major causes of liver transplantation and social problems (*5*). However, there is no treatment for NASH, and lifestyle modifications, such as diet and exercise therapy, are the mainstay of treatment.

Several mouse models have been used in NASH research, including a model induced with a choline-methionine-deficient diet (CDAHFD) (*6*). The liver synthesizes the lipoprotein very low-density lipoprotein (VLDL) and excretes lipid components into the blood.

Phosphatidylcholine (PC) is required for VLDL formation (*7*). The formation of PC, which imposes a burden on the liver, occurs *via* the methylation of phosphatidylethanolamine from active methionine. As 40% of active methionine is used to synthesize PC, reduced PC synthesis under methionine deficiency causes fatty liver because VLDL is not synthesized. Choline is also the starting substrate for PC synthesis in the CDP-choline pathway. In other words, PC is synthesized from choline and methionine *via* different synthesis pathways, and their loss causes substantial damage to hepatocytes. Decreased synthesis of VLDL and increased synthesis of triglycerides lead to the accumulation of fat in the liver and cause fatty degeneration. As a result, lipid peroxidation occurs, damaging the cell membranes and inducing inflammation.

As an environmental factor, high-fat diet intake disturbs the balance of the intestinal microbiota and increases lipopolysaccharide (LPS) concentration, which induces inflammation by exposing hepatocytes to plasma endotoxins. LPS intake induces damage to hepatocytes (*8*). LPS administration induces inflammation in macrophage-like cells (unpublished data).

Lactoferrin, a protein found in breast milk, enhances the immune function in infants, mostly through the action of neutrophils containing lactoferrin (*9,10*). However, in addition to neutrophils, it has been shown to affect macrophages and T cells, and enhance immune function (*11*). In an ovariectomy-induced osteopenia model, lactoferrin also inhibited the loss of bone mineral density by acting on macrophage-derived osteoclasts (*12*). Furthermore, lactoferrin has been shown to have anti-inflammatory effects in models of liver injury induced with acetaminophen and carbon tetrachloride (*13,14*). In hepatocytes, lactoferrin exerts effects on immune abnormalities and inflammation by acting on macrophage-derived Kupffer cells. Previously, we have shown that lactoferrin has an anti-inflammatory effect on hepatocytes in mice fed a high-fat diet (*15*). However, lactoferrin has also been reported to improve the intestinal microbiota (*16*), limiting the ability to test its direct effect on macrophages in high-fat diet models. Therefore, in this study, we aimed to investigate the anti-inflammatory effects of lactoferrin on hepatocyte inflammation and its preventive effects on liver injury in an NASH model with increased hepatocellular damage using a CDAHFD.

## 2. Materials and Methods

### 2.1. Animals

Sixty 5-week-old male C57BL/6JJmsSlc mice (Japan SLC, Shizuoka, Japan) were used in this study after 1 week of preliminary rearing. The rearing environmental conditions were as follows: room temperature of 24°C ± 1°C, 12 h of day light (light period 7:00–19:00 h, dark period 19:00–7:00 h), and humidity of 55%. During the pre-rearing period, the mice were fed CRF-1 (Oriental Yeast Co., Ltd., Tokyo, Japan) and provided with tap water ad libitum. The experimental design of this study was approved by the Experimental Animal Committee of Yokohama University of Pharmacy (2020-009).

### 2.2. Model mice and lactoferrin intake

After 1 week of pre-rearing, the mice were divided into four groups (15 animals per group): control, NASH, NASH+lactoferrin-low (3.3 g/kg), and NASH+lactoferrin-high (6.6 g/kg) groups to ensure that there was no difference in body weight. The control group mice were fed a normal diet (CRF-1), and NASH model mice were fed CDAHFD 60 (choline-deficient methionine reduced 60 kcal% fat diet; EP Trading Co., Ltd., Kanagawa, Japan), as described by Matsumoto *et al*. (*6*). Mice from two of the CDAHFD 60-intake groups were provided lactoferrin at different concentrations 3.3 and 6.6 g/kg ad libitum for 14 days. Bovine lactoferrin was provided by NRL Pharma (NRL Pharma, Inc., Kanagawa, Japan). The group administered 3.3 g/kg lactoferrin was the lactoferrin-low group and the group given 6.6 g/kg was the lactoferrin-high group. The lactoferrin ingested was converted from the daily intake, with 1.65 g/100 mL of dissolved solution for the lactoferrin-low group and 3.3 g/100 mL for the lactoferrin-high group. Food and water intake was measured every 5 days and divided by the number of days and number of mice to obtain the daily food and water intake per mouse. Body weight was measured after pre-rearing and every 5 days from the start of intake.

### 2.3. Aspartate aminotransferase and alanine aminotransferase levels in plasma

Fifteen days after lactoferrin administration, blood samples were collected with the mice under isoflurane anesthesia, placed in a MiniCollect® Tube (Funakoshi Co., Ltd., Tokyo, Japan) and centrifuged; the supernatant was then collected and stored at -80°C until measurement. Aspartate aminotransferase (AST) and alanine aminotransferase (ALT) were measured using an aspartate aminotransferase kit, alanine aminotransferase kit, and transaminase CII-test Wako (Fujifilm Wako Pure Chemicals Corporation, Osaka, Japan).

### 2.4. Histological analysis

Fifteen days after lactoferrin administration, the mice were anesthetized with isoflurane and perfusion-fixed with saline and 10% Mildform® reagent (Fujifilm Wako Pure Chemicals Corporation). The livers were then removed and fixed in 10% Mildform® reagent at 4°C for 24 h. After 24 h, the tissues were immersed in 10%, 20%, and 30% sucrose solution dissolved in phosphate-

buffered saline (PBS) (pH 7.4) sequentially for 24 h at 4°C, embedded in optimal cutting temperature (OCT) compound (Sakura Finetek, Inc. Tokyo, Japan), and frozen. The samples were sectioned to 16-µm thickness using a cryostat HM550 (Thermo Fisher Scientific K.K., Tokyo, Japan). The frozen sections were washed with PBS and stained with hematoxylin–eosin (HE) to evaluate their morphology. The sections were photographed using an all-in-one fluorescence microscope BZ-X710 (KEYENCE, Osaka, Japan).

2.5. Real-time reverse transcription-polymerase chain reaction analysis of gene expression levels

After blood collection, the mice were sacrificed and their livers were removed. Total RNA was extracted by homogenizing the liver with 400 µL of Isogen (Nippon Gene Co., Ltd., Tokyo Japan), followed by centrifugation (16,900× *g*, 15 min) with 80 µL of chloroform. Thereafter, the supernatant was collected, 200 µL of isopropanol was added, and the precipitate was collected using centrifugation (16,900× *g*, 5 min). The precipitate was dissolved in sterile water and reverse-transcribed into cDNA using the SuperScript VIRO cDNA Synthesis kit (*Invitrogen*, Thermo Fisher Scientific Inc., Waltham, MA, USA.). The synthesized cDNA was used as a template with primers for each marker (Table 1) and the expression levels of genes related to inflammatory cytokines, oxidative stress, and apoptosis were detected using the TaqMan probe method on a LightCycler®480II (F. Hoffmann-La Roche, Ltd., Basel, Switzerland.). The expression levels of each gene was corrected using that of *GAPDH*.

2.6. Data analysis

Data are shown as mean ± standard error. Between-group comparisons for each dataset were performed using Dunnett's test after testing with a one-way analysis of variance. The statistical software Stat View 5.0 (SAS Institute Inc., version 5.0) was used for analyses. The significance level was set at $p < 0.05$ and $p < 0.01$.

## 3. Results

3.1. Influence of CDAHFD on food and water intake and body weight of mice

To confirm the influence of CDAHFD, the diet used to generate NASH model mice, on body weight, we measured food and water intake and body weight of mice every 5 days. Food and water intake were measured in group-housed mice. Although statistical comparison was not performed, intake appeared similar across the groups (Table 2); however, the NASH group showed a significant decrease in body weight compared to the control group after 5 days of CDAHFD feeding (Table 3). This weight loss continued until day 15. Lactoferrin intake significantly reduced weight loss induced by CDAHFD feeding from day 10.

**Table 1. Primers for each marker used in real-time RT-PCR**

| Protein/Gene | Universal Probe Library Probe No. | Forward primer (5'→3') | Reverse primer |
|---|---|---|---|
| GAPDH (*GAPDH*) | #9 | agcttgtcatcaacgggaag | tttgatgttagtggggtctcg |
| TNF-α (*TNF*) | #103 | tgctgggaagcctaaagg | cgaattttgagaagatgatcctg |
| IL-6 (*IL6*) | #6 | gctaccaaactggatataatcagga | ccaggtagctatggtactccagaa |
| IL-1β (*IL1B*) | #60 | tcttcctaaagtatgggctgga | aaagggagctccttaacatgc |
| MCP-1( *CCL2*) | #2 | gggacactggctgcttgt | gttgttaagcagaagattcacgtc |
| iNOS (*NOS2*) | #13 | ctttgccacggacgagac | tcattgtactctgagggctgac |
| p53 (*TP53*) | #9 | gacggaggtcgtgagacg | atttccttccacccggatac |
| Caspase 3 (*CASP3*) | #80 | gaggctgacttcctgtatgctt | aaccacgacccgtccttt |

GAPDH: glyceraldehyde-3-phosphate dehydrogenase, TNF-α: tumor necrosis factor-α, IL-6: interleukin-6, IL-1β: interleukin-1β, MCP-1: monocyte chemotactic protein-1, iNOS: inducible nitric oxide synthase.

**Table 2. Food and water intake**

| Group | Food intake (g) | | | Water intake (mL) | | |
|---|---|---|---|---|---|---|
| | Day 5 | Day 10 | Day 15 | Day 5 | Day 10 | Day 15 |
| Control | 3.2 | 3.0 | 3.3 | 4.6 | 4.3 | 4.2 |
| NASH | 2.4 | 2.6 | 3.0 | 4.1 | 5.9 | 5.4 |
| Lactoferrin low | 3.8 | 5.2 | 5.2 | 4.3 | 4.5 | 4.6 |
| Lactoferrin high | 2.3 | 2.0 | 2.4 | 4.0 | 4.4 | 4.8 |

Food and water intake were measured in group-housed mice, and no obvious differences were observed between the groups. NASH: choline-deficient, L-amino acid-defined, high-fat diet fed group, Lactoferrin low: NASH + lactoferrin-low (3.3 g/kg) group, Lactoferrin high: NASH + lactoferrin-low (6.6 g/kg) group.

3.2. Effect of lactoferrin on AST and ALT levels in CDAHFD-fed mice

To assess liver damage caused by CDAHFD feeding, we measured plasma AST and ALT levels. Both AST and ALT levels significantly increased on day 15 of CDAHFD feeding compared with those in the control group (Figure 1). Both low and high doses of lactoferrin significantly suppressed the increase in the AST and ALT levels induced by CDAHFD feeding (Figure 1).

3.3. Effect of lactoferrin on the morphology of the liver

We performed HE staining to morphologically assess the liver damage caused by CDAHFD60 feeding (Figure 2). We observed large fat droplet deposits and vacuoles in hepatocytes after CDAHFD feeding. In mice receiving lactoferrin, the number and size of vacuoles appeared reduced, and hepatocytes showed more regular morphology with less swelling, suggesting partial alleviation of hepatocyte damage. These qualitative observations provide meaningful insights, although the distribution of vacuoles and lipid droplets was highly heterogeneous within and among liver sections.

3.4. Effect of lactoferrin on hepatotoxicity-related gene expression levels in CDAHFD-fed mice

To examine the effect of lactoferrin on liver inflammation, we measured gene expression levels of the inflammatory cytokines tumor necrosis factor (TNF-α), interleukin (IL)-1β, and IL-6 using real-time reverse

**Table 3. Effect of lactoferrin on body weight**

| Group | Body weight (g) | | | |
|---|---|---|---|---|
| | Day 1 | Day 5 | Day 10 | Day 15 |
| Control | 19.6 ± 0.2 | 20.9 ± 0.2 | 21.8 ± 0.2 | 22.0 ± 0.3 |
| NASH | 19.4 ± 0.2 | 19.7 ± 0.2$^{*}$ | 19.7 ± 0.2$^{**}$ | 19.9 ± 0.2$^{**}$ |
| Lactoferrin low | 20.0 ± 0.3 | 20.9 ± 0.3 | 21.0 ± 0.4$^{\#}$ | 21.6 ± 0.4$^{\#}$ |
| Lactoferrin high | 19.8 ± 0.2 | 20.7 ± 0.3 | 20.7 ± 0.3$^{\#}$ | 21.3 ± 0.3$^{\#}$ |

Lactoferrin intake significantly reduced body weight loss due to CDAHFD feeding from day 10 (**$p < 0.01$, *$p < 0.05$ compared to the control, #$p < 0.05$ compared to NASH, Tukey's test). The results are presented as mean ± standard error. NASH: choline-deficient, L-amino acid-defined, high-fat diet fed group, Lactoferrin low: NASH + lactoferrin-low (3.3 g/kg) group, Lactoferrin high: NASH + lactoferrin-low (6.6 g/kg) group.

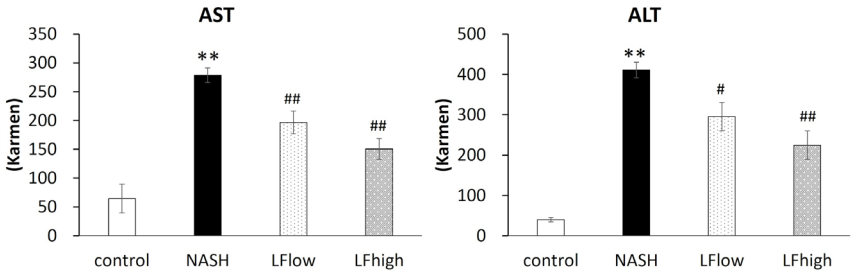


**Figure 1. Effects of lactoferrin on aspartate aminotransferase (AST) and alanine aminotransferase (ALT) level in NASH model mice.** Plasma aspartate aminotransferase (AST) and alanine aminotransferase (ALT) levels. CDAHFD feeding significantly increased the AST and ALT levels. Lactoferrin intake significantly suppressed this increase (**$p < 0.01$, *$p < 0.05$, Dunnett's test). Bars indicate mean ± standard error. NASH: choline-deficient, L-amino acid-defined, high-fat diet fed group, LF low: NASH + lactoferrin-low (3.3 g/kg) group, LF high: NASH + lactoferrin-low (6.6 g/kg) group.

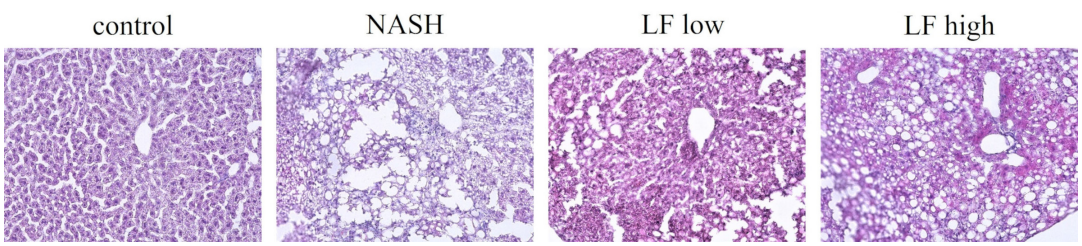


**Figure 2. Effects of lactoferrin on the morphology of liver in NASH model mice, as determined using hematoxylin–eosin (HE) staining.** The control group showed normal lobular cells. The NASH group showed large fat droplet deposits and vacuoles in hepatocytes. Lactoferrin intake decreased the number of vacuoles. NASH: choline-deficient, L-amino acid-defined, high-fat diet fed group, LF low: NASH + lactoferrin-low (3.3 g/kg) group, LF high: NASH + lactoferrin-low (6.6 g/kg) group.

transcription-polymerase chain reaction (RT-PCR). CDAHFD feeding induced a significant increase in the expression of TNF-α, IL-1β, and IL-6 (Figures 3A, 3B, and 3C). High-dose intake of lactoferrin significantly suppressed this increase (Figures 3A and 3B), and the gene expression of IL-6 was significantly suppressed by both low- and high-dose lactoferrin intake (Figure 3C). Next, we measured the gene expression level of the macrophage migration factor (MCP)-1, a macrophage chemotaxis factor. Its expression was significantly increased by CDAHFD feeding and significantly suppressed by high-dose lactoferrin intake (Figure 3D). We measured the gene expression of p53 and caspase 3 to assess hepatocyte apoptosis. The gene expression of p53 and caspase 3 was significantly increased by CDAHFD feeding (Figures 4A and 4B), and high-dose lactoferrin intake significantly suppressed the increase in the gene expression of caspase 3 (Figure 4B). We also measured the gene expression levels of inducible nitric oxide synthase (iNOS) to examine the involvement of oxidative stress; its level was significantly elevated by CDAHFD feeding and significantly suppressed by high-dose lactoferrin intake (Figure 4C).

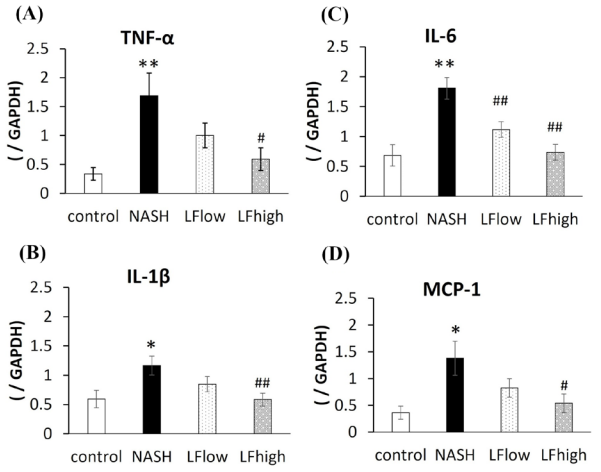


**Figure 3. Effects of lactoferrin on mRNA expression levels of the cytokines tumor necrosis factor (TNF-α), interleukin (IL)-1β, and IL-6 and chemokine monocyte chemoattractant protein 1 (MCP-1) in the liver of NASH model mice.** Expression levels of hepatotoxicity-related genes as determined using real-time RT-PCR. CDAHFD feeding induced a significant increase in the gene expression of TNF-α (A), IL-1β (B), IL-6 (C), and MCP-1 (D). High-dose lactoferrin intake significantly suppressed this increase (**$p < 0.01$, *$p < 0.05$, Dunnett's test). Bars indicate mean ± standard error. NASH: choline-deficient, L-amino acid-defined, high-fat diet fed group, LF low: NASH + lactoferrin-low (3.3 g/kg) group, LF high: NASH + lactoferrin-low (6.6 g/kg) group.

## 4. Discussion

In this study, we investigated the effects of lactoferrin intake in a mouse model of NASH induced with a CDAHFD. We observed a significant decrease in body weight from day 5 of CDAHFD feeding compared with that of the control group, and this decrease continued until day 15 of feeding. Both the low- and high-dose lactoferrin groups showed no weight decrease on day 5 of treatment and significant weight gain compared with that of the NASH group from day 10 of treatment. The amount of food and water intake of mice in each group was measured, and no significant differences were found among the groups. These results suggest that lactoferrin improves weight loss with abnormal lipid metabolism in hepatocytes caused by CDAHFD feeding. We have previously shown that lactoferrin reduced liver inflammation induced by a high-fat diet (*15*). Therefore, we examined the plasma AST and ALT levels to determine whether lactoferrin is involved in the suppression of hepatocyte inflammation. A significant increase in the AST and ALT levels was observed after 16 days of CDAHFD feeding, indicating that CDAHFD feeding induced hepatocyte inflammation. Similar results have been reported by Matsumoto *et al.* (*6*). We also found that lactoferrin intake had a significant concentration-dependent inhibitory effect on the elevation in AST and ALT levels caused by hepatocyte inflammation. It has been reported that lactoferrin exhibited anti-inflammatory effects in a liver injury model developed using acetaminophen and carbon tetrachloride (*13,14*). This finding suggests that lactoferrin exerted an anti-inflammatory effect in our mouse model of NASH

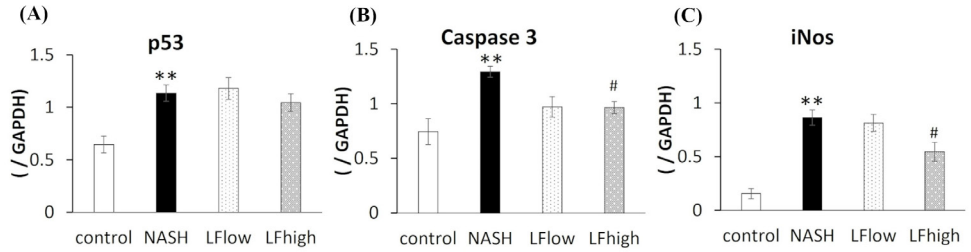


**Figure 4. Effects of lactoferrin on the mRNA expression levels of p53, caspase 3, and inducible nitric oxide synthase (iNOS) in the liver of NASH model mice.** Expression levels of hepatotoxicity-related genes as determined using real-time RT-PCR. CDAHFD feeding significantly increased the gene expression of p53 (A), caspase 3 (B), and iNOS (C). High-dose lactoferrin intake significantly suppressed p53 and iNOS expression (**$p < 0.01$, *$p < 0.05$, Dunnett's test). Bars indicate mean ± standard error. NASH: choline-deficient, L-amino acid-defined, high-fat diet fed group, LF low: NASH + lactoferrin-low (3.3 g/kg) group, LF high: NASH + lactoferrin-low (6.6 g/kg) group.

induced with a CDAHFD.

In this study, lactoferrin suppressed the elevation in plasma AST and ALT levels; therefore, sections of liver tissue were prepared and compared histologically using HE staining. The CDAHFD-fed group had more vacuoles in liver tissue sections than the control group, indicating fatty liver and tissue damage. Therefore, it was considered that lactoferrin intake reduced liver tissue damage; the histological studies also suggested that lactoferrin reduced liver tissue damage caused by CDAHFD feeding.

To further investigate the inhibitory effect of lactoferrin on hepatocyte inflammation, its effect on gene expression was examined using real-time RT-PCR. The gene expression of TNF-α, IL-1β, and IL-6 significantly increased in the CDAHFD group compared with that in the control group. As TNF-α, IL-1β, and IL-6 are inflammatory cytokines released by macrophages, it was suggested that activation of Kupffer cells is involved in hepatocyte inflammation. Ganguly *et al*. reported that different mouse models of NASH exhibit immune changes in hepatocytes, and it is likely that similar changes occurred in the model used in this study (*17*). Lactoferrin intake inhibited the elevation in the levels of these inflammatory cytokines, and significantly suppressed their expression at higher doses. Lactoferrin has been shown to be closely related to immune function in infants and likely involved in the activation of neutrophils (*10*). On the contrary, Hwang *et al*. reported that in *Bacillus* Calmette Guerin and human lactoferrin-treated $CD16^{+}$ macrophages, lactoferrin decreased TNF-α level (*18*). As lactoferrin significantly suppressed the release of inflammatory cytokines from macrophages, we investigated the gene expression of MCP-1, which is involved in macrophage chemotaxis. Lactoferrin intake significantly suppressed the increase in the gene expression of MCP-1 caused by CDAHFD feeding. MCP-1 has been shown to be a migratory factor for macrophages (*19*), suggesting that lactoferrin inhibits macrophage migration. It is also possible that CDAHFD intake causes an imbalance in the intestinal microflora, resulting in increased LPS level and inflammation induced by the activation of Kupffer cells in the liver. Lactoferrin has been reported to improve the imbalance of intestinal microflora (*20*). Although not clarified in the present study, we cannot rule out the possibility that lactoferrin positively affects the intestinal microflora and suppresses the induction of LPS.

In this study, lactoferrin suppressed the increase in plasma AST and ALT levels and histological cell damage caused by CDAHFD feeding, suggesting that lactoferrin also has an effect on hepatocyte cell death. Therefore, we examined the gene expression levels of caspase 3 and p53, which are markers of apoptosis. The results indicated that CDAHFD feeding significantly increased the gene expression of caspase 3 and p53, suggesting the induction of apoptosis in hepatocytes. Lactoferrin intake decreased the gene expression of p53 and significantly suppressed the gene expression of caspase 3. This finding suggests that lactoferrin inhibited the induction of apoptosis in the NASH mouse model used in this study. It has been shown that inflammatory and oxidative stresses are associated with the induction of apoptosis (*21*). NO release is also closely associated with these stresses (*22*). The enzymes neuronal NOS (nNOS), endothelial NOS (eNOS), and iNOS are known to be involved in NO synthesis. Mgbemena *et al*. demonstrated the importance of iNOS in inducing apoptosis *via* oxidative stress in a mouse mode (*23*). Therefore, the gene expression level of iNOS was also examined in this study. The expression of iNOS was significantly higher in the CDSHFD group than in the control group, and this increase was significantly suppressed by lactoferrin intake. These results suggest that lactoferrin suppresses oxidative stress-induced apoptosis induced by CDAHFD feeding. In a study on hepatocellular carcinoma-bearing mice, Abdelmoneem *et al*. showed that lactoferrin inhibited cancer cell growth by suppressing the expression of the transcription factor NF-κB (*24*). As NF-κB expression is known to induce the gene expression of iNOS (*25*), lactoferrin may have suppressed the gene expression of iNOS by suppressing the expression level of NF-κB.

Our results showed that lactoferrin prevented liver injury in the model mice with NASH induced by CDAHFD feeding through anti-inflammatory effect by inhibiting the migration to macrophages and *via* antioxidant stress effects on oxidative stress caused by fat accumulation. However, lactoferrin is known to have multiple functions, and its effects may also involve other immune cells or actions on adipose tissue, which cannot be excluded.

Our study opens up the possibility that lactoferrin could be a new treatment for NASH by reducing the development of lifestyle-related hepatocyte inflammation. Nevertheless, some limitations should be acknowledged. In this study, we focused on the preventive effects of lactoferrin during the early stage of NASH using the CDAHFD model. Previous studies have shown that significant hepatic fibrosis develops after approximately 6 weeks of CDAHFD intake (*6*). Thus, our 14-day experimental period was intended to capture the initial stage of disease progression. However, the pathogenesis of human NASH is more complex and chronic, and whether lactoferrin can suppress long-term progression such as advanced fibrosis or cirrhosis remains to be clarified. This limitation should be addressed in future studies with extended intake periods. Although there are some limitations, our findings suggest that lactoferrin may help prevent the development of NASH, providing a basis for future studies to explore its potential in NASH prevention.

**Acknowledgements**

We thank NRL Pharma for providing the lactoferrin.

*Funding*: None.

*Conflict of Interest*: The authors have no conflicts of interest to disclose.

## References


1. Riazi K, Azhari H, Charette JH, Underwood FE, King JA, Afshar EE, Swain MG, Congly SE, Kaplan GG, Shaheen AA. The prevalence and incidence of NAFLD worldwide: a systematic review and meta-analysis. Lancet Gastroenterol Hepatol. 2022; 7:851-861.
2. Vernon G, Baranova A, Younossi ZM. Systematic review: the epidemiology and natural history of non-alcoholic fatty liver disease and non-alcoholic steatohepatitis in adults: Systematic review: epidemiology of NAFLD and NASH. Aliment Pharmacol Ther. 2011; 34:274-285.
3. Li J, Zou B, Yeo YH, *et al*. Prevalence, incidence, and outcome of non-alcoholic fatty liver disease in Asia, 1999-2019: a systematic review and meta-analysis. Lancet Gastroenterol Hepatol. 2019; 4:389-398.
4. Guo X, Yin X, Liu Z, Wang J. Non-alcoholic fatty liver disease (NAFLD) pathogenesis and natural products for prevention and treatment. Int J Mol Sci. 2022; 23:15489.
5. Terrault NA, Francoz C, Berenguer M, Charlton M, Heimbach J. Liver transplantation 2023: status report, current and future challenges. Clin Gastroenterol Hepatol. 2023; 21:2150-2166.
6. Matsumoto M, Hada N, Sakamaki Y, Uno A, Shiga T, Tanaka C, Ito T, Katsume A, Sudoh M. An improved mouse model that rapidly develops fibrosis in non-alcoholic steatohepatitis. Int J Exp Pathol. 2013; 94:93-103.
7. Vance DE. Role of phosphatidylcholine biosynthesis in the regulation of lipoprotein homeostasis. Curr Opin Lipidol. 2008; 19:229-234.
8. Li Q, Tan Y, Chen S, Xiao X, Zhang M, Wu Q, Dong M. Irisin alleviates LPS-induced liver injury and inflammation through inhibition of NLRP3 inflammasome and NF-κB signaling. J Recept Signal Transduct Res. 2021; 41:294-303.
9. Telang S. Lactoferrin: a critical player in neonatal host defense. Nutrients. 2018; 10:1228.
10. Liang L, Wang ZJ, Ye G, Tang XY, Zhang YY, Kong JX, Du HH. Distribution of lactoferrin is related with dynamics of neutrophils in bacterial infected mice intestine. Molecules. 2020; 25:1496.
11. Nielsen SM, Hansen GH, Danielsen EM. Lactoferrin targets T cells in the small intestine. J Gastroenterol. 2010; 45:1121-1128.
12. Fan F, Shi P, Liu M, Chen H, Tu M, Lu W, Du M. Lactoferrin preserves bone homeostasis by regulating the RANKL/RANK/OPG pathway of osteoimmunology. Food Funct. 2018; 9:2653-2660.
13. Yin H, Cheng L, Holt M, Hail N, Maclaren R, Ju C. Lactoferrin protects against acetaminophen-induced liver injury in mice. Hepatology. 2010; 51:1007-1016.
14. Sugiyama A, Sato A, Takeuchi T. PEGylated lactoferrin enhanced its hepatoprotective effects on acute liver injury induced by carbon tetrachloride in rats. Food Chem Toxicol. 2009; 47:1453-1458.
15. Honma K, Izumo N, Furukawa M, Miyazaki M, Sakurai J, Kuwahara Y, Kagaya S, Hoshino T, Watanabe Y. Effect of lactoferrin on non-alcoholic fatty liver in obese mice. Pharmacometrics. 2019; 96:93-99.
16. Suzuki N, Murakoshi M, Ono T, Morishita S, Koide M, Bae MJ, Totsuka M, Shimizu M, Sugiyama K, Nishino H, Iida N. Effects of enteric-coated lactoferrin tablets containing *Lactobacillus brevis* subsp. *Coagulans* on fecal properties, defecation frequency and intestinal microbiota of Japanese women with a tendency for constipation: a randomized placebo-controlled crossover study. Biosci Microbiota Food Health. 2013; 32:13-21.
17. Ganguly S, Muench GA, Shang L, *et al*. Nonalcoholic steatohepatitis and HCC in a hyperphagic mouse accelerated by Western diet. Cell Mol Gastroenterol Hepatol. 2021; 12:891-920.
18. Hwang S-A, Kruzel ML, Actor JK. Recombinant human lactoferrin modulates human PBMC derived macrophage responses to BCG and LPS. Tuberculosis (Edinb). 2016; 101S:S53-S62.
19. Moreno-Fierros L, García-Hernández AL, Ilhuicatzi-Alvarado D, Rivera-Santiago L, Torres-Martínez M, Rubio-Infante N, Legorreta-Herrera M. Cry1Ac protoxin from *Bacillus thuringiensis* promotes macrophage activation by upregulating CD80 and CD86 and by inducing IL-6, MCP-1 and TNF-α cytokines. Int Immunopharmacol. 2013; 17:1051-1066.
20. Vega-Bautista A, de la Garza M, Carrero JC, Campos-Rodríguez R, Godínez-Victoria M, Drago-Serrano ME. The impact of lactoferrin on the growth of intestinal inhabitant bacteria. Int J Mol Sci. 2019; 20:4707.
21. Shi H, Xu W, Liu Q, Li Y, Dong S, Zhao Z. AKR7A5 knockout promote acute liver injury by inducing inflammatory response, oxidative stress and apoptosis in mice. J Cell Mol Med. 2024; 28:e70129.
22. Ha SK, Chae C. Inducible nitric oxide distribution in the fatty liver of a mouse with high fat diet-induced obesity. Exp Anim. 2010; 59:595-604.
23. Mgbemena V, Segovia J, Chang TH, Bose S. KLF6 and iNOS regulates apoptosis during respiratory syncytial virus infection. Cell Immunol. 2013; 283:1-7.
24. Abdelmoneem MA, Elnaggar MA, Hammady RS, Kamel SM, Helmy MW, Abdulkader MA, Zaky A, Fang JY, Elkhodairy KA, Elzoghby AO. Dual-targeted lactoferrin shell-oily core nanocapsules for synergistic targeted/herbal therapy of hepatocellular carcinoma. ACS Appl Mater Interfaces. 2019; 11:26731-26744.
25. Surh YJ, Chun KS, Cha HH, Han SS, Keum YS, Park KK, Lee SS. Molecular mechanisms underlying chemopreventive activities of anti-inflammatory phytochemicals: down-regulation of COX-2 and iNOS through suppression of NF-kappa B activation. Mutat Res. 2001; 480-481:243-268.


Received June 2, 2025; Revised August 17, 2025; Accepted August 19, 2025.

**Address correspondence to:*
Nobuo Izumo, Laboratory of Pharmacotherapy, Yokohama University of Pharmacy, 601 Matano-cho, Totsuka-ku, Yokohama, Kanagawa 245-0066, Japan.
E-mail: n.izumo@hamayaku.ac.jp

Released online in J-STAGE as advance publication August 26, 2025.

*Original Article*

DOI: 10.5582/ddt.2025.01061

# Piezo1 mediates calcium ion influx, glucose transporter 4 translocation, and glucose uptake in adipocytes under low-frequency vibration

**Dazhuang Huang[1,2], Daijiro Haba[3,4], Sanai Tomida[1,2], Chihiro Takizawa[1], Qi Qin[1], Yukie Kataoka[1], Yuko Mugita[1,2], Hiromi Sanada[5], Gojiro Nakagami[1,4,*]**

[1] Department of Gerontological Nursing/Wound Care Management, Graduate School of Medicine, The University of Tokyo, Tokyo, Japan;
[2] Department of Next-generation Wound Care Innovation, Graduate School of Medicine, The University of Tokyo, Tokyo, Japan;
[3] Department of Well-being Nursing, Graduate School of Nursing, Ishikawa Prefectural Nursing University, Ishikawa, Japan;
[4] Global Nursing Research Center, Graduate School of Medicine, The University of Tokyo, Tokyo, Japan;
[5] Ishikawa Prefectural Nursing University, Ishikawa, Japan.

**SUMMARY**: Diabetic foot ulcers (DFUs) are associated with a high risk of amputation and mortality, necessitating effective wound-healing interventions. Low-frequency vibration (LFV) therapy promotes wound healing by increasing glucose metabolism; however, the mechanisms underlying the effects of LFV on glucose metabolism remain unclear. This study aimed to investigate the role of Piezo1 in glucose uptake induced by LFV in adipocytes. 3T3-L1 adipocytes were subjected to LFV (52 Hz, 600–1,000 mVpp, and 40 min/day) for five days. Cells were divided into non-LFV and LFV groups, both with or without the Piezo1 inhibitor, which was evaluated for intracellular ($Ca^{2+}$) fluorescence intensity, glucose transporter 4 (GLUT4) localization, and glucose uptake. The increased intracellular $Ca^{2+}$ fluorescence intensity induced by LFV was significantly attenuated when combined with Piezo1 inhibitor ($p < 0.0001$). LFV-induced GLUT4 translocation to the plasma membrane was canceled, and glucose uptake was significantly decreased in the LFV group treated with Piezo1 inhibitor ($p < 0.001$) compared to the LFV group without Piezo1 inhibitor. The activation of Piezo1 by LFV may lead to a cascade involving $Ca^{2+}$ influx, GLUT4 translocation, and increased glucose uptake. These findings suggest that Piezo1 plays a critical role in promoting the glucose uptake induced by LFV in adipocytes.

***Keywords***: Diabetic foot ulcers, GLUT4, glycometabolism, hard-to-heal wounds, mechanosensors

## 1. Introduction

The prevalence of diabetes is substantially increasing, driven by lifestyle and social changes (*1*). According to the International Diabetes Federation, the number of people with diabetes was 537 million in 2021, equating to one in every ten adults (*2*). Diabetes is an incurable metabolic disorder characterized by chronic hyperglycemia, which is due to insulin resistance, severely impacting people's quality of life and placing growing economic and medical burdens on society, particularly in those with aging populations (*3-5*). Prolonged hyperglycemia causes extensive cellular damage, leading to complications such as retinopathy, nephropathy, and neuropathy. DFUs are a particularly debilitating complication associated with underlying neuropathy and vascular damage; DFUs are challenging to treat effectively (*6,7*). The estimated lifetime cumulative incidence of DFUs among people with diabetes is 19–34%, with an annual incidence of approximately 2% worldwide (*8*). Recurrence rates within one year of healing are 30–40% (*9*).

The current treatments for DFUs include exercise, pharmacotherapy, dietary interventions, and glycemic control (*10-12*). However, maintaining glycemic control poses significant challenges, and poor patient adherence to treatment often leads to treatment failure and hard-to-heal wounds. Chronic hyperglycemia-induced vascular damage reduces the flow of blood to wounds, impairing the healing of DFUs (*5*). Therefore, promoting blood flow and restoring circulation are critical for effective DFU management.

Local low-frequency vibration (LFV) is a novel non-invasive wound care for enhancing blood circulation and promoting wound healing. Local LFV has been shown to increase blood flow through nitric oxide (NO)-mediated vasodilation and has been used to effectively treat full-thickness wounds in animal studies (*13-15*). Although

NO synthesis is impaired under diabetic conditions due to chronic hyperglycemia (*6*), clinical research has validated that vibration devices placed under mattresses facilitate the healing of DFUs (*16*). In our previous study, we found that LFV benefits the wound healing of DFUs by increasing local glucose metabolism *via* the AMP-activated protein kinase (AMPK)-mediated translocation of GLUT4 to the plasma membrane, thereby promoting wound healing under high-glucose conditions (*17,18*). However, the precise mechanisms underlying the LFV-induced enhancement in glucose uptake remain unclear. Identifying these molecular pathways is critical for optimizing LFV application in DFU treatment and minimizing its potential adverse effects. A deeper understanding of these mechanisms is essential for advancing the implementation of LFV as a therapeutic measure.

In our previous study, we found that the promotion of glucose uptake induced by LFV was closely associated with the influx of $Ca^{2+}$ (*19*). The $Ca^{2+}$ influx induced by mechanical stress is typically mediated by mechanosensors. Mechanosensors are specialized cellular structures or proteins that detect mechanical stimuli, such as vibration, pressure, stretch, or shear stress. Mechanosensors convert these physical forces into biochemical or electrical signals (*20*), playing critical roles in enabling cells and tissues to respond to changes in their mechanical environment. Piezo1 is a mechanosensitive ion channel; a type of protein embedded in cell membranes, that plays a key role in detecting and responding to mechanical stimuli such as vibration (*21*). Piezo1 opens its channels when activated by these forces to allow the influx of positively charged ions such as $Ca^{2+}$ into the cell (*22*). Based on these findings, the following hypothesis was considered: the promotion of glucose uptake induced by vibration would be associated with the activation of Piezo1.

As such, the aim of this study was to elucidate the role of Piezo1 in promoting the LFV-induced glucose uptake in adipocytes, thereby clarifying the molecular mechanisms through which vibration therapy facilitates the healing of DFUs.

## 2. Materials and Methods

### 2.1. Cell culture

The 3T3-L1 cells were obtained from the Japanese Collection of Research Resources Cell Bank (Osaka, Japan). The cells were seeded in a culture plate or chamber slide and cultured in low-glucose Dulbecco's modified Eagle's medium (DMEM; FUJIFILM Wako Pure Chemical Corporation, Osaka, Japan) supplemented with 10% (v/v) heat-inactivated fetal bovine serum (FBS; Cytiva, Marlborough, MA, USA) and 5% (v/v) penicillin-streptomycin (PS) solution (Nacalai Tesque, Kyoto, Japan) until confluence was reached (day 0). After reaching confluence, the cells were cultured for three days in low-glucose DMEM containing 10% FBS, 5% PS, 10 μg/mL insulin (FUJIFILM Wako Pure Chemical Corporation), 1 μM dexamethasone (FUJIFILM Wako Pure Chemical Corporation), and 0.5 mM 3-isobutyl-1-methylxanthine (FUJIFILM Wako Pure Chemical Corporation) (day 3). Subsequently, the cells were maintained in low-glucose DMEM with 10% FBS, 5% PS, and 10 μg/mL insulin for an additional three days (day 6). Finally, the cells were transferred to high-glucose DMEM containing 10% FBS and cultured for two more days (day 8). Fully differentiated 3T3-L1 adipocytes (day 9–13) were used in the experiments.

### 2.2. Adipogenesis assay using oil red O staining

Oil Red O staining was performed to confirm that the differentiation of the adipocytes was successful. This staining method, which is commonly used to evaluate adipocyte differentiation, selectively stains the lipid droplets within cells. The amount of dye extracted from the stained droplets correlates with the volume of accumulated lipids. The treated adipocytes were fixed in 10% formalin, and intracellular lipid droplets were stained using an Oil Red O Stain Kit (Cosmo Bio, Tokyo, Japan). Staining and dye extraction assays were performed according to the manufacturer's instructions. Observations were conducted using a bright-field microscope (Leica CTR 4000, Leica Microsystems, Wetzlar, Germany), and the absorbance of the extracted dye was measured at 540 nm using a plate reader (SpectraMax iD3, Molecular Devices, San Jose, CA, USA).

### 2.3. Real-time reverse-transcription polymerase chain reaction (RT-PCR)

RT-PCR was used to evaluate the gene expression level of *Piezo1* in 3T3-L1 adipocytes. Complementary DNA (cDNA) was synthesized using a high-capacity cDNA Reverse Transcription Kit (Thermo Fisher Scientific, Waltham, MA, USA) with random primers. The target cDNA was amplified using an Mx3000P QPCR System (Agilent Technologies, Santa Clara, CA, USA). *Piezo1* TaqMan® Gene Expression Assay (Mm01241549_m1, Thermo Fisher Scientific) was used. The real-time RT-PCR program was set as follows: 50°C for 2 min, 95°C for 10 min, followed by 50 cycles at 95°C for 15 s, and 60°C for 1 min. All samples were tested in triplicate.

### 2.4. Vibration profiles and experimental set-up

Four groups were designed to verify our hypothesis: an LFV group with and without the Piezo1 inhibitor and a non-LFV group with and without the Piezo1 inhibitor. The vibration settings were as follows: a DC-regulated power supply (AD-8735, A&D, Tokyo, Japan) and

four miniature vibration motors (C1034, SHICOH, Kanagawa, Japan) connected in a parallel circuit were used to generate vibration according to a previous study (*17*). The vibration intensity was changed by adjusting the voltage of the power supply. For LFV groups, LFV was applied at 52 Hz and 600–1,000 mVpp for 40 min per day to the 3T3-L1 adipocytes from day 9 to 13 after differentiation, with the medium and the Piezo1 inhibitor Grammostola spatulata mechanotoxin 4 (GsMTx4; Adooq Bioscience, Irvine, CA, USA) replaced daily (*23*). For with Piezo1 inhibitor groups, GsMTx4 was added to each well 4 h before vibration. For 6-well plates, 10 µL of a 200 µM GsMTx4 solution in 0.9% NaCl was added to each well, and for 96-well plates, 5 µL of a 40 µM GsMTx4 solution in 0.9% NaCl was added to each well. In both cases, the final concentration of GsMTx4 was 1 µM. For groups without Piezo1 inhibitors, the same amount of 0.9% NaCl was added to each well 4 hours before vibration. A 6-well plate, a 96-well plate, or a chamber slide was placed on an oscillator with a rubber foam mat and fixed with bands. LFV was applied to the cells in an incubator at 37°C, transmitting mechanical stimuli to the cells in the medium *via* the plate (Figure 1).

### 2.5. Measurement of intracellular calcium ion levels

To investigate whether vibration stimulation activated the Piezo1 pathway, intracellular $Ca^{2+}$ assays were conducted. The 3T3-L1 cells were seeded into a 96-well culture plate at a density of $1.5 \times 10^4$ cells/well. After differentiation and vibration, the intracellular $Ca^{2+}$ concentrations in the 3T3-L1 adipocytes were measured using a $Ca^{2+}$ Measurement Kit (DOJINDO, Kumamoto, Japan) in all groups. Following the manufacturer's protocol, the intracellular $Ca^{2+}$ concentrations were quantified by measuring the fluorescence intensity using a plate reader with an excitation wavelength of 478 nm and an emission wavelength of 518 nm (SpectraMax iD3, Molecular Devices). The relative fluorescence intensity ratio was calculated by normalizing the fluorescence intensity of non-LFV without GsMTx4 group to 1.

### 2.6. Immunofluorescence staining of GLUT4

The GLUT4 translocation was examined in the fluorescence of GLUT4 following the blockade of the Piezo1 pathway to investigate the relationship between the Piezo1 channel and GLUT4 translocation induced by LFV. The cells were seeded in a chamber slide at a density of $6 \times 10^3$ cells/well. After differentiation and vibration, cells from all groups were fixed with 10% formalin for 30 min and subsequently blocked with 1% bovine serum albumin (BSA)/ phosphate-buffered saline (PBS) for 30 min. The cells were washed six times with PBS and then incubated overnight at 4°C with a GLUT4 primary antibody (1:100; polyclonal rabbit antibody, #NBP1-49533, Novus Biologicals, Littleton, CO, USA). After removing the primary antibody, the cells were washed six times with PBS again and incubated with a secondary antibody, Alexa Fluor® 488 (1:1,000; polyclonal donkey antibody, 711-545-152, Jackson ImmunoResearch, West Grove, PA,

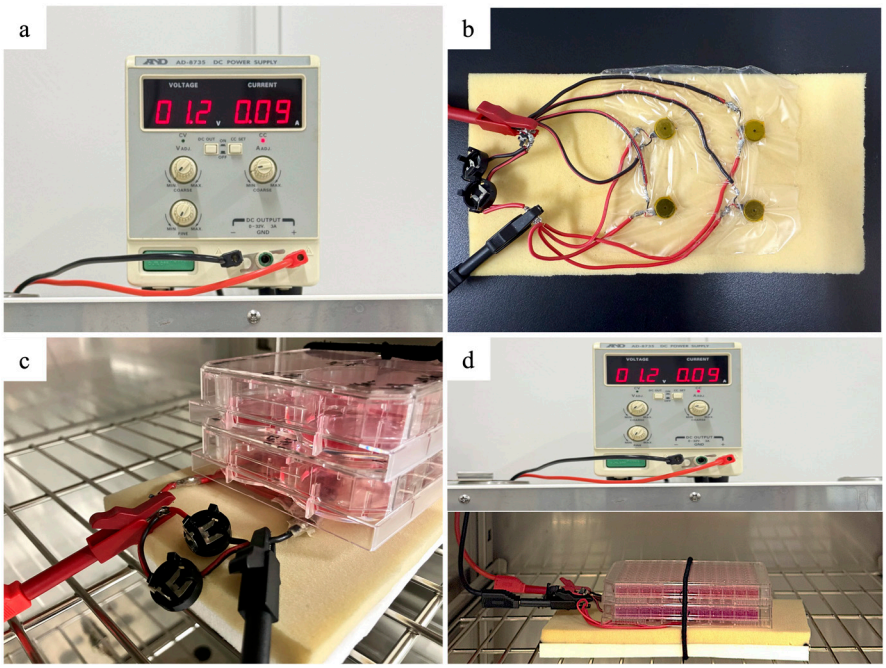


**Figure 1. Vibration experimental set-up. a:** DC-regulated power supply; **b:** four miniature vibration motors connected in a parallel circuit; **c:** the plate was placed on an oscillator with a rubber foam mat and fixed with bands; **d:** LFV was applied to the cells in a dry heat sterilizer at 37°C, transmitting mechanical stimuli to the cells in the medium *via* the plate.

USA) for 1 h, followed by mounting with DAPI (H-1200-10, Vector Laboratories, Newark, NJ, USA). The GLUT4 fluorescence was observed using a fluorescence microscope (BZ-X810, Keyence, Osaka, Japan).

2.7. 2-Deoxy-D-glucose (2-DG) uptake test

We measured 2-DG uptake while blocking the Piezo1 pathway to elucidate the relationship between the Piezo1 channel and the LFV-induced glucose uptake. A 2-DG Uptake Measurement Kit (Cosmo Bio) was used to evaluate the uptake of glucose in the 3T3-L1 adipocytes in all groups. The cells were seeded in a 6-well culture plate at a density of $6 \times 10^4$ cells/well. After differentiation and vibration, adipocytes on day 14 were preincubated in serum-free high-glucose DMEM. 10 µL of a 200 µM GsMTx4 solution in 0.9% NaCl was added to each well GsMTx4 2 h after replacing the medium with serum-free high-glucose DMEM, and then incubated for 4 h. After the total 6-h preincubation, the medium was replaced with 2 mL of Krebs-Ringer phosphate-HEPES buffer (KRPH; 50 mM HEPES, 1.2 mM $KH_2PO_4$, 137 mM NaCl, 4.8 mM KCl, 1.85 mM $CaCl_2$, and 1.3 mM $MgSO_4$, pH 7.4) containing 2% BSA, and GsMTx4 was added again. The non-LFV group remained in the incubator at 37°C, 5% $CO_2$, whereas the LFV group was placed in a dry heat sterilizer at 37°C for vibration. After 20 min of vibration, 2-DG (1 mM) was added to both groups, followed by an additional 20 min of incubation or vibration. The cells were subsequently washed three times with PBS and lysed with 1 mL of Tris/HCl buffer (10 mM, pH 8.0). The lysate was collected into tubes, heated to 80°C for 15 min, and centrifuged at 15,000× *g* for 20 min at 4°C. The supernatant was transferred to a new tube and diluted fivefold. The diluted supernatant was combined with each reaction solution according to the manufacturer's instructions. The absorbance of each sample was measured at 420 nm using a plate reader (SpectraMax iD3, Molecular Devices). 2-DG uptake was calculated using a linear plot of the luminescence signal versus the concentration of authentic 2-DG 6-phosphate (µmol/well). The relative ratio was calculated by normalizing the 2-DG uptake of the non-LFV without GsMTx4 group to 1.

2.8. Statistical analyses

All data were presented as the mean ± standard deviation. The differences in the intracellular $Ca^{2+}$ fluorescence intensity and the absorbance of 2-DG between groups were determined using Tukey's multiple comparison test. Statistical analyses were performed using the R software system (version 4.3.3; R Foundation for Statistical Computing, Vienna, Austria). A *p*-value of less than 0.05 was considered statistically significant.

## 3. Results

3.1. Piezo1 gene expression levels

We confirmed the expression levels of the Piezo1 gene in the 3T3-L1 adipocytes using real-time RT-PCR. All samples exhibited threshold cycle values for *Piezo1* below 30, indicating detectable expression.

3.2. Comparison of intracellular $Ca^{2+}$ fluorescence intensity

The relative intracellular $Ca^{2+}$ fluorescence intensity ratio was significantly higher in the LFV group than in the non-LFV group ($p < 0.0001$). The intracellular $Ca^{2+}$ was significantly lower in the LFV group treated with GsMTx4 than in the LFV group without GsMTx4 ($p < 0.0001$), while the non-LFV group treated with GsMTx4 had no significant difference ($p = 0.590$) (Figure 2).

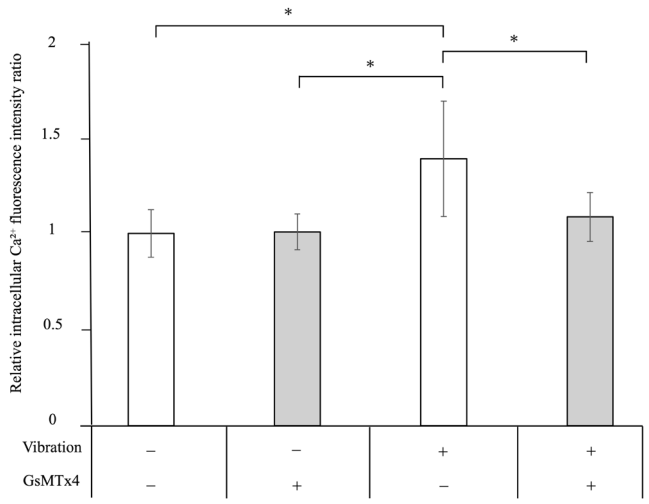


**Figure 2. Relative intracellular $Ca^{2+}$ fluorescence intensity ratio under the tested conditions.** $n = 18$, *$p < 0.0001$, Tukey's multiple comparison test, means ± standard deviation.

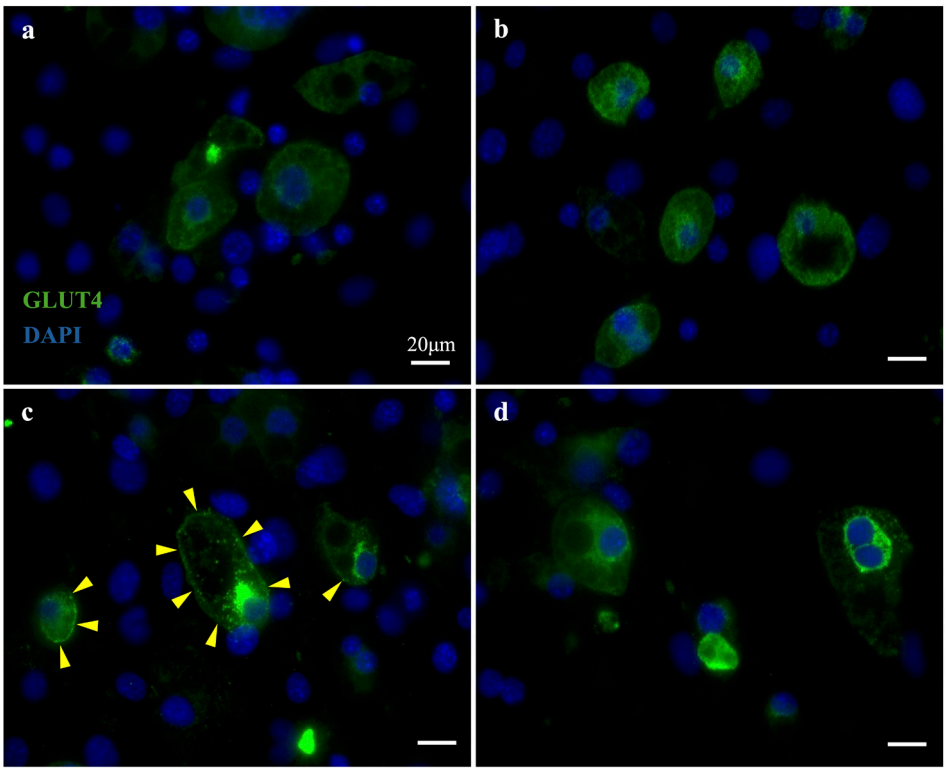


**Figure 3. GLUT4 immunofluorescence under the tested conditions.** The immunofluorescence staining of GLUT4 under the following conditions: non-LFV groups without GsMTx4 **(a)** and with GsMTx4 **(b)**; LFV groups without GsMTx4 **(c)** and with GsMTx4 **(d)**. In the LFV groups without GsMTx4 (c), the GLUT4 fluorescence was enhanced in the plasma membrane (yellow arrowheads), indicating GLUT4 translocation from the cytoplasm to the plasma membrane by LFV. Scale bar: 20 μm.

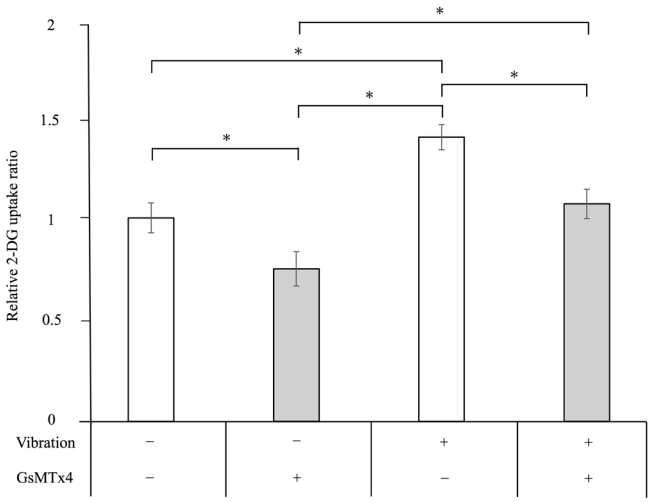


**Figure 4. Relative 2-DG uptake ratio under tested conditions.** 2-DG uptake in each group was measured in the presence or absence of GsMTx4, and the relative ratio was calculated by normalizing the 2-DG uptake of the non-LFV without GsMTx4 group to 1. ($n = 5$, $*p < 0.01$, Tukey's multiple comparison test, means ± standard deviation).

### 3.3. Immunofluorescence of GLUT4 under GsMTx4 staining

GLUT4 immunofluorescence staining was performed on the adipocytes from the non-LFV and LFV groups with or without GsMTx4 treatment. Strong GLUT4 fluorescence was observed to be concentrated on the plasma membrane in the LFV group (Figure 3c) compared to the non-LFV group (Figure 3a). In the LFV group treated with GsMTx4 (Figure 3d), GLUT4 fluorescence on the plasma membrane was not as strong compared to the LFV group without GsMTx4 (Figure 3c).

### 3.4. 2-DG uptake reduced by GsMTx4 treatment

The 2-DG uptake was significantly higher in the LFV group compared to the non-LFV group without GsMTx4 ($p < 0.001$). Moreover, 2-DG uptake was significantly lower

in the LFV group treated with GsMTx4 than in the LFV group without GsMTx4 treatment ($p < 0.001$) However, the 2-DG uptake was also significantly lower in the non-LFV group treated with GsMTx4 compared to the non-LFV group without GsMTx4 ($p < 0.01$) (Figure 4).

## 4. Discussion

To our knowledge, this is the first report on the effects of Piezo1 on glucose uptake induced by LFV in 3T3-L1 adipocytes. The results of this study demonstrated that LFV stimulated intracellular $Ca^{2+}$ influx, promoted GLUT4 translocation to the plasma membrane, and enhanced 2-DG uptake, which was significantly attenuated by the Piezo1 inhibitor, GsMTx4. These results reveal that Piezo1 is the primary mediator of LFV-induced glucose uptake in 3T3-L1 adipocytes. These findings provide new insights into the mechanistic role of Piezo1 in regulating LFV-induced glucose uptake and metabolism in 3T3-L1 adipocytes. Our findings support the advancement of non-invasive vibration therapy for treating DFUs and encourage the implementation of LFV-based wound care to various clinical settings.

Piezo1, a mechanosensitive ion channel, responds to mechanical stimuli by facilitating the influx of cations, particularly $Ca^{2+}$ (*20-22*). $Ca^{2+}$ influx is an activator of AMPK, a critical regulator of glucose uptake, through the calcium/calmodulin-dependent protein kinase kinase β (CaMKKβ) pathway (*24*). In a previous study, Caco-2 cells (epithelial cells) were subjected to mechanical stretch, which activated the CaMKK2-AMPKα signaling pathway (*25*). This finding of LFV-induced $Ca^{2+}$ influx aligns with the finding in other studies, which used different cell types, where Piezo1 activation was found to initiate calcium signaling pathways (*22,26*).

AMPK plays a central role in energy homeostasis *via* facilitating GLUT4 translocation to the plasma membrane under energy stress or mechanical stimulation (*27*). AMPK-mediated GLUT4 translocation occurs through the transient elevation of the intracellular $Ca^{2+}$ levels or an increased AMP-to-ATP ratio (*28*). In this study, LFV-induced GLUT4 translocation to the plasma membrane was observed. Thus, LFV-induced GLUT4 translocation may potentially be due to AMPK activation *via* $Ca^{2+}$ influx.

In skeletal muscle, exercise or whole-body LFV triggers intracellular $Ca^{2+}$ influx, leading to muscle contraction, AMPK activation, and subsequent glucose uptake *via* GLUT4 translocation (*29,30*). This mechanism parallels the findings of our study, where LFV in adipocytes stimulated $Ca^{2+}$ influx, promoted GLUT4 translocation, and enhanced 2-DG uptake, suggesting that LFV-induced glucose uptake is linked to AMPK signaling.

We primarily focused on the Piezo1-mediated glucose uptake induced by LFV; thus, the potential interplay between Piezo1 and AMPK needs further investigation. Piezo1 activation likely initiates calcium influx, which subsequently triggers AMPK activation. This cascade could provide a mechanistic explanation for the GLUT4 translocation and glucose uptake observed during LFV stimulation. Future studies could examine whether Piezo1 directly modulates AMPK activation through calcium influx, CaMKK, or other intermediary pathways, providing a deeper understanding of the molecular mechanisms underlying LFV-induced glucose metabolism.

Despite these promising findings, several limitations should be acknowledged: First, this study relied solely on GsMTx4, a pharmacological inhibitor commonly used to block Piezo1, to assess its role in calcium influx and glucose uptake. While generally regarded as a selective blocker of mechanosensitive ion channels, GsMTx4 may have off-target effects. Notably, GsMTx4 alone, without LFV, reduced 2-DG uptake, suggesting possible actions on other mechanosensitive channels or related pathways. Therefore, these findings cannot confirm Piezo1 as the sole mediator, and future studies using gene knockdown or knockout approaches are needed. Second, this study used only the 3T3-L1 adipocyte cell line, which is widely applied and well-characterized in adipogenesis and glucose uptake research. Although previous studies have shown that LFV enhances glucose uptake in this cell type (*18*), the *in vitro* system does not fully reproduce the complex biological and physiological environment of primary adipocytes or adipose tissue *in vivo*. Validation using primary adipocytes and animal models, particularly those representing diabetic conditions or diabetic foot ulcers, is needed to confirm the present findings and assess their translational relevance. Third, LFV in this study was tested under only one condition (52 Hz, 600–1,000 mVpp), chosen based on a prior report demonstrating wound-healing effects under these parameters (*17*). While this setting elicited biological responses, the narrow parameter range limits understanding of the dose–response relationship for Piezo1 activation and glucose uptake. Systematic testing of different frequencies, amplitudes, and durations is needed to optimize LFV protocols for potential therapeutic applications. Fourth, other mechanosensitive channels, such as members of the transient receptor potential channel family (*e.g.*, TRPV4, TRPC1), are also known to regulate calcium signaling in response to mechanical stimuli (*31,32*). Although our findings are consistent with Piezo1 involvement, the contribution of these alternative pathways cannot be excluded. Future studies using specific inhibitors or genetic ablation of these mechanosensors are needed to clarify whether Piezo1 is the sole or predominant mediator of LFV-induced effects.

By addressing these limitations in future research, we can more precisely delineate the molecular pathways involved in LFV-induced glucose uptake and strengthen

the translational potential of this approach for metabolic and wound-healing applications.

## 5. Conclusions

Piezo1 may contribute to glucose uptake induced by LFV in adipocytes, although the involvement of other mechanosensitive channels cannot be ruled out. The key findings are as follows: (i) LFV-induced $Ca^{2+}$ influx in adipocytes is at least partially associated with Piezo1. (ii) Piezo1 contributes to LFV-induced GLUT4 translocation. (iii) Piezo1 is a potential mediator of LFV-induced glucose uptake. Further studies are needed to clarify the involvement of other mechanosensitive ion channels.

*Funding*: This study was supported by JSPS KAKENHI (grant numbers: 21K18287 and 23H00547) and JST Fusion Oriented Research for Disruptive Science and Technology (FOREST) (grant number: JPMJFR205H).

*Conflict of Interest*: Dazhuang Huang, Sanai Tomida and Yuko Mugita are affiliated with a department funded by Nichiban Co., Ltd.; Daijiro Haba is affiliated with a department funded by Molten Corporation. However, this study was conducted independently and is unrelated to these sponsors.

## References

1. Kolb H, Martin S. Environmental/lifestyle factors in the pathogenesis and prevention of type 2 diabetes. BMC Med. 2017; 15:131.
2. IDF Diabetes Atlas, 10th ed. 2021. https://diabetesatlas.org/ (accessed December 19, 2024).
3. Martinengo L, Olsson M, Bajpai R, Soljak M, Upton Z, Schmidtchen A, Car J, Järbrink K. Prevalence of chronic wounds in the general population: systematic review and meta-analysis of observational studies. Ann Epidemiol. 2019; 29:8-15.
4. Banday MZ, Sameer AS, Nissar S. Pathophysiology of diabetes: an overview. Avicenna J Med. 2020; 10:174-188.
5. Rohm TV, Meier DT, Olefsky JM, Donath MY. Inflammation in obesity, diabetes, and related disorders. Immunity. 2022; 55:31-55.
6. Alavi A, Sibbald RG, Mayer D, Goodman L, Botros M, Armstrong DG, Woo K, Boeni T, Ayello EA, Kirsner RS. Diabetic foot ulcers: Part I. Pathophysiology and prevention. J Am Acad Dermatol. 2014; 70:1.e1-18.
7. Azevedo MM, Lisboa C, Cobrado L, Pina-Vaz C, Rodrigues A. Hard-to-heal wounds, biofilm and wound healing: an intricate interrelationship. Br J Nurs. 2020; 29:S6-S13.
8. Armstrong DG, Boulton AJM, Bus SA. Diabetic foot ulcers and their recurrence. N Engl J Med. 2017; 376:2367-2375.
9. Van Netten JJV, Price PE, Lavery LA, Monteiro-Soares M, Rasmussen A, Jubiz Y, Bus SA. International Working Group on the Diabetic Foot, Prevention of foot ulcers in the at-risk patient with diabetes: a systematic review. Diabetes Metab Res Rev. 2016; 32 (Supplement 1):84-98.
10. Tran MM, Haley MN. Does exercise improve healing of diabetic foot ulcers? A systematic review. J Foot Ankle Res. 2021; 14:19.
11. Basiri R, Spicer M, Levenson C, Ledermann T, Akhavan N, Arjmandi B. Improving dietary intake of essential nutrients can ameliorate inflammation in patients with diabetic foot ulcers. Nutrients. 2022; 14:2393.
12. Hasan R, Firwana B, Elraiyah T, Domecq JP, Prutsky G, Nabhan M, Prokop LJ, Henke P, Tsapas A, Montori VM, Murad MH. A systematic review and meta-analysis of glycemic control for the prevention of diabetic foot syndrome. J Vasc Surg. 2016; 63(Supplement):22S-28S.e2.
13. Nakagami G, Sanada H, Matsui N, Kitagawa A, Yokogawa H, Sekiya N, Ichioka S, Sugama J, Shibata M. Effect of vibration on skin blood flow in an *in vivo* microcirculatory model. BioSci Trends. 2007; 1:161-166.
14. Ichioka S, Yokogawa H, Nakagami G, Sekiya N, Sanada H. *In vivo* analysis of skin microcirculation and the mole of nitric oxide during vibration. Ostomy Wound Manage. 2011; 57:40-47.
15. Sari Y, Sanada H, Minematsu T, Nakagami G, Nagase T, Huang L, Noguchi H, Mori T, Yoshimura K, Sugama J. Vibration inhibits deterioration in rat deep-tissue injury through HIF1-MMP axis. Wound Repair Regen. 2015; 23:386-393.
16. Mahran HG, Helal OF, El-Fiky AAR. Effect of mechanical vibration therapy on healing of foot ulcer in diabetic polyneuropathy patients. J Am Sci. 2013; 9:76-87.
17. Haba D, Ohmiya T, Sekino M, Qin Q, Takizawa C, Tomida S, Minematsu T, Sanada H, Nakagami G. Efficacy of wearable vibration dressings on full-thickness wound healing in a hyperglycemic rat model. Wound Repair Regen. 2023; 31:816-826.
18. Haba D, Nakagami G, Minematsu T, Sanada H. Low-frequency vibration promotes AMPK-mediated glucose uptake in 3T3-L1 adipocytes. Heliyon. 2021; 7:e07897.
19. Haba D, Qin Q, Takizawa C, Tomida S, Minematsu T, Sanada H, Nakagami G. Investigation of ultrasound and low-frequency vibration for glycometabolism promotion in 3T3-L1 adipocytes. Jpn J Electrophysical Agents. 2023; 30:83-92. (in Japanese)
20. Takahashi K, Matsuda Y, Naruse K. Mechanosensitive ion channels. AIMS Biophys. 2016; 3:63-74.
21. Lewis AH, Grandl J. Mechanical sensitivity of Piezo1 ion channels can be tuned by cellular membrane tension. eLife. 2015; 4:e12088.
22. Zhu H, He W, Ye P, Chen J, Wu X, Mu X, Wu Y, Pang H, Han F, Nie X. Piezo1 in skin wound healing and related diseases: mechanotransduction and therapeutic implications. Int Immunopharmacol. 2023; 123:110779.
23. Fei LY, Xu M, Wang HH, Zhong C, Jiang S, Lichtenberger FB, Erdoğan C, Wang H, Bonk JS, Lai EY, Persson PB, Kovács R, Zheng Z, Patzak A, Khedkar PH. Piezo1 mediates vasodilation induced by acute hyperglycemia in mouse renal arteries and microvessels. Hypertension. 2023; 80:1598-1610.
24. Yamashita Y, Jiang H, Okada F, Kitakaze T, Yoshioka Y, Ashida H. Single oral administration of quercetin glycosides prevented acute hyperglycemia by promoting GLUT4 translocation in skeletal muscles through the activation of AMPK in mice. J Clin Biochem Nutr. 2024; 74:37-6.
25. Tao T, Shu Q, Zhao YW, Guo WQ, Wang JT, Shi YH, Jia SQ, Zhai HN, Chen H, Wang CC, Xu GY. Mechanical regulation of lipid and sugar absorption by Piezo1 in

enterocytes. Acta Pharmaceutica Sinica B. 2024; 14:3576-3590.
26. Xie L, Wang XY, Ma YK, Ma H, Shen J, Chen JY, Wang YD, Su SA, Chen KJ, Xu LX, Xie Y, Xiang MX. Piezo1 (piezo-type mechanosensitive ion channel Component 1)-mediated mechanosensation in macrophages impairs perfusion recovery after hindlimb ischemia in mice. Arterioscler Thromb Vasc Biol. 2023; 43:504-518.
27. Bradley H, Shaw CS, Worthington PL, Shepherd SO, Cocks M, Wagenmakers AJM. Quantitative immunofluorescence microscopy of subcellular GLUT4 distribution in human skeletal muscle: effects of endurance and sprint interval 93 training. Physiol Rep. 2014; 2:e12085.
28. Witczak CA, Sharoff CG, Goodyear LJ. AMP-activated protein kinase in skeletal muscle: from structure and localization to its role as a master regulator of cellular metabolism. Cell Mol Life Sci. 2008; 65:3737-3755.
29. Musi N, Hayashi T, Fujii N, Hirshman MF, Witters LA, Goodyear LJ. AMP-activated protein kinase activity and glucose uptake in rat skeletal muscle. Am J Physiol Endocrinol Metab. 2001; 280:E677-E684.
30. Ren Z, Lan Q, Chen Y, Chan YWJ, Mahady GB, Lee SM-Y. Low-magnitude high-frequency vibration decreases body weight gain and increases muscle strength by enhancing the p38 and AMPK pathways in db/db mice. Diabetes Metab Syndr Obes. 2020; 13:979-989.
31. Thodeti CK, Matthews B, Ravi A, Mammoto A, Ghosh K, Bracha AL, Ingber DE. TRPV4 channels mediate cyclic strain-induced endothelial cell reorientation through integrin to integrin signaling. Circ Res. 2009; 104:1123-1130.
32. Maroto R, Raso A, Wood TG, Kurosky A, Martinac B, Hamill OP. TRPC1 forms the stretch-activated cation channel in vertebrate cells. Nat Cell Biol. 2005; 7:179-185.

Received June 30, 2025; Revised August 15, 2025; Accepted August 21, 2025.

**Address correspondence to:*
Gojiro Nakagami, Department of Gerontological Nursing/ Wound Care Management, Graduate School of Medicine, The University of Tokyo, 7-3-1 Hongo, Bunkyo-Ku, Tokyo 113-0033, Japan.
E-mail: gojiron@g.ecc.u-tokyo.ac.jp

Released online in J-STAGE as advance publication August 28, 2025.

*Original Article*

DOI: 10.5582/ddt.2025.01066

# Evaluation of electrospun composite biomaterial and porcine small intestine submucosa patch in open inguinal herniorrhaphy: A prospective, randomized, single-blind, controlled, multicenter, 72-month clinical study

**Zhiying Qiu[1,§], Liang Fang[1,§], Shaojie Li[2], Jianxiong Tang[2], Yun Pang[1], Jing Wang[3,4], Jing Zhou[5], Ling Wang[6,7,*], Lin Chen[1,*]**

[1] Department of Ultrasonic Diagnosis, Huadong Hospital Affiliated to Fudan University, Shanghai, China;
[2] Department of General Surgery, Huadong Hospital Affiliated to Fudan University, Shanghai, China;
[3] Guizhou University of Traditional Chinese Medicine, Guiyang, Guizhou, China;
[4] Hainan Women and Children's Medical Center, Haikou, Hainan, China;
[5] Department of Obstetrics and Gynecology, Nanfang Hospital, Southern Medical University, Guangzhou, Guangdong, China;
[6] Department of Obstetrics and Reproductive Immunology, Shanghai East Hospital, Tongji University School of Medicine, Shanghai, China;
[7] Department of Obstetrics, The First Affiliated Hospital, Guizhou University of Traditional Chinese Medicine, Guiyang, China.

**SUMMARY**: The aim of this study was to compare postoperative complications and long-term clinical efficacy of electrospun composite biomaterial and porcine small intestine submucosa (SIS) patch in open inguinal herniorrhaphy. A prospective, randomized, single-blind, controlled, multicenter study was used to select 172 patients with inguinal hernia who met the inclusion criteria in 3 hospitals. All participants were randomly assigned (1:1) and treated by open inguinal herniorrhaphy. The experimental group used electrospun composite biomaterial patch and the control group used SIS patch. Complications were assessed by ultrasonic volume auto-scan (UVAS) at 6, 33 and 72 months after operation. The results showed that 53 cases were found to be positive by UVAS, including 20 cases of encapsulated effusion (12.74%), 11 cases of soft tissue edema (6.40%), 4 cases of recurrence (3.01%), 2 cases of testicular ischemic atrophy (1.50%), 7 cases of testicular hydrocele (5.26%), 6 cases of varicocele (4.51%), 2 cases of spermatic cord cyst (1.27%) and 1 case of epididymal head cyst (0.64%). At 33-month follow-up, 2 cases recurred in the control group (2/79, 2.53%) while none in the experimental group (0/78) (the 95% CI difference in effective rates between the two groups was -0.93% to 6.00%, within the preset non-degradation range of Δ10%). At 72-month follow-up, there were 4 cases of recurrence in the control group (4/59, 6.78%), while none in the experimental group (0/60) (the lower limit of 95% CI difference in effective rates between the two groups was 0.27% > 0). The main clinical efficacy of the experimental group was better than that of the control group. There was no statistical difference in the secondary efficacy between the two groups. The postoperative safety evaluation effect of the two groups was the same. Long-term follow-up with UVAS after operation showed that the main clinical efficacy of electrospun composite biomaterial applied in this procedure was superior to that of SIS patch, and there was no significant difference in the secondary efficacy between the two biological patches.

***Keywords***: biological patch, tension-free inguinal herniorrhaphy, postoperative complications, ultrasonic volume auto-scan

## 1. Introduction

Inguinal hernia is a common surgical disease, and surgical treatment is the preferred method for treating inguinal hernia. In the past 30 years, the tension-free repair technology using repair patches has become very mature and has basically replaced traditional tissue suturing techniques. Traditional patch is usually made of polypropylene. Although it has been widely used in clinic, the incidence of postoperative chronic pain is as high as 10%~12% due to its non-absorbable characteristics (*1-3*), and more than 25% of patients' daily activities and weight-bearing functions are restricted, which affects their quality of life (*4-6*).

In recent years, the material science has developed rapidly. Biological repair materials such as porcine small

intestinal submucosa (SIS) patch, electrospun composite biomaterial and porcine basement membrane patch have been accepted by surgeons and are gradually used in inguinal and incisional herniorrhaphy. Compared with traditional synthetic patches, biological patches have significant advantages such as good biocompatibility, no excess scar tissue, no long-term chronic inflammation, and light tissue adhesion, which can effectively reduce the risk of long-term complications after adult open inguinal herniorrhaphy (*7-8*). Its degradability effectively increases the compliance of the abdominal wall and the postoperative comfort of patients, which can significantly improve the quality of patients' postoperative life and protect their fertility (*9*). Of course, the use of biological patches in herniorrhaphy may also result in postoperative complications such as encapsulated fluid accumulation or recurrence. The current guidelines for the treatment of adult inguinal hernia do not provide detailed recommendations for the comparison and selection of different types of biological patches.

This study compared the use of two different biomaterials in adult inguinal hernia repair surgery, diagnosed postoperative complications through ultrasonic volume auto-scan (UVAS), and explored the mid to long term clinical efficacy of using biomaterials in open tension-free inguinal herniorrhaphy.

## 2. Methods

### 2.1. Ethical statement

This study was approved by the Clinical Research Ethics Committee of the local hospital and was retrospectively registered in 2017 (ChiCTRINR-17010723).

### 2.2. Participants

From July 2014 to March 2015, patients with unilateral inguinal hernia were recruited from Huadong Hospital, Shanghai Tenth People's Hospital and Shanghai Putuo Hospital. All subjects in the study, who were Han adult man, participated voluntarily and signed informed consent forms.

The subjects aged 18-79 years who had a unilateral primary inguinal hernia with American Society of Anesthesiology grade I-III, were eligible for this study. According to the Chinese classification of groin hernia recommended by the Committee of Hernia and Abdominal Wall Surgeons of the Chinese College of Surgeons, inguinal hernia can be divided into type I-III. Exclusion criteria were: bilateral hernia, recurrent hernia or incarcerated hernia; patients who were allergic to anti-adhesive film; patients with contraindications to surgery, such as serious cardiopulmonary disease, coagulation dysfunction, and abnormal liver and kidney function; patients with previous reproductive dysfunction or undergoing genitourinary surgery that may affect reproductive function; patients with malignant tumors whose life expectancy were less than 6 months; patients with mental and neurological illness who were noncompliant with their doctors.

### 2.3. Study design and procedures

According to one published study, the recurrence rate of SIS patch was 4.9% (*10*). So, 5% was used as the established recurrence rate in this study. The sample size was based on the main clinical efficacy measure (recurrence rate) and the non-inferiority evaluation formula: $n = [(Z1-\alpha/2+Z1-\beta)/(PT-PC-\delta)]2\times[PT(1-PT)+PC(1-PC)]$, $\alpha = 0.025$, $\beta = 0.10$, non-inferiority threshold $\delta = 10\%$, the required number of cases in each group was 75. Assuming that the exclusion rate was 10% and the recurrence rate of the experimental group was similar to that of the control group, the sample size was 86 cases in each group, a total of 172 cases.

In this randomized, single blind, controlled, multi-center study, 172 subjects selected from three hospitals were randomly assigned to the experimental group and control group according to a ratio of 1:1. The experimental group was treated with electrospun composite biomaterial patch (P[LLA-CL]/fibrinogen patch; Shanghai Pine&Power Biotech Co., Ltd., China), while the control group was treated with SIS patch (Biodesign Surgisis; Cook Biotech Inc., USA). Both groups used a custom-made patch of the same size (6 × 14cm). The surgical method of open tension-free inguinal herniorrhaphy was technique of abdominal wall reinforcement with biological mesh (*11*). All participating surgeons were invited to participate in a specific training course organized by the Training Center of Huadong Hospital of Fudan University to ensure that they used the same standard techniques in this study. Only the surgeon performing the operation was aware of the assignment. Patients, investigators, and other researchers were blind to the allocation information throughout the entire study.

Siemens Acuson S3000 UVAS, with probe model 14L5BV and 1 mm scan spacing, was used to examine the surgical incision, chronic pain site and scrotum of the patient at 6, 33 and 72 months postoperative. A single scan captured ultrasonic volume images of a 15.4 cm (length) × 16.8 cm (width) × 6.0 cm (depth) area. Positive ultrasound diagnoses after operation, all of whom were confirmed by puncture, surgery or other imaging examinations, included encapsulated effusion, soft tissue edema, recurrent hernia, hydrocele of testis, atrophy of testis, varicocele, *etc*. Negative ultrasound diagnostic criteria after surgery were: good peritoneal continuity in the repair area, flat patch, no hydrops in the preperitoneal space, free movement of spermatic cord at the reconstructed inner ring and no abnormal echo in the ipsilateral spermatic cord and scrotum.

Simple verbal scale (SVS) and visual analogue scale (VAS) questionnaires were administered to assess

patients' pain at rest and cough at each follow-up period. SVS included 5 grades: none, mild, moderate, severe and intolerable. VAS used a 100 mm straight line without numbers, scales or words. The left end of the line (0 mm) represented no pain. The right end (100 mm) represented maximum pain. The middle part indicated different levels of pain. Let the patient make a mark on the horizontal line to indicate the level of pain.

Activities of daily living (ADL) questionnaire was used to assess the patients' quality of life at each follow-up period (*12*). ADL was scored by the Barthel index (*13*) during daily work, strolling, jogging, sexual life and weight-bearing exercise. There were four level of 100 points. Level 0: ability intact, 100 points. Level 1: mild dependence, 61-99 points. Level 2: moderate dependence, 45-60 points. Level 3: heavy dependence, ≤ 40 points.

2.4. Curative effect evaluation

The primary clinical efficacy was determined by effective rate and recurrence rate at 6, 33 and 72 months after surgery. Effective rate = 1 - recurrence rate. Recurrence rate = Recurrence cases/total study cases × 100%. The secondary efficacy at each follow-up period was evaluated based on other positive ultrasound diagnoses, SVS and VAS scores and ADL scores. The postoperative safety was judged according to serious complications such as incision infection, patch infection and bladder injury.

2.5. Statistical analysis

PASS 22.0 was used for statistical analysis. Count data were described by composition ratio. The independent *t*-test was used for inter group comparison of normally distributed measurement data, and Wilcoxon rank sum test was used to compare numerical data with a non-normally distributed. The non-inferiority test and superiority test of two groups were conducted for the main evaluation indexes, and the non-inferiority margin was -10%. The comparison between enumeration data was conducted by the chi square test or Fisher's exact test.

## 3. Results

3.1. Comparison of the basic characteristics of the two groups

One hundred and seventy-two patients with inguinal hernia who met the inclusion criteria were selected in this study. There were 86 cases in the experimental group and the control group. No cases were lost at the 6-month follow-up after surgery. The total number of patients was 157 at the 33-month follow-up, including 8 cases lost in the experimental group and 7 cases lost in the control group. At the 72nd month, 133 people completed follow-up, including 12 cases lost in both the experimental group and the control group. Among these lost cases, 5 cases withdrew consents due to patients' own choices, 22 cases had insufficient data or missing examinations, 2 cases had colon mass lesions, 1 case had pancreatitis, 1 case had fever, 1 case had myocarditis, and 1 case had lung mass lesions. 6 cases were lost for unknown reasons. There was no statistical significance in the comparison of basic characteristic data between the two groups ($P > 0.05$, Table 1).

3.2. Postoperative complications diagnosed by UVAS

During 72 months after operation, 53 positive ultrasound diagnoses were found, including 4 cases (3.01%) of recurrent hernia, 20 cases (12.74%) of encapsulated

**Table 1. Comparison of basic characteristics of 172 enrolled patients**

| Variable | | Experimental group ($n$ = 86) | Control group ($n$ = 86) | $P$ |
|---|---|---|---|---|
| Cases in each center | Huadong Hospital | 40 | 40 | > 0.05 |
| | Shanghai Putuo Hospital | 11 | 13 | > 0.05 |
| | Shanghai Tenth People's Hospital | 15 | 13 | > 0.05 |
| Age (years) | | 58.15 ± 12.61 | 57.20 ± 13.44 | > 0.05 |
| gender | male | 86 (100.00%) | 86 (100.00%) | > 0.05 |
| Height (cm) | | 170.87 ± 5.44 | 171.61 ± 6.04 | > 0.05 |
| Weight (kg) | | 68.25 ± 9.70 | 68.25 ± 9.03 | > 0.05 |
| BMI (kg/m$^2$) | | 23.33 ± 2.78 | 23.15 ± 2.61 | > 0.05 |
| Marital status | Be married | 78 (90.69%) | 79 (91.86%) | > 0.05 |
| | Unmarried | 8 (9.30%) | 7 (8.13%) | > 0.05 |
| Job | Physical work | 23 (26.74%) | 26 (30.23%) | > 0.05 |
| | Non-physical work | 63 (73.25%) | 60 (69.76%) | > 0.05 |
| Inguinal hernia classification (case/%) | Type I | 26 (30.23) | 23 (26.74) | > 0.05 |
| | Type II | 53 (61.63) | 57 (66.28) | > 0.05 |
| | Type III | 7 (8.23) | 6 (6.98) | > 0.05 |
| Preoperative ASA grade assessment (case/%) | Grade I | 45 (52.33) | 46 (53.49) | > 0.05 |
| | Grade II | 40 (46.51) | 39 (45.35) | > 0.05 |
| | Grade III | 1 (1.16) | 1 (1.16) | > 0.05 |

effusion in the surgical area (Figure 1), 11 cases (6.40%) of soft tissue edema, 2 cases (1.50%) of ischemic shrinkage in testis (Figure 2), 7 cases (5.26%) of hydrocele, 6 cases (4.51%) of varicocele, 2 cases (1.27%) of spermatic cyst and 1 case (0.64%) of epididymal head cyst. There was no significant difference in positive ultrasound diagnosis between the two groups in each follow-up period ($P > 0.05$).

3.3. Analysis of the primary clinical efficacy of the two groups

According to the Clopper-Pearson method, the lower limit of the 95% confidence interval (CI) for the difference of effective rate between the two groups was -0.93% at 33 months and 0.27% at 72 months after surgery. When the lower limit of the difference was greater than the pre-set non-inferior cut-off value (-10%), the invalid hypothesis was rejected. Therefore, the efficacy of the experimental group at both 33 and 72 months after inguinal herniorrhaphy was not worse than that of the control group. Based on the superiority test, when the lower limit of the 95% CI for the efficiency difference between the two groups, which was 0.27% at 72 months after surgery, was greater than 0, the effective

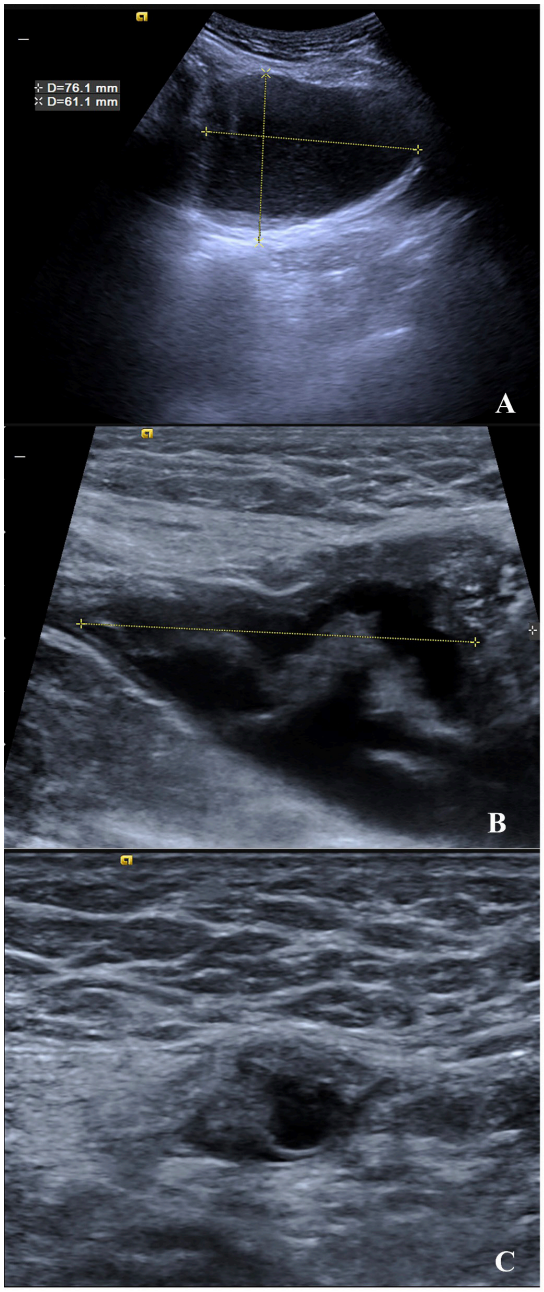


**Figure 1. The encapsulated effusion caused by the degradation of the biological patch in the same patient at 6 (part A), 18(part B), and 33(part C) months after surgery.**

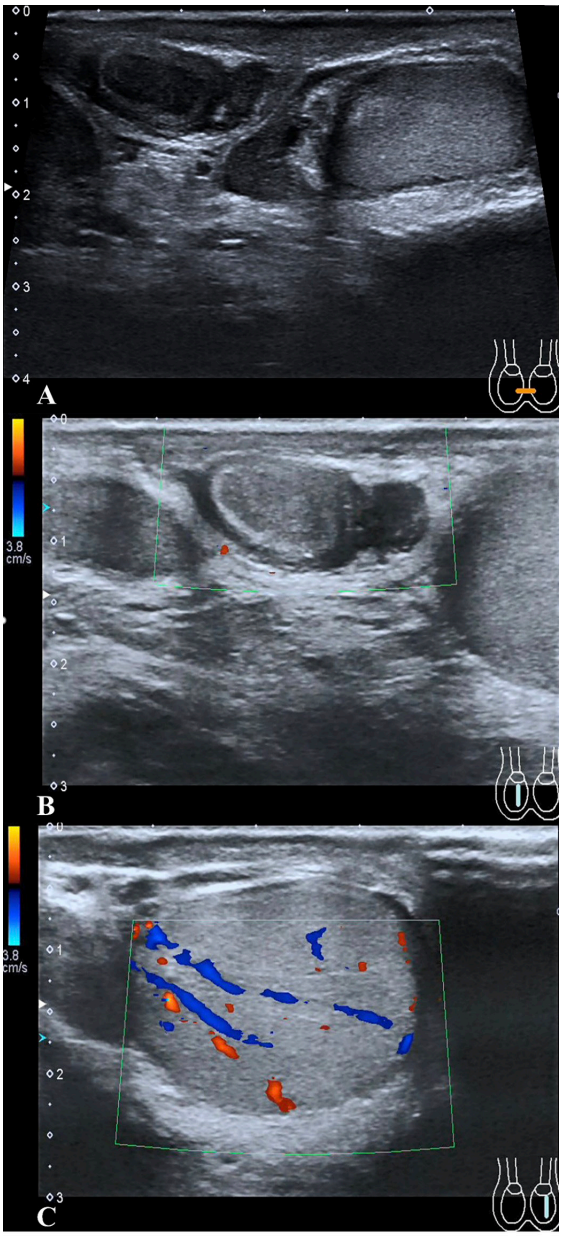


**Figure 2. The comparison between the right testicular ischemic shrinkage and the left normal testis.** Part A: the comparative image of testes on both sides. Part B: no color blood flow signal in the right reduced testis. Part C: color blood flow signal in the left normal testis.

rate of the experimental group was better than that of the control group. Therefore, the efficacy of the experimental group at 72 months after inguinal herniorrhaphy was better than that of the control group (Table 2).

### 3.4. Comparison of the secondary efficacy and the postoperative safety

When the patients' postoperative pain was assessed by SVS and VAS scores, there was no statistical significance in the evaluation of SVS and VAS of resting state and coughing between the two groups during each follow-up period ($P > 0.05$).

We used ADL scores to evaluate the patients' postoperative quality of life, and found that there was no statistical significance between the two groups in the scores of daily work, walking, jogging, riding, sexual life and weight-bearing exercise during each follow-up period ($P > 0.05$). Among all patients, there were significant differences in the ability impairment in jogging, sexual life and weight-bearing exercise compared to that of walking in each follow-up period ($P < 0.05$). The incidence of moderate and severe ability impairment in jogging, sexual life and weight-bearing exercise is higher than that in walking, as shown in Table 3.

No other complications such as patch or incision infection or bladder injury occurred in both two groups, so the safety evaluation effect of the two groups was equal.

## 4. Discussion

The rapid development of materials science has further promoted the research and development of new biological patches and their application in inguinal herniorrhaphy. The clinical application of acellular matrix biological patch was early. Currently, available acellular matrix biological materials include human dermis, porcine small intestinal submucosa, porcine dermis, and fetal bovine pericardium, *etc.* (*14*). It takes homologous or xenogenic skin, intestinal submucosal tissue and other collagen matrix as materials, and uses special methods to retain the collagen fiber network structure of the extracellular matrix as the skeleton, stimulates and induces the patient's own fibroblasts or

**Table 2. Non-inferiority test and superior test of postoperative effective rate of two groups**

| | 33 months follow-up | | | 72months follow-up | | |
|---|---|---|---|---|---|---|
| | Experimental group | Control group | Efficiency difference | Experimental group | Control group | Efficiency difference |
| Case, *n* | 78 | 79 | | 78 | 79 | |
| Recurrence, *n* | 0 | 2 | | 0 | 2 | |
| effective rate (%) | 100 | 97.47 | 2.53 | 100 | 97.47 | 2.53 |
| 95% CI | 95.38-100 | 91.15-99.69 | -0.93-6.00 | 95.38-100 | 91.15-99.69 | -0.93-6.00 |

**Table 3. Comparison of postoperative activities of daily living of all patients in each follow-up period**

| | ADL grade | | | | No such activity | Chi-square test | *P* |
|---|---|---|---|---|---|---|---|
| | 0 | 1 | 2 | 3 | | | |
| 6 months follow-up, *n* | | | | | | | |
| Walking | 162 | 10 | 0 | 0 | 0 | | |
| Daily work | 147 | 11 | 2 | 0 | 12 | 2.345 | 0.3096 |
| Riding | 149 | 9 | 4 | 2 | 8 | 6.409 | 0.0933 |
| Jogging | 137 | 15 | 5 | 2 | 13 | 9.595 | 0.0223 |
| Sexual life | 135 | 9 | 5 | 6 | 17 | 12.658 | 0.0054 |
| Weight-bearing exercise | 131 | 13 | 13 | 8 | 7 | 24.536 | < 0.0001 |
| 33 months follow-up, *n* | | | | | | | |
| Walking | 150 | 7 | 0 | 0 | 0 | | |
| Daily work | 137 | 8 | 0 | 1 | 11 | 1.378 | 0.4999 |
| Riding | 141 | 9 | 1 | 1 | 5 | 2.657 | 0.4476 |
| Jogging | 128 | 11 | 4 | 3 | 11 | 9.828 | 0.0201 |
| Sexual life | 130 | 6 | 2 | 5 | 14 | 8.219 | 0.0417 |
| Weight-bearing exercise | 125 | 8 | 13 | 6 | 5 | 22.274 | 0.0001 |
| 72 months follow-up, *n* | | | | | | | |
| Walking | 127 | 6 | 0 | 0 | 0 | | |
| Daily work | 117 | 6 | 0 | 1 | 9 | 1.096 | 0.5781 |
| Riding | 120 | 8 | 1 | 1 | 3 | 2.45 | 0.4844 |
| Jogging | 106 | 10 | 4 | 3 | 10 | 9.517 | 0.0232 |
| Sexual life | 111 | 4 | 3 | 4 | 11 | 8.016 | 0.0457 |
| Weight-bearing exercise | 101 | 10 | 10 | 7 | 5 | 20.877 | 0.0001 |

collagen to use this skeleton for adhesion and migration (*15*), and constantly repairs and strengthens itself, thus achieving the purpose of repairing peritoneal defects (*16*). At the same time, the material itself can be degraded in the body (*17*).

In recent years, an electrospun composite biomaterial has shown unique advantages in the field of hernia treatment. It is made of fibrinogen and absorbable polymer, using nano electrostatic spinning technology. The material has excellent superhydrophilicity and histocompatibility, which is conducive to the recruitment and adhesion of wound healing factors and regenerated cells. Its stable three-dimensional mesh scaffold structure and large specific surface area can make the new tissue grow in and reshape regeneration while the material degrades. The metabolites are non-toxic, non-allergenic and can be completely degraded and absorbed (*18-19*).

Of course, the biological patch also has some defects. In the ideal state, there is a dynamic balance between biological patch degradation and tissue remodeling. But in fact, when the patch degrades too early, the extracellular matrix cannot maintain local tension in time, which can easily lead to local swelling or even recurrence after surgery (*20*). Some researches found that there were certain similarities in the changes of mechanical properties and degradation processes between electrospun composite biomaterials and SIS patches. After being implanted into dogs, the burst strength of SIS patch and PLCL/Fg patch rapidly decreased within the first two weeks. Subsequently, the biological scaffold gradually remodelled and recovered its strength, maintaining it for at least two years (*21-22*). This early decline in strength load was related to the rapid degradation of the biological scaffold, cell infiltration, and deposition of new host matrix (*23*). Meanwhile, the strength of the host abdominal wall itself also played a very important role in success or recurrence of the early time in repair (*24*). Some studies found that the postoperative recurrence rate of using SIS patch was 4.9% (*25,26*). In our study, the recurrence rate of electrospun composite biomaterial was 0%. However, the compliance of the subjects decreased during the long 6-year period, and the follow-up loss rate of the experimental group was 23.2%. Therefore, it cannot be ruled out that there may be a bias in the lower recurrence rate of the research data. The cross-linking structure greatly increases the mechanical strength of the acellular matrix biological patch. However, if the cross-linking is excessive, chronic inflammatory stimulation will be formed in the long-term degradation process of this collagen fiber network structure, and the proliferation of fiber tissue will far exceed the remodeling of biological scaffold tissue, which ultimately causes postoperative foreign body sensation or chronic pain (*27-29*). Other studies reported that the incidence of chronic pain after biological patch surgery exceeded 4.0% (*30*). In this study, the chronic pain and long-term quality of patients' life using biological patch were preliminarily explored. Chronic pain still affected a small number of patients' jogging, sexual life and weight-bearing exercise after operation. The hyperacute rejection caused by the active surface area of biological patch is an important reason for the seroma after implantation of biological patch (*31*). Some researches showed that the incidence of the seroma after implantation of biological patch was higher than that of synthetic patch (*32-33*). In our study, a patient who used electrospun composite biomaterial patch developed encapsulated hydrops after operation. During the follow-up period, he underwent five punctures, all of which the transparent light-yellow jelly-like substances were extracted. Finally, the hydrops disappeared completely 36 months after operation. For obese patients, the wound is prone to fat liquefaction, and the incidence of hydrops after using biological patches is also high. Therefore, wound healing will be affected and even patch infection may occur (*34*).

The diagnosis rate of various complications after inguinal herniorrhaphy by ultrasonography is as high as 90% (*35*). Ultrasound can display the full anatomical picture from the skin to the abdominal wall, clearly observe the conditions of the patch, peritoneum, and surgical area (*36*), and easily diagnose common postoperative complications such as recurrence and fluid accumulation. Meanwhile, ultrasound can also accurately observe the subtle morphological and structural changes such as patch folds, spermatic cord slippage and intestinal adhesion, which can help patients avoid reoperation to find the cause of postoperative chronic pain (*37*). In addition, ultrasonography, due to its advantages of fast operation, good repeatability, no radiation and flexible change of examination position, has a higher diagnostic efficiency than other imaging examinations (such as CT and MRI) for obese patients and recurrent hernias with thick hernia sac wall or small hernia sac (*38*). UVAS plays a complementary role to traditional ultrasound by adding coronal image display on the basis of two-dimensional ultrasound image, providing surgeons with the intuitive surgical visual plane (*39*). Therefore, using ultrasound and UVAS together has important application value in the diagnosis of various postoperative complications of inguinal hernia repair.

## 5. Conclusion

In conclusion, the long-term follow-up of open tension-free inguinal herniorrhaphy with biological patches through UVAS showed that the long-term clinical efficacy of electrospun composite biomaterials applied in this operation was superior to that of SIS patches. There was no significant difference between these two biological patches in chronic pain after surgery and the quality of patient's postoperative life. The postoperative safety of both was equal.

**Acknowledgements**

We thank all patients for their participation and the staff of the Department of Ultrasonic Diagnosis and the Department of Surgery in all participating hospitals (including Huadong Hospital affiliated with Fudan University [Shanghai, China], Tenth People's Hospital affiliated with Tongji University [Shanghai, China] and Putuo Hospital affiliated with Shanghai University of Traditional Chinese Medicine [Shanghai, China]).

*Funding*: This work was supported by a grant from Shanghai Municipal Health Commission (grant No. 202340140 to ZY Qiu), Shanghai Shenkang Hospital Development Center (grant No. SHDC2022CRD021 to SJ Li) and the National Natural Science Foundation of China (grant No. 82374243 to L Wang).

*Conflict of Interest*: The authors have no conflicts of interest to disclose.

**References**

1. Luijendijk RW, Hop WC, van den Tol MP, de Lange DC, Braaksma MM, IJzermans JN, Boelhouwer RU, de Vries BC, Salu MK, Wereldsma JC, BruijninckxCM, Jeekel J. A comparison of suture repair with mesh repair for incisional hernia. N Engl J Med. 2000; 343:392-398.
2. Poobalan AS, Bruce J, Smith WC, King PM, Krukowski ZH, Chambers WA. A Review of Chronic Pain After Inguinal Herniorrhaphy. Clin J Pain. 2003; 19:48-54.
3. Konschake M, Zwierzina M, Moriggl B, Függer R, Mayer F, Brunner W, Schmid T, Chen DC, Fortelny R. The inguinal region revisited: the surgical point of view: An anatomical-surgical mapping and sonographic approach regarding postoperative chronic groin pain following open hernia repair. Hernia. 2020; 24:883-894.
4. Poobalan AS, Bruce J, King PM, Chambers WA, Krukowski ZH, Smith WC. Chronic pain and quality of life following open inguinal hernia repair. Br J Surg. 2001; 88:1122-1126.
5. Rutegård M, Gümüşçü R, Stylianidis G, Nordin P, Nilsson E, Haapamäki MM. Chronic pain, discomfort, quality of life and impact on sex life after open inguinal hernia mesh repair: an expertise-based randomized clinical trial comparing lightweight and heavyweight mesh. Hernia. 2018; 22:411-418.
6. Palmqvist E, Larsson K, Anell A, Hjalmarsson C. Prospective study of pain, quality of life and the economic impact of open inguinal hernia repair. Br J Surg. 2013; 100:1483-1488.
7. Bochicchio GV, Jain A, Mcgonigal K, Turner D, Ilahi O, Reese S, Bochicchio K. Biologic vs Synthetic Inguinal Hernia Repair: 1-Year Results of a Randomized Double-Blinded Trial. J Am Coll Surg. 2014; 218:751-757.
8. Deng MH, Zhong YS, Yan J, Hu KP, Yao ZC, Chen C, Xu GF. An eligible biological allograft patch in tension-free herniorrhaphy of swine. Biosci Trends. 2012; 6:333-339.
9. Li SJ, Tang JX, Li SC. Clinical analysis on the technique of transverse fascia reinforcement with biological mesh in young inguinal hernia patients. Zhongguo Shi Yong Wai Ke Za Zhi. 2019; 39:821-824. (in Chinese)
10. Edelman DS, Hodde JP. Bioactive prosthetic material for treatment of hernias. Surg Technol Int. 2006; 15:104-108.
11. Tang JX, Li SJ, Huang L. The standardization implementation and quality control specification of inguinal hernia surgery in China. Zhongguo Shi Yong Wai Ke Za Zhi. 2018; 38:72-74. (in Chinese)
12. Hao XN, Gu J, Ying XJ, Bo T, Fu W. Social support and care needs of the disabled elderly population: An empirical study based on survey data from Beijing, China. Biosci Trends. 2017; 11:507-515.
13. Yang H, Chen Y, Wang J, Wei H, Chen Y, Jin J. Activities of daily living measurement after ischemic stroke: Rasch analysis of the modified Barthel Index. Medicine (Baltimore). 2021; 100: e24926.
14. Jin CH, Shen YM, Sun L. Safety and effectiveness of a new-type domestic biologic mesh. Zhonghua Shan He Fu Bi Wai Ke Za Zhi. 2019; 13:16-20. (in Chinese)
15. Ansaloni L, Catena F, Coccolini F, Gazzotti F, D'Alessandro L, Pinna AD. Inguinal hernia repair with porcine small intestine submucosa: 3-year follow-up results of a randomized controlled trial of Lichtenstein's repair with polypropylene mesh versus Surgisis Inguinal Hernia Matrix. Am J Surg. 2009; 198:303-312.
16. Mestak O, Matouskova E, Spurkova Z, Benkova K, Vesely P, Mestak J, Molitor M, Pombinho A, Sukop A. Mesenchymal stem cells seeded on cross—linked and noncross—linked acellular porcine dermal scaffolds for long-term full-thickness hernia repair in a small animal model. Artif Organs. 2014; 38:572-529.
17. Du M, Liu W, Cao YL. Current status of the epidermis reconstruction on acellular dermal matrix in clinical use. Zhongguo Kang Fu Yi Xue Za Zhi. 2003; 7:1686-1687. (in Chinese)
18. Li S, Xiao H, Yang L, Hua L, Qiu ZY, Hu X, Ping D, Zheng K, He H, Tang J. Electrospun P(LLA-CL) nanoscale fibrinogen patch vs porcine small intestine submucosa graft repair of inguinal hernia in adults: A randomized, single-blind, controlled, multicenter, non-inferiority trial. J Am Coll Surg. 2019; 229:541-551.
19. Han J, Yang Y, Lu JR, Wang C, Xie Y, Zheng X, Yao Z, Zhang C. Sustained release vancomycin-coated titanium alloy using a novel electrostatic dry powder coating technique may be a potential strategy to reduce implant-related infection. Biosci Trends. 2017; 11:346-354.
20. Chen SY, Dai WG, Chen CQ. Progress of clinical application of biological patch in hernia and abdominal surgery. Zhonghua Shan He Fu Bi Wai Ke Za Zhi. 2018; 12:90-93. (in Chinese)
21. Wu X, Wang Y, Zhu C, Tong X, Yang M, Yang L, Liu Z, Huang W, Wu F, Zong H, Li H, He H. Preclinical animal study and human clinical trial data of co-electrospun poly(l-lactide-cocaprolactone) and fibrinogen mesh for anterior pelvic floor reconstruction. Int J Nanomedicine. 2016; 11:389-397.
22. Badylak S, Kokini K, Tullius B, Whitson B. Strength over time of a resorbable bioscaffold for body wall repair in a dog model. J Surg Res. 2001; 99:282-287.
23. Obermiller FJ, Hodde JP, McAlexander CS, Kokini K, Badylak SF. A comparison of suture retention strengths for three biomaterials. Med Sci Monit. 2004; 10:1-5.
24. Franz MG, Smith PD, Wachtel TL, Wright TE, Kuhn MA, Ko F, Robson MC. Fascial incisions heal faster than skin: a new model of abdominal wall repair. Surgery. 2001; 129:203-208.
25. Edelman DS, Hodde JP. Bioactive prosthetic material for

treatment of hernias. Surg Technol Int. 2006; 15:104-108.
26. Ansaloni L, Catena F, Coccolini F, Gazzotti F, D'Alessandro L, Pinna AD. Inguinal hernia repair with porcine small intestine submucosa: 3-year follow-up results of a randomized controlled trial of Lichtenstein's repair with polypropylene mesh versus Surgisis Inguinal Hernia Matrix. Am J Surg. 2009; 198:303-312.
27. Liu Y, Shen Y, Chen J. Effects of non-woven mesh in preperitoneal tension-free inguinal hernia repair: a retrospective cohort study. Minerva Chir. 2017; 72:311-316.
28. David CS, Goldenberg A. Prospective ultrasonographic study of blood flow and testicular volume in patients submitted to surgical repair of inguinal hernia without using prosthesis. Acta Cir Bras. 2018; 33:268-281.
29. Ma SZ. Some new understanding about biological materials used for hernia and abdominal wall surgery. Zhongguo Shi Yong Wai Ke Za Zhi. 2015; 35:1153-1156. (in Chinese)
30. Li SJ, Tang JX, Xiao HB, Hua L, Huang L, Ping D, Si XK, Hu X, Cai Z. Multi-center study of electrospun composite biomaterial and SIS biological mesh in adult inguinal hernia surgery. Zhonghua Shan He Fu Bi Wai Ke Za Zhi. 2020; 14:336-341. (in Chinese)
31. Qin CF, Shen YM. Application of biodegradable meshes in inguinal hernia repair of adolescents and young adults. Zhonghua Xiao Hua Wai Ke Za Zhi. 2023; 22:1047-1053. (in Chinese)
32. López Cano M, Armengol Carrasco M, Quiles Pórez MT, Arbós Via MA. Biological implants in abdominal wall hernia surgery. Cir Esp. 2013; 91:217-223.
33. Köckerling F, Alam NN, Narang SK, Daniels IR, Smart NJ. Biological meshes for inguinal hernia repair–review of the literature. Front Surg. 2015; 2:48.
34. Wu XP, Ping T, Jin Z, Chen L, Shuai W. Comparative analysis of traditional hernia repair and biological mesh hernia repair on young adults of childbearing age. Zhonghua Shan He Fu Bi Wai Ke Za Zhi. 2018; 12:271-276. (in Chinese)
35. Wei ZH, Tao YY, Hu QL. Application and accuracy analysis of high frequency ultrasound in clinical diagnosis of indirect inguinal hernia. Zhonghua Shan He Fu Bi Wai Ke Za Zhi. 2021; 15:44-47. (in Chinese)
36. Qiu ZY, Chen Y, Chang C. Comparison of Ultrasonic Volume Auto-scan and regular ultrasonography for the diagnostic classification of the hernia. Zhongguo Chao Sheng Yi Xue Za Zhi. 2012; 28:446-449. (in Chinese)
37. Qiu ZY, Chen Y, Tang JX, Chen L. Ultrasonography in diagnosis and analysis of chronic pain following anterior open inguinal herniorrhaphy. BMC Surgery. 2018; 18:28.
38. China Hernia Society, Chinese Hernia College of Surgeons. Guidelines for diagnosis and treatment on the adult groin hernia (2018 edition). Zhonghua Wai Ke Za Zhi. 2018; 56:495-498. (in Chinese)
39. Qiu ZY, Chen Y, Tang JX, Chen G. Value of Auto Ultrasonic Volume Scan in the diagnostic classification of the hernia. Lin Chuang Wai Ke Za Zhi. 2011; 19:5-8. (in Chinese)

Received July 2, 2025; Revised August 18, 2025; Accepted August 23, 2025.

[§]These authors contributed equally to this work.

**Address correspondence to:*
Lin Chen, Department of Ultrasonic Diagnosis, Huadong Hospital Affiliated to Fudan University, 221 West Yanan Road, Shanghai 200040, China.
E-mail: hdchenlin@fudan.edu.cn

Ling Wang, Department of Obstetrics and Reproductive Immunology, Shanghai East Hospital, Tongji University School of Medicine, No. 1800 Yuntai Road, Shanghai 200100, China.
E-mail: dr.wangling@vip.163.com

Released online in J-STAGE as advance publication August 26, 2025.

*Original Article*

DOI: 10.5582/ddt.2025.01044

# Switching from originator infliximab to biosimilar infliximab in Japanese patients with rheumatoid arthritis achieving clinical remission (the IFX-SIRIUS study I): An interventional, multicenter, open-label, single-arm clinical trial with clinical, ultrasound and biomarker assessments

**Toshimasa Shimizu[1,2], Shin-ya Kawashiri[1,3,*], Tomohiro Koga[1], Rieko Kiya[2], Michiko Morita[2], Shohei Kuroda[2], Shigeki Tashiro[2], Shuntaro Sato[2], Hiroshi Yano[2], Tomoyuki Asano[4], Kazuyoshi Saito[5], Tamami Yoshitama[6], Yukitaka Ueki[7], Nobutaka Eiraku[8], Yutaro Yamada[9], Tadashi Okano[10], Yusuke Ushio[11], Hiroaki Dobashi[11], Tetsu Itami[12], Daisuke Tomita[12], Yuji Nozaki[12], Naoki Hosogaya[2], Hiroshi Yamamoto[2], Atsushi Kawakami[1]**

[1] Department of Immunology and Rheumatology, Division of Advanced Preventive Medical Sciences, Naga-saki University Graduate School of Biomedical Sciences, Nagasaki, Japan;
[2] Clinical Research Center, Nagasaki University Hospital, Nagasaki, Japan;
[3] Department of Community Medicine, Division of Advanced Preventive Medical Sciences, Nagasaki University Graduate School of Biomedical Sciences, Nagasaki, Japan;
[4] Department of Rheumatology, Fukushima Medical University School of Medicine, Fukushima, Japan;
[5] Department of Internal Medicine, Tobata General Hospital, Kitakyushu, Japan;
[6] Yoshitama Clinic for Rheumatic Diseases, Kagoshima, Japan;
[7] Department of Rheumatology, Hakujyujikai Sasebo Chuo Hospital, Sasebo, Japan;
[8] Eiraku Internal Medicine Clinic, Kagoshima, Japan;
[9] Department of Orthopedic Surgery, Osaka Metropolitan University Graduate School of Medicine, Osaka, Japan;
[10] Center for Senile Degenerative Disorders (CSDD), Osaka Metropolitan University Graduate School of Medicine, Osaka, Japan;
[11] Division of Rheumatology, Department of Internal Medicine, Kagawa University Hospital, Kagawa, Japan;
[12] Department of Hematology and Rheumatology, Kindai University Faculty of Medicine, Osaka, Japan.

**SUMMARY**: Rheumatoid arthritis (RA) is a systemic inflammatory disease characterized by the presence of autoantibodies, with infliximab (IFX), the first biological disease-modifying anti-rheumatic drug (DMARD) targeting tumor necrosis factor α, significantly improving treatment but prompting the development of cost-effective biosimilar DMARDs due to its high cost. This study aimed to investigate the efficacy and safety of switching from originator to biosimilar IFX, CT-P13, in patients with RA using musculoskeletal ultrasound (MSUS) and clinical disease activity indices. This prospective, open-label, interventional, single-arm clinical trial involved a 24-week follow-up, enrolling patients with RA who had achieved clinical remission during treatment with originator IFX. CT-P13 was switched from the originator IFX with an unchanged dosing regimen for 24 weeks. The study utilized not only clinical disease activity indices but also MSUS and serum cytokines/chemokines. Eighteen patients were evaluated during the study period. From baseline to week 24, two of the 18 patients experienced clinical relapse (11.1% [95% CI: 3.1–32.8]). No changes were observed in the MSUS score, including total grayscale and power Doppler scores, Disease Activity Score 28 (DAS28)-erythrocyte sedimentation rate, DAS28-C-reactive protein, Health Assessment Questionnaire-Disability Index, and van der Heijde-modified total Sharp score from baseline to week 24. Serum levels of multiple cytokines/chemokines showed no apparent changes. Three non-serious adverse events occurred, with no study discontinuations due to adverse events. In conclusion, most RA patients undergoing treatment with originator IFX in clinical remission could safely switch to CT-P13 without an increased risk of relapse, as evidenced by MSUS, clinical indices, and biomarker levels.

***Keywords***: rheumatoid arthritis, biosimilar, CT-P13, musculoskeletal ultrasound, biomarker

## 1. Introduction

Rheumatoid arthritis (RA) is characterized by persistent synovitis, systemic inflammation, and autoantibodies (*1*). Uncontrolled active RA leads to joint damage, dis-ability, reduced quality of life, and comorbidities. Therefore, tight control of disease activity using the treat-to-target strategy is recommended (*2*). Advances in RA treatment, including biological disease-modifying anti-rheumatic drugs (bDMARDs), have improved clinical outcomes, such as achieving clinical remission. Clinicians also aim for imaging and immunological remission (*3*).

RA pathophysiology involves multiple inflammatory cascades, notably the over-production and overexpression of tumor necrosis factor (TNF), which drives synovial inflammation and joint destruction (*1*). Infliximab (IFX), a chimeric monoclonal antibody targeting TNF-α, was the first bDMARD to significantly alter RA's course/prognosis, effectively suppressing disease activity and joint destruction progression (*4-6*). However, the high cost of bDMARDs imposes a significant financial burden, making it difficult for certain patients to begin or maintain these therapies. Consequently, biosimilar DMARDs (bsDMARDs) have emerged as cost-effective alternatives that reduce the economic burden. A "biosimilar" is a biotherapeutic product comparable in quality, safety, and efficacy to a licensed reference biotherapeutic product (*i.e.*, originator).

CT-P13, developed by Celltrion (Incheon, South Korea), was approved in 2014 as the first bsDMARD for RA treatment in Japan (*7*). The biosimilar CT-P13 and originator IFX have been shown to be pharmacokinetically equivalent with comparable efficacy and safety (*7*). Previous studies have reported that switching from originator IFX to CT-P13 maintained clinical efficacy (*8,9*). However, previous research relied on clinical disease activity indices as efficacy endpoints without utilizing high-sensitivity imaging modalities, such as joint musculoskeletal ultrasound (MSUS), to assess disease activity.

MSUS is primarily used to evaluate RA disease activity (*10,11*). MSUS is recommended for its superior visualization of synovial inflammation compared with clinical examination (*10,11*). Employing MSUS to assess therapeutic response can be highly beneficial in clinical practice (*10-13*). MSUS is a non-invasive, objective, cost-effective, and reproducible imaging modality ideal for treatment monitoring (*10,11*). Although clinical remission can be achieved in a relatively large number of patients with RA by introducing bDMARD therapy, residual synovitis detected by MSUS remains at a certain frequency, even in patients who achieve clinical remission (*14,15*). Residual synovitis is an important finding that can predict joint destruction and clinical relapse. Therefore, it is important to accurately evaluate disease activity at the joint level using MSUS, as well as clinical disease activity indices, including subjective parameters.

This study evaluated the impact of switching from originator IFX to CT-P13 using MSUS as well as clinical disease activity indices so that the patients' disease activity could be more accurately assessed.

## 2. Materials and Methods

### 2.1. Study design

This study was a prospective, open-label, interventional, single-arm clinical trial. The study was conducted at the following 19 centers: Nagasaki University Hospital, Asahi General Hospital, Chiba-East Hospital, Eiraku Clinic, Fukushima Medical University Hospital, Hamanomachi Hospital, Japanese Red Cross Nagasaki Genbaku Hospital, Kagawa University Hospital, Kindai University Hospital, University of Miyazaki Hospital, Miyazaki Zenjinkai Hospital, Nagasaki Kita Hospital, Osaka Metropolitan University Hospital, Osaka Medical and Pharmaceutical University Hospital, Sagawa Akira Rheumatology Clinic, Sasebo Chuo Hospital, Tobata General Hospital, Utazu Hospital, and Yoshitama Clinic for Rheumatic Diseases. This study was registered in the Japan Registry of Clinical Trials (*https://jrct.niph.go.jp*) as jRCTs071190030. The study has been approved by the certified review board of Nagasaki University. The reference number was CRB19-010. Written informed consent was provided by patients before enrollment. The study was conducted in accordance with the principles of the Declaration of Helsinki (*16*), the Clinical Trials Act (since February 2019), the Act on the Protection of Personal Information and related regulatory notifications, and this clinical study protocol. The protocol for this study was previously published (*17*).

### 2.2. Patients

The inclusion criteria were (1) age ≥ 20 years, (2) diagnosis of RA based on the American College of Rheumatology (ACR)/European League Against Rheumatism (EULAR) 2010 RA Classification Criteria (*18*); (3) treatment with originator IFX for ≥ 24 weeks and achieving clinical remission defined as a Disease Activity Score 28 (DAS28)-erythrocyte sedimentation rate (ESR) < 2.6 at the last administration of originator IFX and at baseline; and (4) able and willing to give written informed consent and comply with the requirements of the study protocol.

The exclusion criteria were (1) concurrent use of a glucocorticoid equivalent to > 10 mg/day of prednisolone; (2) previous use of a biosimilar for IFX; (3) treatment with a bDMARD other than originator IFX, a bsDMARD, or a Janus kinase (JAK) inhibitor at the baseline visit; (4) a history of infusion reaction due to originator IFX that required medication; (5) treatment with a glucocorticoid or conventional synthetic

DMARDs and changed the dose within 8 weeks prior to the baseline visit; (6) use of a prohibited drug or therapy within 8 weeks prior to the baseline visit; (7) current pregnancy, breastfeeding, or noncompliance with a medically approved contraceptive regimen during and 6 months after the study period; or (8) being considered unsuitable for this study by the investigator.

2.3. Intervention

CT-P13 was administered at the same dose (dose per kg) and the same interval as the originator IFX before switching with an unchanged dosing regimen for 24 weeks. All patients had to continue to take the same doses of methotrexate (MTX) and oral glucocorticoids that they were taking before the switch throughout the study period. During the study period, the following treatments were prohibited: administration of a bDMARD or JAK inhibitor, the concomitant use of an immunosuppressant (azathioprine, cyclophosphamide, or cyclosporine) or oral glucocorticoids equivalent to > 10 mg/day of prednisolone (PSL), intra-articular corticosteroid injections at joints, and non-steroidal anti-inflammatory drugs (NSAIDs) suppositories. During the study period, the dosage of any NSAID could be modified within the range of its approved doses in Japan.

If a patient experienced a clinical relapse, the patient was discontinued from this study. Clinical relapse was defined as (1) a change from the baseline value in the DAS28-ESR (ΔDAS28-ESR) ≥ 1.2 or in the DAS28-ESR ≥ 3.2, and (2) an increase in the DAS28-ESR value due to elevated disease activity of RA, rather than other factors.

2.4. Outcome measurements

The study visits took place at baseline and after 12 and 24 weeks of treatment, respectively. These assessments are shown in Supplementary Figure S1 (*https://www.ddtjournal.com/action/getSupplementalData.php?ID=268*). The clinical assessors were blinded to joint assessments using MSUS.

Clinical disease activity was evaluated by each attending physician (Japan College of Rheumatology [JCR]-certified rheumatologists) based on the values of the DAS28-ESR and DAS28-C-reactive protein (CRP) (*19*). The patients' functional assessment was evaluated using the Health Assessment Questionnaire-Disability Index (HAQ-DI) (*20*).

The participants underwent MSUS imaging at baseline, week 12, and week 24. MSUS examinations for each patient were performed by one of the JCR-certified sonographers, defined as having at least one year of MSUS experience and practical experience with more than 50 cases. A systematic multiplanar grayscale (GS) and power Doppler (PD) examination of each patient's joint was performed using a multifrequency linear transducer (12–24 MHz). PD was used depending on which Doppler modality was the most sensitive on the individual machines. The Doppler settings were adjusted at each hospital according to published recommendations (*21*). There were no changes in the MSUS settings during the study and no software upgrades. Joint synovitis was assessed by MSUS at dorsal views of 22 joints: bilateral wrist joints, 1st–5th metacarpophalangeal (MCP) joints, the interphalangeal (IP) joints, and the 2nd–5th proximal interphalangeal (PIP) joints. Each joint was scored for GS and PD on a scale from 0 to 3 in a semi-quantitative manner. The sum of the GS and PD scores was considered the total GS and PD scores, respectively. We also assessed the Global Outcome Measures in Rheumatology (OMERACT)-EULAR Synovitis Score (GLOESS) (*22,23*). GLOESS has been combined with synovial hypertrophy, as shown by GS and PD.

X-ray images of bilateral hands and feet were conducted at posteroanterior and anteroposterior views, respectively. Trained JCR-certified rheumatologists (T.K. and T.S.) evaluated joint damage progression based on the van der Heijde-modified total Sharp score (vdH-mTSS) method as previously described (*24*), including 16 areas in each hand for erosions and 15 for joint-space narrowing (*25*).

2.5. Biomarker measurements

The serum concentrations of the following biomarkers were measured. Rheumatoid factor (RF) was measured by a latex agglutination turbidimetric immunoassay (LTIA) (LZ test "Eiken" RF) (Eiken Chemical Co., Ltd., Tokyo, Japan). Anti-cyclic citrullinated peptide antibodies (ACPA) were measured by a chemiluminescent enzyme immunoassay (CLEIA) (STACIA MEBLux test CCP) (Medical & Biological Laboratories Co., Ltd., Tokyo, Japan). Matrix metalloproteinase-3 (MMP-3) was measured by a latex turbidimetric immunoassay (LTIA) (Panaclear MMP-3 "Latex") (Sekisui Medical Co., Ltd., Tokyo, Japan). Multiplex cytokine/chemokine bead assays were performed using diluted serum supernatants and a MILLIPLEX MAP Human Cytokine/Chemokine Magnetic Bead Panel (Merck KGaA, Darmstadt, Germany). Bio-Plex Pro Human Cytokine Assays (Bio-Rad, Hercules, CA) were analyzed with a Bio-Plex MAGPIX™ Multiplex Reader (Bio-Rad) according to the manufacturer's instructions.

The cytokines/chemokines that were measured by the bead panel include inter-leukin (IL)-1α, IL-1β, IL-1 receptor antagonist, IL-2, IL-3, IL-4, IL-5, IL-6, IL-7, IL-8, IL-9, IL-10, IL-12 (p40), IL-12 (p70), IL-13, IL-15, IL-17, IL-18, interferon-gamma (IFN-γ), IFN-α2, CXCL1 (growth-related oncogene [GRO]), granulocyte-macrophage colony-stimulating factor (GM-CSF), granulocyte colony-stimulating factor (G-CSF), CX3CL1 (fractalkine), flt-3 ligand, fibroblast growth factor (FGF)-2, eotaxin, epidermal growth

factor (EGF), soluble CD40 ligand (sCD40L), vascular endothelial growth factor (VEGF), TNF-β, TNF-α, transforming growth factor (TGF)-α, CCL4 (macrophage inflammatory protein [MIP]-1β), CCL3 (MIP-1α), CCL22 (macrophage-derived chemokine [MDC]), CCL7 (monocyte chemotactic protein [MCP]-3), CCL2 (MCP-1), CXCL10 (IFN-γ-inducible protein [IP]-10), vascular cell adhesion molecule-1 (VCAM-1), and intercellular adhesion molecule-1 (ICAM-1). Serum levels of IL-6 and TNFα were measured using specific enzyme-linked immunosorbent assay (ELISA) kits (R&D Systems, Minneapolis, MN).

### 2.6. Study endpoints

The primary endpoint was the proportion of patients who experienced a clinical relapse during the period from baseline to week 24. Clinical relapse was defined as (1) a change from the baseline value in the DAS28-ESR (ΔDAS28-ESR) ≥ 1.2 or in the DAS28-ESR ≥ 3.2, and (2) an increase in the DAS28-ESR value due to elevated disease activity of RA, rather than other factors.

The secondary endpoints of this study were as follows: (1) the proportion of patients who experienced a clinical relapse during the period from baseline to week 12, (2) changes in the total PD and GS scores and the GLOESS from baseline to weeks 12 and 24, (3) the changes in the DAS28-ESR and DAS28-CRP values from baseline to weeks 12 and 24, (4) the change in vdH-mTSS from baseline to week 24, (5) the change in the HAQ-DI score from baseline to weeks 12 and 24, and (6) the changes in the serum levels of biomarkers from baseline to weeks 12 and 24. In addition, the safety endpoint was an occurrence of adverse events.

### 2.7. Statistical analysis method

The non-inferiority margin and sample size determination are described in detail in the protocol for this study (*17*). Briefly, this study aimed to test the non-inferiority of CT-P13 to the originator IFX, using a non-inferiority margin based on two clinical studies (*26,27*). The null hypothesis for noninferiority was rejected if the upper boundary of the confidence interval for the difference in relapse proportions did not exceed 27.2% (*i.e.*, the sum of the 11.2% margin and the 16.0% expected relapse proportion). The required sample size was calculated as 80 patients. However, due to insufficient enrollment of the expected number of cases, we determined that testing for non-inferiority would not be appropriate. Therefore, analyses of endpoints were limited to summarization and estimation. Baseline characteristics data were expressed as medians and interquartile ranges (IQR) for continuous variables and numbers with percentages for discrete variables. For interval estimation such as a confidence interval (CI), an Wilson's score method was used. R version 4.4.0 (R Project for Statistical Computing, Vienna, Austria) was used for statistical analyses.

## 3. Results

### 3.1. Patients' characteristics

This study included 19 patients between October 11, 2019, and March 31, 2023, although the target enrollment was 80 patients. Among the enrolled patients, 18 patients were evaluated for DAS28-ESR at 24 weeks or study discontinuation (full analysis set [FAS]) (Figure 1).

Table 1 shows the baseline characteristics of the patients. The age of the patients was 63 years (51, 72), with 6 males (33%) and 12 females (67%). The disease duration of RA was 9 years (6, 12.3). Fifteen (83%) were RF positive, and 17 (94%) were ACPA positive. The duration of the originator IFX treatment was 6.4 years (3.4, 9.5), and the duration of maintenance of clinical remission was 83 weeks (25, 151). The baseline originator IFX dose was 4.5 mg/kg (3, 8.25), and the dosing interval was 8 weeks (8, 8.75). The methotrexate dose at baseline was 8 mg/week (8, 10), and two patients (11%) were receiving concomitant PSL at baseline at a dose of 4 mg/day (3.5, 4.5). Before the baseline visit, prior use of other bDMARDs or JAK inhibitors was observed in two patients with etanercept, one with tocilizumab, one with abatacept, and one with tofacitinib.

### 3.2. Primary endpoint

The proportion of study subjects who experienced clinical relapse from baseline to week 24 after the start of treatment was 2 out of 18 [11.1% (95% CI: 3.1–32.8)]. One case relapsed at week 11 and the other at week 24.

### 3.3. Secondary endpoints

The proportion of study subjects who experienced clinical relapse from baseline to week 12 was 1 of 18 (5.5% [95% CI: 1.0–25.8]).

Table 2 presents the changes in the total GS and

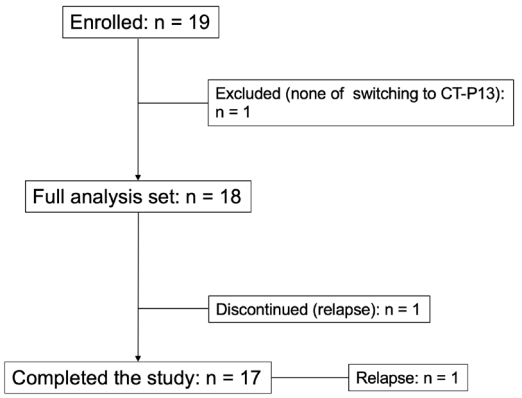


**Figure 1. Patient flow chart.**

PD scores, GLOESS, DAS28-ESR, DAS28-CRP, and HAQ-DI values from baseline to weeks 12 and 24, and the changes in vdH-mTSS from baseline to week 24. Figure 2 illustrates the distribution of the actual values for each outcome measure. Patients who discontinued treatment due to relapse had increased total GS and PD scores, GLOESS, DAS28-ESR, DAS28-CRP, and HAQ-DI values. However, no changes in these values were observed overall from baseline to weeks 12 and 24. The PD scores at weeks 12 and 24 remained at 0, indicating PD remission in the MSUS assessment. The clinical assessments at weeks 12 and 24 revealed sustained remission.

Figure 3 shows the changes in multiple cytokine arrays and ELISA from baseline to weeks 12 and 24 and stop visit and Supplementary Table S1 (*https://www.ddtjournal.com/action/getSupplementalData.php?ID=268*) shows cytokine/chemokine levels at the baseline. All the cytokines/chemokines showed no apparent changes from baseline to weeks 12 and 24. However, in a single patient in whom the study was discontinued because of relapse, serum levels of G-CSF, IL-6, PDGF-AA, MCP-1, VEGF-A, and IL-27 increased, whereas serum levels of eotaxin, IL-5, and MDC decreased. In addition, RF, ACPA, and MMP-3 levels did not change from baseline to weeks 12 and 24 (data not shown).

**Table 1. Baseline characteristics**

| | *n* = 18 |
|---|---|
| Age, years | 63 (51, 72) |
| Female | 12 (67) |
| Height, cm | 162 (154, 167) |
| Weight, kg | 54 (46, 63) |
| Disease Duration, year | 9.0 (0.0, 6.5) |
| Rheumatoid factor-positive | 15 (83) |
| Anti-cyclic citrullinated peptide antibody-positive | 17 (94) |
| Duration of remission, week | 83 (25, 151) |
| Duration of Infliximab use, year | 6.4 (3.4, 9.5) |
| Infliximab dose, mg/kg | 4.5 (3.0, 8.25) |
| Infliximab dose interval, week | 8 (8, 8.75) |
| History of infusion reaction to Infliximab | 0 (0) |
| Smoking history | 9 (50) |
| Current smoker | 2 (11) |
| Former smoker | 7 (39) |
| Pretreatment for rheumatoid arthritis | |
| Biologics agents | |
| Etanercept | 2 (11) |
| Tocilizumab | 1 (5.6) |
| Abatacept | 1 (5.6) |
| JAK inhibitors | |
| Tofactinib | 1 (5.6) |
| Concomitant medications | |
| Methotrexate | 18 (100) |
| Methotrexate dose, mg/week | 8 (8.0, 10.0) |
| Prednisolone | 2 (11) |
| Prednisolone dose, mg/day | 4 (3.5, 4.5) |
| Iguratimod | 3 (16.7) |
| Tacrolimus | 1 (5.6) |
| Tacrolimus, Iguratimod, and Salazosulfapyridine | 1 (5.6) |

Data are shown as *n* (%) or median (IQR). IQR, interquartile range; JAK, Janus kinase.

### 3.4. Safety

In the safety analysis set (18 patients), three adverse events (eczema, dry dermatitis, and COVID-19) occurred from the start of treatment to week 24. Serious adverse events were not observed. All non-serious adverse events were grade 2 and moderate in severity (requiring minimal/local/non-invasive treatment for adverse events). No adverse events led to study discontinuation.

## 4. Discussion

In this study, most patients who underwent treatment with originator IFX in clinical remission could safely switch to biosimilar IFX, CT-P13, without increased relapse risk. In addition, few changes were observed in MSUS scores, levels of cytokines/chemokines, as well as clinical indices, including DAS28-ESR and DAS28-CRP, among the patients who completed the 24-week

**Table 2. Assessment of efficacy**

| Items | Median (IQR) |
|---|---|
| **Total GS score** | |
| changes 0-12 weeks (*n* = 17) | 0 (0, 0) |
| changes 0-24 weeks (*n* = 17) | 0 (-1, 0) |
| changes 0 week-stop (*n* = 1) | 3 |
| **Total PD score** | |
| changes 0-12 weeks (*n* = 17) | 0 (0, 0) |
| changes 0-24 weeks (*n* = 17) | 0 (0, 0) |
| changes 0 week-stop (*n* = 1) | 2 |
| **GLOESS** | |
| changes 0-12 weeks (*n* = 17) | 0 (0, 0) |
| changes 0-24 weeks (*n* = 17) | 0 (-1, 0) |
| changes 0 week-stop (*n* = 1) | 3 |
| **DAS28-ESR** | |
| changes 0-12 weeks (*n* = 17) | -0.06 (-0.22, 0.36) |
| changes 0-24 weeks (*n* = 17) | 0.15 (-0.08, 0.81) |
| changes 0 week-stop (*n* = 1) | 2.6 |
| **DAS28-CRP** | |
| changes 0-12 weeks (*n* = 16) | 0.08 (-0.01, 0.29) |
| changes 0-24 weeks (*n* = 17) | 0.13 (-0.05, 0.54) |
| changes 0 week-stop (*n* = 1) | 3.4 |
| **HAQ-DI** | |
| changes 0-12 weeks (*n* = 17) | 0 (0, 0) |
| changes 0-24 weeks (*n* = 17) | 0 (0, 0) |
| changes 0 week-stop (*n* = 1) | 0 |
| **vdH-mTSS** | |
| changes 0-24 weeks (*n* = 17) | 0 (0, 0) |

CRP, C-reactive protein; DAS28, Disease Activity Score-28; ESR, erythrocyte sedimentation rate; GLOESS, Global Outcome Measures in Rheumatology European Alliance of Associations for Rheumatology Synovitis Score; GS, gray scale; HAQ-DI, Health Assessment Questionnaire-Disability Index; IQR, Interquantile range, vdH-mTSS, van der Heijde-modified total Sharp score; PD, power Doppler.

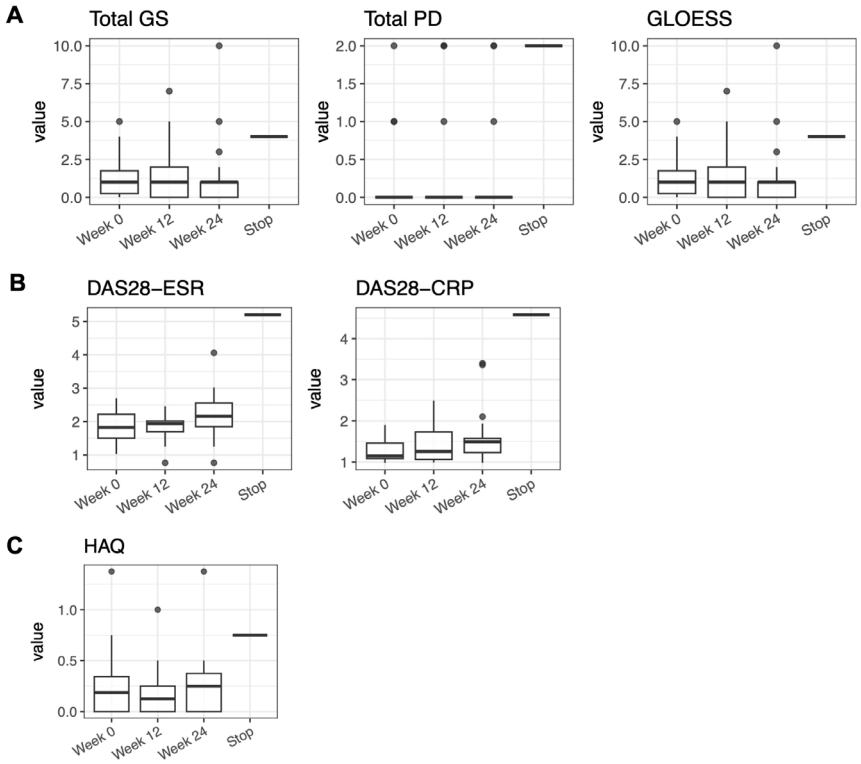


**Figure 2. Changes in MSUS scores, clinical disease activity, and HAQ-DI during the study period.** A. MSUS scores, B. clinical disease indices, and C. HAQ-DI. Horizontal bar: median; boxes: 25th and 75th percentiles; bars: 5th and 95th percentiles. CRP, C-reactive protein; DAS28, Disease Activity Score-28; ESR, erythrocyte sedimentation rate; GLOESS, Global OMERACT-EULAR Synovitis Score; GS, grayscale; HAQ-DI, Health Assessment Questionnaire-Disability Index; MSUS, musculoskeletal ultrasound; PD, power Doppler.

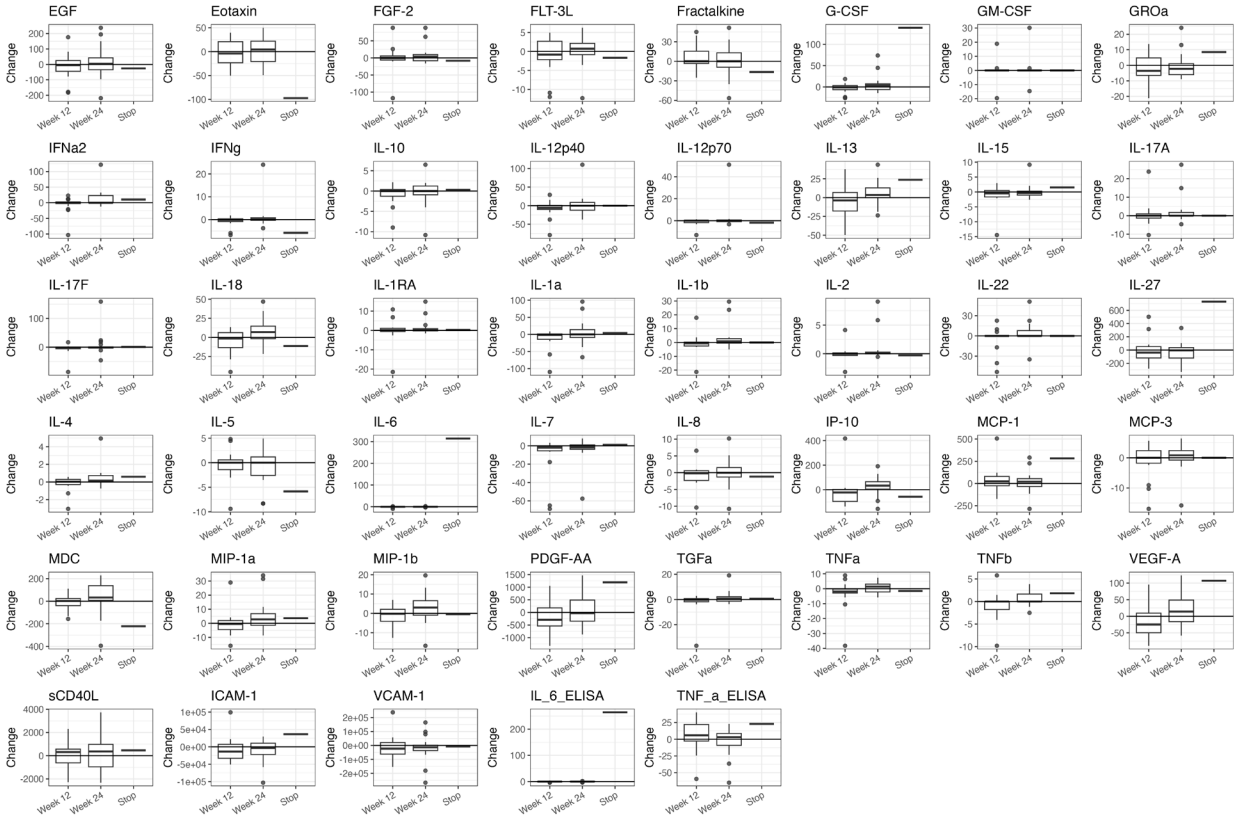


**Figure 3. Changes in multiple cytokine and chemokine levels during the study period.** Horizontal bar: median; boxes: 25th and 75th percentiles; bars: 5th and 95th percentiles.

study duration.

Introducing biologics into clinical practice has dramatically improved the management of various immune-mediated inflammatory diseases, including RA (*28*). However, the high cost of currently available biologics limits access to treatment for patients with RA (*29,30*). Biosimilars provide potential cost savings and health benefits, playing a crucial role in the treatment of rheumatic diseases (*8,30,31*). The price of a pharmaceutical product is a key factor in drug selection, and the cost reduction for CT-P13 was 38% (in terms of the average NHI price as of December 2024) compared with the originator IFX in Japan. Therefore, the Japanese government has promoted using biosimilars to reduce healthcare costs. However, some physicians are cautious about their clinical use, questioning their efficacy and safety. Additionally, there are concerns regarding the nocebo effect of switching to biosimilars (*32,33*).

The efficacy and safety equivalence of biosimilar IFX, including CT-P13, to originator IFX in patients with RA have been demonstrated (*7,34,35*). In addition, several studies have shown the efficacy and safety of switching from originator IFX to biosimilar IFX (*8,9,30,36*). One randomized control trial reported that patients with several inflammatory diseases, including RA, after switching from originator IFX to CT-P13, were not inferior to continued treatment with originator IFX (*8*). In a Danish registry, clinical relapse ($\Delta$DAS28 $\geq$ 1.2) was observed in 10 of 346 patients with RA and psoriatic arthritis within 3 months after switching from originator IFX to CT-P13 (*36*). Similarly, in this study, clinical relapse following the switch to CT-P13 was infrequent, with only one of 18 patients experiencing relapse at week 12 and another 1 of 18 at week 24.

The strength of this study is its prospective evaluation of therapeutic efficacy using not only clinical disease activity indices but also MSUS to accurately and objectively evaluate disease activity at the joint level in a patient series. Actually, the results of this study demonstrated that in non-clinical relapsed cases, there were no changes in imaging evaluations with MSUS as well as in clinical disease activity indices. In addition, the results showed no alterations in functional assessments using HAQ-DI and multiple serum biomarker levels, confirming the absence of disease progression in RA from multiple perspectives.

In the pathophysiology of RA, it has been elucidated that intracellular signaling activity mediated by inflammatory cytokines, such as TNF-α and IL-6, plays a critical role in developing synovitis and the progression of joint destruction (*37*). In this study, we evaluated the serum levels of multiple cytokines/chemokines after switching to biosimilar IFX. Previous studies have reported that baseline multi-biomarker disease activity scores, including serum IL-6 and VEGF-A, can predict disease relapse following discontinuation of TNF inhibitors in patients with RA who have low disease activity while on TNF inhibitors (*38*). However, no study has investigated the relationship between longitudinal changes in cytokine/chemokine levels and clinical relapse. In this study, no changes in cytokine/chemokine levels were observed in non-clinical relapsed cases. In contrast, one relapsed case showed fluctuations in multiple cytokines, including IL-6, at the time of relapse. Nevertheless, because this observation was based on a single case, further studies are warranted to elucidate the relationship between cytokine dynamics and disease relapse.

This study had some limitations. First, the sample size was small. Only 18 patients were evaluated, although 80 patients were expected to be enrolled. Thus, the initially planned test of non-inferiority to originator IFX could not be evaluated, and analyses of primary endpoint were limited to summarization and estimation. In addition, the analysis of the other endpoints primarily consisted of summarization. Second, the present study only covered a period of 24 weeks, indicating the need for future studies to assess the long-term outcomes. Third, immunogenicity such as anti-drug antibodies and neutralizing antibodies was not assessed; thus, their relationship with relapse was not investigated. Fourth, another aim of this study was to identify the predictive factors for clinical relapse after switching from originator IFX to CT-P13. However, due to the limited number of relapse cases, it was not feasible to conduct an analysis to identify the predictive factors. Despite these limitations, this study represents a prospective evaluation of therapeutic efficacy utilizing not only clinical disease activity indices but also MSUS and several biomarkers; consequently, these results possess considerable clinical value.

In conclusion, this study revealed that although the results were limited to estimations due to the small number of cases, a large proportion of Japanese patients with RA who achieved clinical remission were able to maintain non-clinical relapse after switching from originator infliximab to biosimilar infliximab. This study highlighted the potential for cost-effective biosimilars to maintain remission in patients with RA, suggesting significant implications for reducing treatment costs and improving accessibility.

**Acknowledgements**

We thank Shin-Ichiro Kagami (Asahi General Hospital), Takuya Nakazawa (Chiba-East Hospital), Seiji Yoshizawa (Hamanomachi Hospital), Takahisa Suzuki (Japanese Red Cross Nagasaki Genbaku Hospital), Etsuo Chosa (University of Miyazaki Hospital), Toshihiko Hidaka (Miyazaki Zenjinkai Hospital), Masako Furuyama (Nagasaki Kita Hospital), Toru Takeuchi (Osaka Medical and Pharmaceutical University Hospital), Akira Sagawa (Sagawa Akira Rheumatology Clinic), and Ikuko Onishi (Utazu Hospital), all of which are investigators of joint research institutions. We thank our colleagues and staff

at the Department of Immunology and Rheumatology, Nagasaki University Hospital for their support. We thank Editage (*www.editage.jp*) for English language editing.

*Funding*: This study was funded by Celltrion Healthcare Co., Ltd. (Inchon, South Korea).

*Conflict of Interest*: AK received research funding from AYUMI Pharmaceutical Co., Celltrion Healthcare Co., Ltd., Gilead Sciences Inc., KIYAN PHARMA Co. Ltd., Janssen Pharmaceutical K.K., ONO Pharmaceutical Co., Asahi Kasei Pharma Corporation, Taisho Pharmaceutical Co. Ltd., Teijin Pharma Co., Chugai Pharmaceutical Co., Kyowa Kirin Co., Boehringer Ingelheim Japan, Abbvie GK, Eli Lilly Japan, Daiichi Sankyo Co., Mitsubishi Tanabe Pharma Co., Bristol-Myers Squibb, and Eisai Co. The other authors have no conflicts of interest to declare.

**References**

1. Scott DL, Wolfe F, Huizinga TW. Rheumatoid arthritis. Lancet. 2010; 376:1094-1108.
2. Smolen JS, Breedveld FC, Burmester GR, *et al.* Treating rheumatoid arthritis to target: 2014 update of the recommendations of an international task force. Ann Rheum Dis. 2016; 75:3-15.
3. Schett G, Emery P, Tanaka Y, Burmester G, Pisetsky DS, Naredo E, Fautrel B, van Vollenhoven R. Tapering biologic and conventional DMARD therapy in rheumatoid arthritis: current evidence and future directions. Ann Rheum Dis. 2016; 75:1428-1437.
4. St Clair EW, van der Heijde DM, Smolen JS, Maini RN, Bathon JM, Emery P, Keystone E, Schiff M, Kalden JR, Wang B, Dewoody K, Weiss R, Baker D. Combination of infliximab and methotrexate therapy for early rheumatoid arthritis: a randomized, controlled trial. Arthritis Rheum. 2004; 50:3432-3443.
5. Lipsky PE, van der Heijde DM, St Clair EW, Furst DE, Breedveld FC, Kalden JR, Smolen JS, Weisman M, Emery P, Feldmann M, Harriman GR, Maini RN. Infliximab and methotrexate in the treatment of rheumatoid arthritis. Anti-Tumor Necrosis Factor Trial in Rheumatoid Arthritis with Concomitant Therapy Study Group. N Engl J Med. 2000; 343:1594-1602.
6. Yamanaka H, Tanaka Y, Sekiguchi N, Inoue E, Saito K, Kameda H, Iikuni N, Nawata M, Amano K, Shinozaki M, Takeuchi T. Retrospective clinical study on the notable efficacy and related factors of infliximab therapy in a rheumatoid arthritis management group in Japan (RECONFIRM). Mod Rheumatol. 2007; 17:28-32.
7. Takeuchi T, Yamanaka H, Tanaka Y, Sakurai T, Saito K, Ohtsubo H, Lee SJ, Nambu Y. Evaluation of the pharmacokinetic equivalence and 54-week efficacy and safety of CT-P13 and innovator infliximab in Japanese patients with rheumatoid arthritis. Mod Rheumatol. 2015; 25:817-824.
8. Jorgensen KK, Olsen IC, Goll GL, Lorentzen M, Bolstad N, Haavardsholm EA, Lundin KEA, Mork C, Jahnsen J, Kvien TK. Switching from originator infliximab to biosimilar CT-P13 compared with maintained treatment with originator infliximab (NOR-SWITCH): a 52-week, randomised, double-blind, non-inferiority trial. Lancet. 2017; 389:2304-2316.
9. Tanaka Y, Yamanaka H, Takeuchi T, Inoue M, Saito K, Saeki Y, Lee SJ, Nambu Y. Safety and efficacy of CT-P13 in Japanese patients with rheumatoid arthritis in an extension phase or after switching from infliximab. Mod Rheumatol. 2017; 27:237-245.
10. Colebatch AN, Edwards CJ, Ostergaard M, *et al*. EULAR recommendations for the use of imaging of the joints in the clinical management of rheumatoid arthritis. Ann Rheum Dis. 2013; 72:804-814.
11. D'Agostino MA, Terslev L, Wakefield R, Østergaard M, Balint P, Naredo E, Iagnocco A, Backhaus M, Grassi W, Emery P. Novel algorithms for the pragmatic use of ultrasound in the management of patients with rheumatoid arthritis: from diagnosis to remission. Ann Rheum Dis. 2016; 75:1902-1908.
12. Naredo E, Moller I, Cruz A, Carmona L, Garrido J. Power Doppler ultrasonographic monitoring of response to anti-tumor necrosis factor therapy in patients with rheumatoid arthritis. Arthritis Rheum. 2008; 58:2248-2256.
13. Kawashiri SY, Nishino A, Shimizu T, *et al.* Ultrasound disease activity of bilateral wrist and finger joints at three months reflects the clinical response at six months of patients with rheumatoid arthritis treated with biologic disease-modifying anti-rheumatic drugs. Mod Rheumatol. 2017; 27:252-256.
14. Nguyen H, Ruyssen-Witrand A, Gandjbakhch F, Constantin A, Foltz V, Cantagrel A. Prevalence of ultrasound-detected residual synovitis and risk of relapse and structural progression in rheumatoid arthritis patients in clinical remission: a systematic review and meta-analysis. Rheumatology (Oxford). 2014; 53:2110-2118.
15. Kawashiri SY, Suzuki T, Nakashima Y, Horai Y, Okada A, Iwamoto N, Ichinose K, Tamai M, Arima K, Nakamura H, Origuchi T, Uetani M, Aoyagi K, Eguchi K, Kawakami A. Ultrasonographic examination of rheumatoid arthritis patients who are free of physical synovitis: power Doppler subclinical synovitis is associated with bone erosion. Rheumatology (Oxford). 2014; 53:562-569.
16. World Medical Association. World Medical Association Declaration of Helsinki: ethical principles for medical research in-volving human subjects. JAMA. 2013; 310:2191-2194.
17. Kawashiri SY, Shimizu T, Sato S, Morimoto S, Kawazoe Y, Sumiyoshi R, Hosogaya N, Fukushima C, Yamamoto H, Kawakami A. Switching from originator infliximab to biosimilar infliximab in Japanese patients with rheumatoid arthritis achieving clinical remission (the IFX-SIRIUS study I): Study protocol for an interventional, multicenter, open-label, single-arm and noninferiority clinical trial with clinical, ultrasound, and biomarker assessments. Medicine (Baltimore). 2020; 99:e21151.
18. Aletaha D, Neogi T, Silman AJ, *et al.* 2010 Rheumatoid arthritis classification criteria: an American College of Rheumatology/European League Against Rheumatism collaborative initiative. Arthritis Rheum. 2010; 62:2569-2581.
19. Prevoo ML, van 't Hof MA, Kuper HH, van Leeuwen MA, van de Putte LB, van Riel PL. Modified disease activity scores that include twenty-eight-joint counts. Development and validation in a prospective longitudinal study of patients with rheumatoid arthritis. Arthritis Rheum. 1995; 38:44-48.
20. Fries JF, Spitz P, Kraines RG, Holman HR. Measurement of patient outcome in arthritis. Arthritis Rheum. 1980;

23:137-145.
21. Torp-Pedersen ST, Terslev L. Settings and artefacts relevant in colour/power Doppler ultrasound in rheumatology. Ann Rheum Dis. 2008; 67:143-149.
22. D'Agostino MA, Boers M, Wakefield RJ, Berner Hammer H, Vittecoq O, Filippou G, Balint P, Möller I, Iagnocco A, Naredo E, Østergaard M, Gaillez C, Le Bars M. Exploring a new ultrasound score as a clinical predictive tool in patients with rheumatoid arthritis starting abatacept: results from the APPRAISE study. RMD Open. 2016; 2:e000237.
23. Terslev L, Naredo E, Aegerter P, Wakefield RJ, Backhaus M, Balint P, Bruyn GAW, Iagnocco A, Jousse-Joulin S, Schmidt WA, Szkudlarek M, Conaghan PG, Filippucci E, D'Agostino MA. Scoring ultrasound synovitis in rheumatoid arthritis: a EULAR-OMERACT ultrasound taskforce-Part 2: reliability and application to multiple joints of a standardised consensus-based scoring system. RMD Open. 2017; 3:e000427.
24. Tanaka Y, Oba K, Koike T, *et al*. Sustained discontinuation of infliximab with a raising-dose strategy after obtaining remission in patients with rheumatoid arthritis: the RRRR study, a randomised controlled trial. Ann Rheum Dis. 2020; 79:94-102.
25. van der Heijde D. How to read radiographs according to the Sharp/van der Heijde method. J Rheumatol. 2000; 27:261-263.
26. Brocq O, Millasseau E, Albert C, Grisot C, Flory P, Roux CH, Euller-Ziegler L. Effect of discontinuing TNFalpha antagonist therapy in patients with remission of rheumatoid arthritis. Joint bone spine. 2009; 76:350-355.
27. Nishino A, Kawashiri SY, Koga T, *et al.* Ultrasonographic efficacy of biologic and targeted synthetic disease-modifying antirheumatic drug therapy in rheumatoid arthritis from a multicenter rheumatoid arthritis ultrasound prospective cohort in Japan. Arthritis Care Res. 2018; 70:1719-1726.
28. Kuek A, Hazleman BL, Ostör AJ. Immune-mediated inflammatory diseases (IMIDs) and biologic therapy: a medical revolution. Postgrad Med J. 2007; 83:251-260.
29. Modena V, Bianchi G, Roccatello D. Cost-effectiveness of biologic treatment for rheumatoid arthritis in clinical practice: an achievable target? Autoimmun Rev. 2013; 12:835-838.
30. Yoo DH, Prodanovic N, Jaworski J, *et al.* Efficacy and safety of CT-P13 (biosimilar infliximab) in patients with rheumatoid arthritis: comparison between switching from reference infliximab to CT-P13 and continuing CT-P13 in the PLANETRA extension study. Ann Rheum Dis. 2017; 76:355-363.
31. Dörner T, Strand V, Cornes P, Gonçalves J, Gulácsi L, Kay J, Kvien TK, Smolen J, Tanaka Y, Burmester GR. The changing landscape of biosimilars in rheumatology. Ann Rheum Dis. 2016; 75:974-982.
32. Glintborg B, Loft AG, Omerovic E, *et al*. To switch or not to switch: results of a nationwide guideline of mandatory switching from originator to biosimilar etanercept. One-year treatment outcomes in 2061 patients with inflammatory arthritis from the DANBIO registry. Ann Rheum Dis. 2019; 78:192-200.
33. Colloca L, Panaccione R, Murphy TK. The Clinical Implications of Nocebo Effects for Biosimilar Therapy. Front Pharmacol. 2019; 10:1372.
34. Yoo DH, Hrycaj P, Miranda P, *et al*. A randomised, double-blind, parallel-group study to demonstrate equivalence in efficacy and safety of CT-P13 compared with innovator infliximab when coadministered with methotrexate in patients with active rheumatoid arthritis: the PLANETRA study. Ann Rheum Dis. 2013; 72:1613-1620.
35. Yoo DH, Racewicz A, Brzezicki J, Yatsyshyn R, Arteaga ET, Baranauskaite A, Abud-Mendoza C, Navarra S, Kadinov V, Sariego IG, Hong SS, Lee SY, Park W. A phase III randomized study to evaluate the efficacy and safety of CT-P13 compared with reference infliximab in patients with active rheumatoid arthritis: 54-week results from the PLANETRA study. Arthritis Res Ther. 2016; 18:82.
36. Glintborg B, Sørensen IJ, Loft AG, *et al.* A nationwide non-medical switch from originator infliximab to biosimilar CT-P13 in 802 patients with inflammatory arthritis: 1-year clinical outcomes from the DANBIO registry. Ann Rheum Dis. 2017; 76:1426-1431.
37. Smolen JS, Aletaha D, McInnes IB. Rheumatoid arthritis. Lancet. 2016; 388:2023-2038.
38. Ghiti Moghadam M, Lamers-Karnebeek FBG, Vonkeman HE, *et al.* Multi-biomarker disease activity score as a predictor of disease relapse in patients with rheumatoid arthritis stopping TNF inhibitor treatment. PLoS One. 2018; 13:e0192425.

Received May 16, 2025; Revised August 11, 2025; Accepted August 17, 2025.

**Address correspondence to:*
Shin-ya Kawashiri, Department of Community Medicine, Division of Advanced Preventive Medical Sciences, Nagasaki University Graduate School of Biomedical Sciences, 1-12-4 Sakamoto, Nagasaki 852-8523, Japan.
E-mail: shin-ya@nagasaki-u.ac.jp

Released online in J-STAGE as advance publication August 22, 2025.

**Brief Report**

DOI: 10.5582/ddt.2025.01052

# Anti-*Mycobacterium avium* complex activities of streptcytosine analogs from a marine actinomycete as nucleoside antibiotics

**Natsuki Oshima, Akiho Yagi*, Hiroyuki Yamazaki, Ryuji Uchida***

Division of Natural Product Chemistry, Faculty of Pharmaceutical Sciences, Tohoku Medical and Pharmaceutical University, Miyagi, Japan.

**SUMMARY**: To examine the potential of nucleoside antibiotics as therapeutic agents against *Mycobacterium avium* complex (MAC), the *in vitro* and *in vivo* anti-MAC activities of streptcytosine A (**1**), plicacetin (**2**), and bamicetin (**3**) derived from a marine actinomycete were evaluated. Compounds **1**–**3** exhibited antimicrobial activities against *M. avium* and *M. intracellulare*, with minimum inhibitory concentration values of 4.0 and 16 μg/mL, respectively, as assessed by the microdilution method. In silkworm infection models of *M. avium* and *M. intracellulare*, these compounds also exhibited therapeutic efficacies at lower doses than clarithromycin, with 50% effective doses of between 7.6 and 28 μg/larva·g, and no toxicity was observed. A pharmacokinetic analysis further revealed elimination half-lives of 3.0, 2.3, and 5.1 hours, respectively, in the silkworm hemolymph. These results suggest the potential of **1**–**3** as lead candidates for the development of potent anti-MAC drugs.

***Keywords***: Streptcytosine, plicacetin, bamicetin, silkworm infection model, *Mycobacterium avium* complex (MAC), natural product

## 1. Introduction

Non-tuberculous mycobacterial (NTM) disease is an infectious disease that primarily affects the lungs, and its incidence has been increasing globally in recent years (*1,2*). Unlike tuberculosis, NTM disease is mainly caused by non-tuberculous mycobacteria found in environmental sources. Among these infections, *Mycobacterium avium* complex (MAC) infection, primarily caused by *M. avium* and *M. intracellulare*, accounts for more than 80% of NTM disease cases in Japan (*2*). The standard treatment for MAC infection consists of a multidrug regimen comprising macrolides, such as clarithromycin and azithromycin, in combination with rifampicin and ethambutol. However, despite prolonged administration exceeding 6 months, the attenuation of symptoms is often inadequate due to the emergence of drug-resistant strains, rendering the disease refractory. In such cases, injectable aminoglycosides or amikacin liposome inhalation suspensions are recommended as adjunctive therapy. Nevertheless, an optimal treatment regimen for MAC infection has yet to be established. Therefore, the development of novel anti-MAC drugs remains an urgent medical priority.

In the search for novel drug candidates, a key requirement is the presence of a unique structure that has not been previously identified. Nucleoside compounds, such as mavintramycin and amicetin, were recently reported to exhibit anti-MAC activity (*3*), underscoring the potential of nucleoside antibiotics as promising anti-MAC agents. Therefore, we focused on nucleoside antibiotics, specifically streptcytosine analogs, which were previously identified as antimicrobial agents against *M. smegmatis* during our screening of anti-tuberculosis compounds derived from marine invertebrates and microorganisms (*4*). In the present study, we examined the anti-MAC activities of streptcytosine analogs isolated from the marine actinomycete *Streptomyces* sp. TPU1236A using *in vitro* and *in vivo* assays, namely, the liquid microdilution method and silkworm infection model, respectively. In addition, their elimination half-lives ($t_{1/2}$) in the silkworm hemolymph were assessed by high-performance liquid chromatography (HPLC).

## 2. Materials and Methods

### 2.1. Materials

Streptcytosine A (**1**), plicacetin (**2**), and bamicetin (**3**) were purified from the culture broth of marine-derived *Streptomyces* sp. TPU1236A (*4*). Rifampicin was obtained from FUJIFILM Wako Pure Chemical Industries (Osaka, Japan), and clarithromycin was purchased from Tokyo Chemical Industries (Tokyo, Japan).

2.2. Microorganisms

*M. avium* JCM 15430 and *M. intracellulare* JCM 6384 were obtained from the Japan Collection of Microorganisms, RIKEN BRC, which is part of the National BioResource Project of MEXT, Japan.

2.3. Measurement of minimum inhibitory concentration (MIC) values using the liquid microdilution method

The MIC values of **1**–**3** against *M. avium* and *M. intracellulare* were evaluated using the liquid microdilution method according to a previously established protocol (*5,6*). *M. avium* and *M. intracellulare* were cultured at 37°C for seven days in Middlebrook 7H9 broth (1.04% Middlebrook 7H9 broth, 0.05% Tween 80, 0.5% bovine serum albumin, 0.2% glucose, and 0.085% NaCl) until reaching approximately $1.0 \times 10^9$ colony-forming units (CFU)/mL. Bacterial cultures were then diluted 500-fold with the same fresh broth. A 95-µL aliquot of the diluted suspension was dispensed into each well of a 96-well microplate with or without test samples (5 µL in methanol). The microplate was incubated at 37°C for seven days. Turbidity was assessed by measuring absorbance at 550 nm using a spectrophotometer. MIC was defined as the lowest concentration of the test compound that inhibited bacterial growth by 90% of the control (without the compound).

2.4. Evaluation of the 50% effective dose ($ED_{50}$) in the silkworm infection model

The silkworm infection model was conducted following a previously established protocol (*5,7–14*). Fertilized silkworm eggs of *Bombyx mori* (Hu·Yo × Tukuba·Ne) were obtained from Ehime Sansyu (Ehime, Japan) and reared on an artificial diet (Silk Mate 2M; Nihon Nosan Kogyo, Kanagawa, Japan) in an incubator at 27°C until the fourth-instar larval molting stage. On the first day of the fifth-instar larval stage following molting, silkworms were fed the artificial diet until their body weight reached approximately 2 g. On the next day, a suspension of *M. avium* or *M. intracellulare* ($2.5 \times 10^7$ CFU/larva·g in 50 µL Middlebrook 7H9 broth) was injected into the hemolymph of silkworm larvae (2.0 g, $n = 5$) using a disposable 1-mL syringe (NIPRO, Osaka, Japan) equipped with a 27-G needle (TERUMO, Tokyo, Japan). Within 30 minutes of infection, test samples (50 µL in saline or 10% DMSO) were administered *via* injection. After the injection, silkworms were maintained at 37ºC without feeding, and their survival rate was monitored for 96 hours post-injection. $ED_{50}$ values were defined as the dose required to achieve a 50% survival rate, normalized per gram of silkworm body weight.

2.5. Evaluation of drug metabolism in silkworm larvae

Drug metabolism in silkworm larvae was assessed according to a previously established protocol (*15*,*16*). Hemolymph samples were collected at the time points specified in the figure legends after injecting **1**–**3** (50 µL of 1 mg/mL) directly into the hemolymph. The collected hemolymph (50–100 µL) was mixed with an equal volume of acetonitrile, followed by centrifugation at 10,000 rpm at 4°C for 5 min. The resulting supernatant was analyzed by HPLC under the following conditions: column, SUPELCO Express C18 (2.1 mm × 50 mm, Sigma-Aldrich Chemical Company, St. Louis, MO, USA); mobile phase, acetonitrile with a 0.1% formic acid gradient (5–95% over 10 min); flow rate, 0.4 mL/min; column temperature, 50ºC; injection volume, 10 µL; detection, UV at 320 nm.

## 3. Results and Discussion

The *in vitro* activities of **1**–**3** against *M. avium* and *M. intracellulare* were evaluated using the liquid microdilution method, and their MIC values are summarized in Table 1. Compounds **1**–**3** exhibited antimicrobial activities against *M. avium*, each with an MIC value of 4.0 µg/mL. They also showed antimicrobial activities against *M. intracellulare* with consistent MIC values of 16 µg/mL. In our previous study, **1**–**3** were isolated as antimicrobial compounds that were active against *M. smegmatis* and identified as nucleoside antibiotics containing cytosine, amosamine, amicetose, and *p*-aminobenzoic acid (PABA) (Figure 1) (*4*). The findings obtained demonstrated that streptcytosines B–E, which lack amosamine and PABA, did not exhibit anti-*M. smegmatis* activity, suggesting that the presence of amosamine and PABA, whether individually or together, is essential for this activity.

Hosoda *et al*. (*3*) reported that the structurally related compounds, mavintramycin and amicetin, exhibited

**Table 1. MIC and $ED_{50}$ values of 1-3 against *M. avium* and *M. intracellulare***

| | *M. avium* | | *M. intracellulare* | |
|---|---|---|---|---|
| | MIC (µg/mL) | $ED_{50}$ (µg/larva·g) | MIC (µg/mL) | $ED_{50}$ (µg/larva·g) |
| Streptcytosine A (**1**) | 4.0 | 9.1 | 16 | 28 |
| Plicacetin (**2**) | 4.0 | 15 | 16 | 26 |
| Bamicetin (**3**) | 4.0 | 7.6 | 16 | 12 |
| Clarithromycin | 0.098 | 23 | 0.012 | 42 |

anti-MAC activities. Since mavintramycin lacks PABA, this finding indicates that the amosamine moiety is critical for anti-NTM activity. In the present study, **1**–**3**, which contain cytosine, amosamine, and amicetose, similar to amicetin and mavintramycin, exhibited anti-MAC activities. Mavintramycin A has been shown to inhibit *M. avium* by binding to 23S ribosomal RNA and interfering with protein synthesis (*3*). Furthermore, a crystallographic analysis revealed that amicetin bound to the 70S ribosomal subunit of *Thermus thermophilus*, occupying the P-site in the peptidyl transferase center (*17*), which differs from the binding sites of clinically used antibiotics, such as clarithromycin and amikacin. Therefore, **1**–**3** may interact with similar ribosomal sites in *M. avium* and *M. intracellulare*, potentially conferring efficacy against drug-resistant clinical strains.

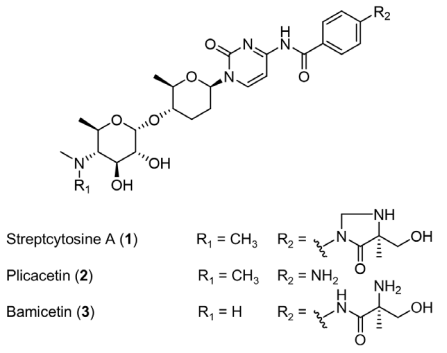


**Figure 1. Structures of 1-3.**

The therapeutic efficacies of **1**–**3** were further evaluated using silkworm infection models of *M. avium* and *M. intracellulare* ($n$ = 5). These models closely mimic *in vivo* conditions and are useful for examining the therapeutic efficacies and pharmacokinetics of antimicrobial agents, similar to murine models, while requiring minimal sample quantities and enabling rapid evaluations (*15,18*). As shown in Figure 2 and Table 1, the administration of **1**–**3** to silkworms infected with *M. avium* resulted in dose-dependent therapeutic

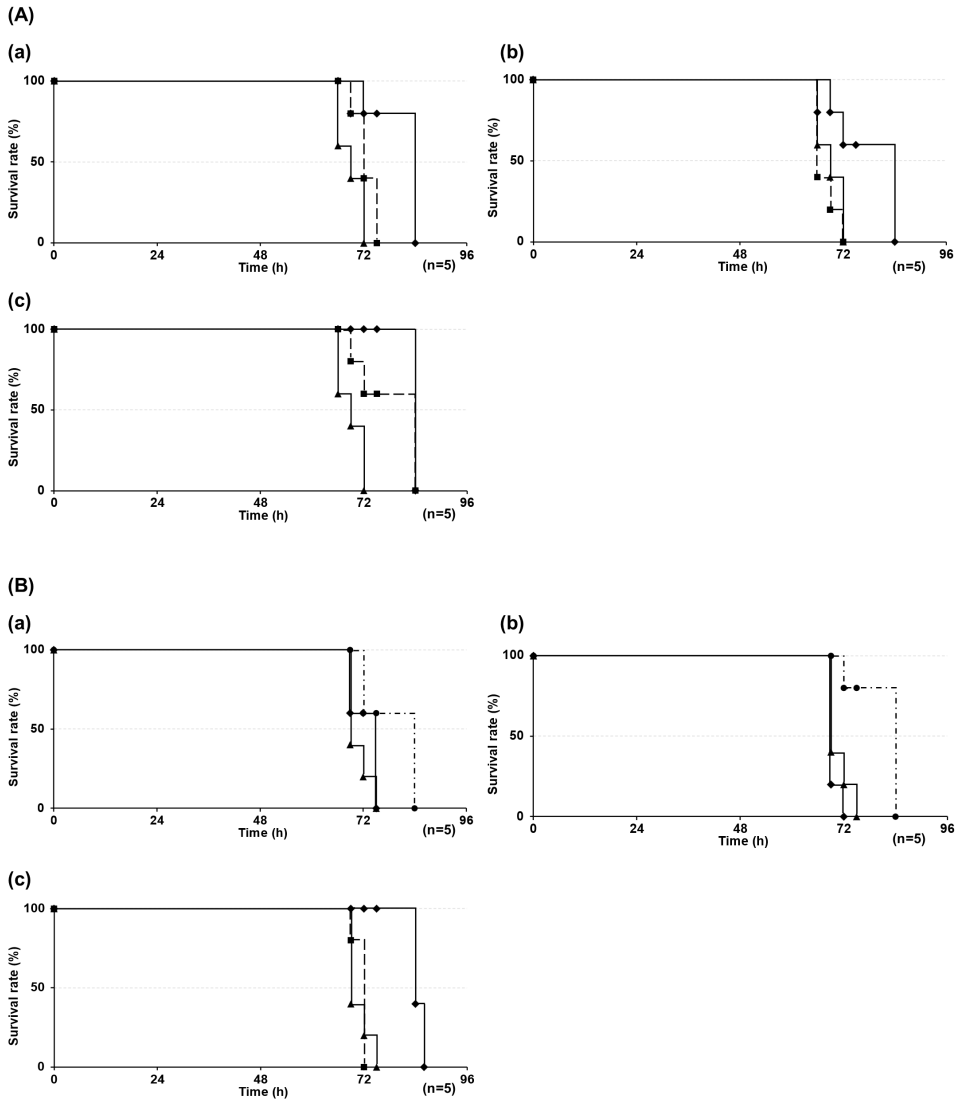


**Figure 2. Therapeutic effects of 1–3 in silkworm infection models of (A) *M. avium* and (B) *M. intracellulare*.** (a) Streptcytosine A (**1**), (b) plicacetin (**2**), and (c) bamicetin (**3**). ●: 32, ♦: 16, ■: 8.0, ▲: 0 μg/larva·g. Experiments were performed twice, and reproducible data were obtained.

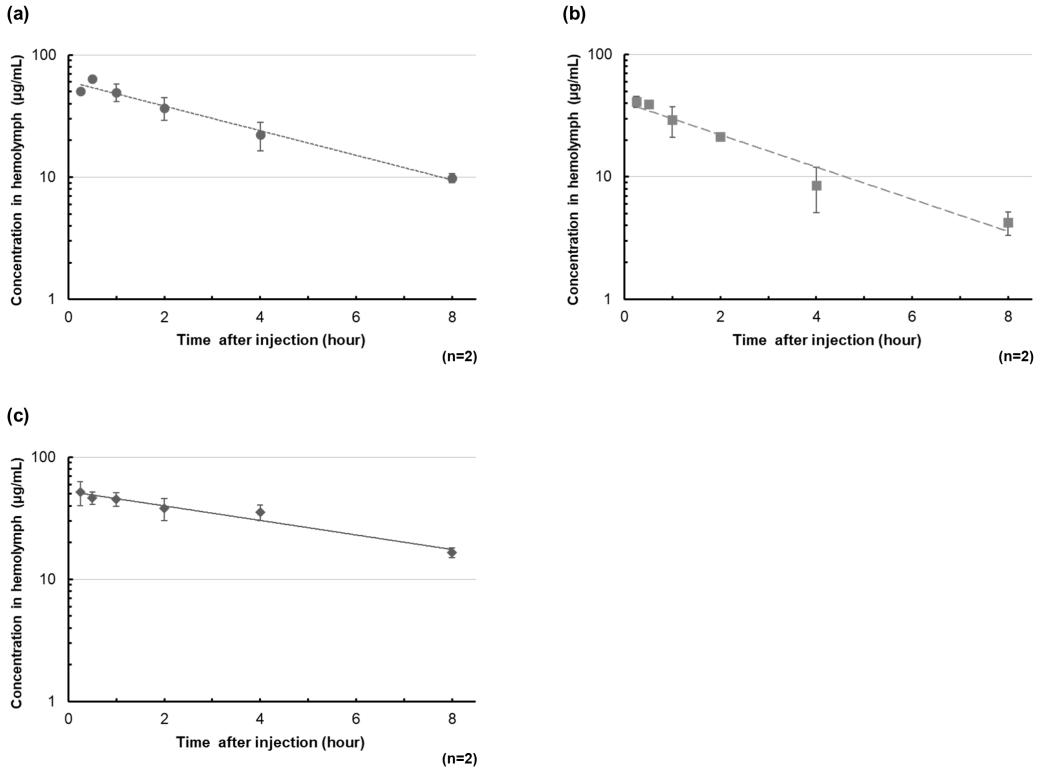


**Figure 3. Time-dependent concentration profiles of 1–3 in the silkworm hemolymph.** ●: Streptcytosine A (**1**) ($t_{1/2}$ = 3.0 hours) (a); ■: plicacetin (**2**) ($t_{1/2}$ = 2.3 hours) (b); ♦: bamicetin (**3**) ($t_{1/2}$ = 5.1 hours) (c). The silkworm hemolymph ($n$ = 2) was collected 0.25, 0.5, 1.0, 2.0, 4.0 and 8.0 hours after the injection of **1**–**3**. Experiments were performed twice, yielding consistent results.

effects, with $ED_{50}$ values of 9.1, 15, and 7.6 μg/larva·g, respectively. Similarly, in the *M. intracellulare*-infected silkworm model, the corresponding $ED_{50}$ values were 28, 26, and 12 μg/larva·g, respectively. Moreover, none of the compounds exhibited toxicity towards silkworms within a 72-hour observation period (data not shown). These results indicate that **1**–**3** exhibited potent *in vivo* anti-MAC activities, with $ED_{50}$ values that correlated with their MIC values. Since mavintramycin A was previously shown to exhibit therapeutic efficacy in a murine *M. avium* infection model (*3*), **1**–**3** may also be effective in mammalian systems. Moreover, the $ED_{50}$ values of clarithromycin in the silkworm models of *M. avium* and *M. intracellulare* were 23 and 42 μg/larva·g, respectively, which were markedly higher than those of **1**–**3**, suggesting their strong potential as anti-MAC agents.

A pharmacokinetic analysis was conducted by collecting the silkworm hemolymph at various time points after the administration of **1**–**3** and subjecting it to a HPLC analysis (*15*). The $t_{1/2}$ of **1**–**3** were 3.0, 2.3, and 5.1 hours, respectively (Figure 3). These moderate $t_{1/2}$ are consistent with their therapeutic efficacies observed *in vivo*, suggesting that **1**–**3** maintain pharmacologically active concentrations in the hemolymph during the dosing interval. Moreover, these values were within the typical range reported for clinically used antimicrobial agents in the silkworm model (*19*). This pharmacokinetic profile supports their potential as anti-MAC agents. To the best of our knowledge, this is the first study to investigate the pharmacokinetics of these related compounds, and the results obtained provide valuable insights for future *in vivo* studies.

In conclusion, the present study demonstrated that nucleoside antibiotics, specifically streptcytosine analogs derived from a marine actinomycete, exhibited significant anti-MAC activities both *in vitro* and *in vivo*. Future research needs to focus on optimizing these compounds through *in vivo* structure-activity relationship studies, particularly by investigating structurally related compounds, such as amicetin and mavintramycins. In addition, their potential for synergistic effects in combination with existing clinical drugs merits further research to accelerate the development of novel anti-MAC therapeutics.

*Funding*: None.

*Conflict of Interest*: The authors have no conflicts of interest to disclose.

## References

1. Bents SJ, Mercaldo RA, Powell C, Henkle E, Marras TK, Prevots DR. Nontuberculous mycobacterial pulmonary disease (NTM PD) incidence trends in the United States, 2010-2019. BMC Infect Dis. 2024; 24:1094.
2. Namkoong H, Kurashima A, Morimoto K, Hoshino

Y, Hasegawa N, Ato M, Mitarai S. Epidemiology of pulmonary nontuberculous mycobacterial disease, Japan. Emerg Infect Dis. 2016; 22:1116-1117.
3. Hosoda K, Koyama N, Shigeno S, Nishimura T, Hasegawa N, Kanamoto A, Ohshiro T, Tomoda H. Mavintramycin A is a promising antibiotic for treating *Mycobacterium avium* complex infectious disease. Antimicrob Agents Chemother. 2024; 68:e0091723.
4. Bu YY, Yamazaki H, Ukai K, Namikoshi M. Anti-mycobacterial nucleoside antibiotics from a marine-derived *Streptomyces* sp. TPU1236A. Mar Drugs. 2014; 12:6102-6112.
5. Hosoda K, Koyama N, Hamamoto H, Yagi A, Uchida R, Kanamoto A, Tomoda H. Evaluation of anti-mycobacterial compounds in a silkworm infection model with *Mycobacteroides abscessus*. Molecules. 2020; 25:4971.
6. Hosoda K, Koyama N, Kanamoto A, Tomoda H. Discovery of nosiheptide, griseoviridin, and eamycin as potent anti-mycobacterial agents against *Mycobacterium avium* complex. Molecules. 2019; 24:1495.
7. Uchida R, Iwatsuki M, Kim YP, Ohte S, Ōmura S, Tomoda H. Nosokomycins, new antibiotics, discovered in an *in vivo*-mimic infection model using silkworm larvae. I. Fermentation, isolation and biological properties. J Antibiot (Tokyo). 2010; 63:151-155.
8. Uchida R, Iwatsuki M, Kim YP, Ōmura S, Tomoda H. Nosokomycins, new antibiotics, discovered in an *in vivo*-mimic infection model using silkworm larvae. II. Structure elucidation. J Antibiot (Tokyo). 2010; 63:157-163.
9. Uchida R, Hanaki H, Matsui H, Hamamoto H, Sekimizu K, Iwatsuki M, Kim YP, Tomoda H. *In vitro* and *in vivo* anti-MRSA activities of nosokomycins. Drug Discov Ther. 2014; 8:249-254.
10. Hamamoto H, Urai M, Ishii K, *et al*. Lysocin E is a new antibiotic that targets menaquinone in the bacterial membrane. Nat Chem Biol. 2015; 11:127-133.
11. Uchida R, Namiguchi S, Ishijima H, Tomoda H. Therapeutic effects of three trichothecenes in the silkworm infection assay with *Candida albicans*. Drug Discov Ther. 2016; 20:44-48.
12. Tominaga T, Uchida R, Koyama N, Tomoda H. Anti-*Rhizopus* activity of tanzawaic acids produced by the hot spring-derived fungus *Penicillium* sp. BF-0005. J Antibiot (Tokyo). 2018; 71:626-632.
13. Yagi A, Uchida R, Hamamoto H, Sekimizu K, Kimura K, Tomoda H. Anti-*Mycobacterium* activity of microbial peptides in a silkworm infection model with *Mycobacterium smegmatis*. J Antibiot (Tokyo). 2017; 70:685-690.
14. Yagi A, Yamazaki H, Terahara T, Yang T, Hamamoto H, Imada C, Tomoda H, Uchida R. Development of an *in vivo*-mimic silkworm infection model with *Mycobacterium avium* complex. Drug Discov Ther. 2021; 14:287-295.
15. Hamamoto H, Tonoike A, Narushima K, Horie R, Sekimizu K. Silkworm as a model animal to evaluate drug candidate toxicity and metabolism. Comp Biochem Physiol C Toxicol Pharmacol. 2009; 149:334-339.
16. Yagi A, Sato T, Kano C, Igari T, Oshima N, Ohte S, Ohshiro T, Uchida R. Evaluation of tirandamycins with selective activity against Enterococci in the silkworm infection model. J Antibiot (Tokyo). 2025; 78:211-218.
17. Serrano CM, Kanna Reddy HR, Eiler D, Koch M, Tresco BIC, Barrows LR, VanderLinden RT, Testa CA, Sebahar PR, Looper RE. Unifying the aminohexopyranose- and peptidyl-nucleoside antibiotics: implications for antibiotic design. Angew Chem Int Ed Engl. 2020; 59:11330-11333.
18. Hamamoto H, Kurokawa K, Kaito C, Kamura K, Manitra Razanajatovo I, Kusuhara H, Santa T, Sekimizu K. Quantitative evaluation of the therapeutic effects of antibiotics using silkworms infected with human pathogenic microorganisms. Antimicrob Agents Chemother. 2004; 48:774-779.
19. Hamamoto H, Horie R, Sekimizu K. Pharmacokinetics of anti-infectious reagents in silkworms. Sci Rep. 2019; 9:9451.

Received June 9, 2025; Revised August 18, 2025; Accepted August 20, 2025.

**Address correspondence to:*
Ryuji Uchida and Akiho Yagi, Division of Natural Product Chemistry, Faculty of Pharmaceutical Sciences, Tohoku Medical and Pharmaceutical University, 4-4-1 Komatsushima, Aoba-ku, Sendai, Miyagi 981-8558, Japan.
E-mail: uchidar@tohoku-mpu.ac.jp (RU) and yagia@tohoku-mpu.ac.jp (AY)

Released online in J-STAGE as advance publication August 24, 2025.

***Brief Report***

DOI: 10.5582/ddt.2025.01063

# Implementation and evaluation of a structured lecture-based training program for early-career pharmacists

**Yuma Nonomiya[1,2,*], Masashi Nakamura[2], Tomonori Nakamura[1], Masakazu Yamaguchi[2]**

[1] Division of Pharmaceutical Care Sciences, Center for Social Pharmaceutical Care Sciences, Keio University Faculty of Pharmacy, Tokyo, Japan;
[2] Department of Pharmacy, Cancer Institute Hospital, Japanese Foundation for Cancer Research, Tokyo, Japan.

**SUMMARY**: Since 2022, the Cancer Institute Hospital of the Japanese Foundation for Cancer Research (JFCR) has participated in a postgraduate clinical training program organized by the Japanese Society of Hospital Pharmacists. Subsequently, the training system for newly employed pharmacists was reviewed. Beginning in 2023, a structured lecture-based training program was introduced for young pharmacists (employees in their first to fifth years of practice). To evaluate the effectiveness and usefulness of the newly implemented lecture-based training program (LBTP), a questionnaire survey was conducted using open-ended and multiple-choice questions based on a 5-point Likert scale. The lectures were conducted with the participation of 12 individuals, all of whom had less than five years of professional experience. All lectures received high ratings in terms of content and the participants' level of understanding, suggesting a high degree of overall satisfaction. Furthermore, after the lectures, the lecturers reported an increased understanding of the lecture-based training program and expressed their willingness to contribute actively in the following fiscal year. Both the participants and lecturers reported high levels of satisfaction, demonstrating the usefulness of the program. As the JFCR is a cancer-specialized hospital, there is a need for more proactive learning on topics beyond oncology. The LBTP had a positive impact on both participants and lecturers, contributing to the enhancement of education for new staff members.

***Keywords***: Questionnaire survey, postgraduate clinical training, psychological safety

## 1. Introduction

Since 2022, the Department of Pharmacy at the Cancer Institute Hospital of the Japanese Foundation for Cancer Research (JFCR) has participated in the postgraduate clinical training program organized and implemented by the Japan Society of Hospital Pharmacists. The aim of this training program is to contribute to the development of a standardized postgraduate training curriculum used in healthcare institutions and pharmacies, with a view to linking it to future preclinical education in pharmaceutical studies. The postgraduate clinical training guidelines set 13 training items, and it was mandated that each item would be evaluated through rubric-based assessments. Additionally, pharmacists were required to deepen their understanding of their roles within team-based healthcare and to enhance their knowledge of pharmacotherapy across a broad range of medical specialties (*1*). JFCR is a cancer-specialized hospital, and while adequate lectures and education in the oncology field are provided, the training items related to other areas had not been clearly defined. Therefore, we considered it crucial to reevaluate the pharmacist training program at JFCR and to develop a novel educational lecture-based training program (LBTP).

Unlike traditional university-style lectures where information is passively absorbed, LBTP incorporates small-group learning approaches such as Problem-Based Learning (PBL) and Team-Based Learning (TBL), fostering active engagement and collaborative learning (*2*). The participants of the LBTP were designated as early-career pharmacists (from their 1st to 5th year of practice). Except for first-year pharmacists, early-career pharmacists were tasked not only with attending the lectures but also with lecturing. The purpose of having early-career pharmacists serve as lecturers was to enhance and refine their own knowledge through the process of teaching (*3*). In response to the growing emphasis placed by the Japan Hospital Pharmacists Association on the active involvement of pharmacists in team-based medical care, pharmacists actively engaged in intra-hospital teams were appointed as lecturers. These individuals not only introduced their respective teams but also provided comprehensive lectures on the professional functions and roles of pharmacists within these teams.

This study aims to evaluate the effectiveness and practical utility of LBTP primarily designed for early-career pharmacists.

## 2. Methods

### 2.1. Questionnaire survey

A questionnaire survey was conducted targeting 12 pharmacists belonging to the pharmacy department of the JFCR, following the LBTP held from June 2023 to February 2024. The questionnaire survey was conducted with both 12 participants and 16 lecturers (Supplementary Figure S1, A and B, *https://www.ddtjournal.com/action/getSupplementalData.php?ID=269*). After the final lecture, a survey regarding new employee training lectures was conducted (Supplementary Figure S1, C, *https://www.ddtjournal.com/action/getSupplementalData.php?ID=269*). The questions were developed by the authors.

### 2.2. Evaluation methods

A simple tabulation was performed using a 5-point Likert scale for the attributes and surveys related to each lecture. Changes in questionnaire scores before and after the lecture were analyzed using the Wilcoxon signed-rank test. Statistical analyses were performed using SPSS software version 24 (IBM Corp.), with the level of significance set at less than 5%. Changes in the lecturers' mindset before and after the lectures were evaluated by asking questions and requesting responses on a 5-point scale (1 = "Do not agree," 2 = "Somewhat disagree," 3 = "Neutral," 4 = "Somewhat agree," and 5 = "Agree"). Box plots were created using JMP Pro 18 software (SAS Institute, Japan).

### 2.3. Ethical considerations

This study was submitted to the Ethics Review Committee of the Cancer Institute Hospital of JFCR; however, it was determined that the study did not fall under the category of life sciences or medical research, and therefore, a review was deemed unnecessary. The purpose of the study, questionnaire items, response methods, privacy protection measures, data handling, and contact information were explained to the survey participants, and their consent was obtained. Personally identifiable information was not obtained.

## 3. Results and Discussion

As shown in Table 1 and Figure S2 (*https://www.ddtjournal.com/action/getSupplementalData.php?ID=269*), participants reported high scores for all lectures across multiple dimensions, including interest in the topic, clarity of the lecture slides, content comprehension, and overall satisfaction. These positive results are likely attributable to the program's clearly defined target audience—early-career pharmacists with less than five years of experience—and the deliberate optimization of lecture content based on the participants' expected baseline knowledge and professional context. This targeted approach helped to reduce mismatches between content difficulty and audience capability, thereby enhancing learning effectiveness. Furthermore, the 30-minute lecture format (20 minutes for presentation and 10 minutes for Q&A) appeared appropriate, aligning with prior studies that suggest shorter lectures more effectively maintain attention and satisfaction among adult learners (*4,5*). The active learning environment, supported by a robust Q&A structure, further contributed to increased participant engagement (*6*). Lecturer

**Table 1. Overview of new employee training lectures and questionnaire collection rates**

| | Content | Pharmacist career (year) | Questionnaire collection rate *n* (%) |
|---|---|---|---|
| 1st | Certified pharmacist system | 5 | 12/12 (100) |
| 2nd | Pediatrics | 5 | 12/12 (100) |
| 3rd | Head and Neck Surgery Procedures and Oral medication management | 4 | 12/12 (100) |
| 4th | Insulin Injection | 2 | 10/12 (83.3) |
| 5th | Suppositories | 2 | 10/12 (83.3) |
| 6th | Renal function and injury | 4 | 10/12 (83.3) |
| 7th | Hepatic function and injury | 4 | 8/11 (72.7) |
| 8th | Pharmacist intervention points in head and neck cancer | 5 | 10/12 (83.3) |
| 9th | High-risk medicine | 15 | 11/12 (91.7) |
| 10th | TDM | 21 | 11/12 (91.7) |
| 11th | Preoperative drug discontinuation | 9 | 10/12 (83.3) |
| 12th | Medical fee calculation | 10 | 10/12 (83.3) |
| 13th | PUT | 20 | 11/12 (91.7) |
| 14th | ICT | 13 | 11/12 (91.7) |
| 15th | NST | 10 | 11/12 (91.7) |
| 16th | PCT | 12 | 10/12 (83.3) |

PUT, Pressure Ulcer Care Team. ICT, Infection Control Team. NST, Nutrition Support Team. PCT, Palliative Care Team.

feedback (Figure 1) adds another layer of insight into the program's impact. While 50% of lecturers did not find the slide preparation burdensome, 37.5% did feel burdened by the process.

Nevertheless, 75% of the lecturers agreed that a 30-minute session was appropriate, and 68.8% reported spending 2 to 6 hours on slide preparation (Figure 1A), suggesting a moderate and manageable workload. Importantly, lecturers' self-reported motivation significantly increased from a pre-lecture median score of 2.8 to a post-lecture median of 4.3 ($p < 0.01$; Figure 1B), indicating a marked shift from initial reluctance or anxiety to greater engagement and satisfaction. Additionally, willingness to deliver the same or a different topic in the following year also increased, with median scores of 4.2 and 3.7, respectively (Figure 1C), both showing statistically significant improvements.

These findings suggest that the lecture experience itself served as a form of professional development, helping early-career pharmacists gain confidence and derive a sense of achievement through successful knowledge sharing. Indeed, such successful experiences positively impact one's mindset (*7*), fostering not only competence but also intrinsic motivation and professional identity formation. The program was independently developed at our institution to address existing gaps in non-oncology education, particularly given Japan's increasing emphasis on the training of generalist pharmacists. Our hospital, being oncology-focused, has limited opportunities for early-career pharmacists to gain exposure to a broader spectrum of diseases. The LBTP was thus designed not only as a knowledge dissemination platform but also as a professional development tool. By encouraging junior pharmacists to select lecture topics, create educational materials, and deliver presentations, the program fostered key competencies such as proactivity, planning, communication, and professionalism (*8,9*). This structure allowed for both horizontal (peer-based) and vertical (mentor-based) learning.

Despite its successes, the program has notable limitations. First, this study was conducted as a cross-sectional survey within a single institution, limiting the generalizability of the findings. Without longitudinal

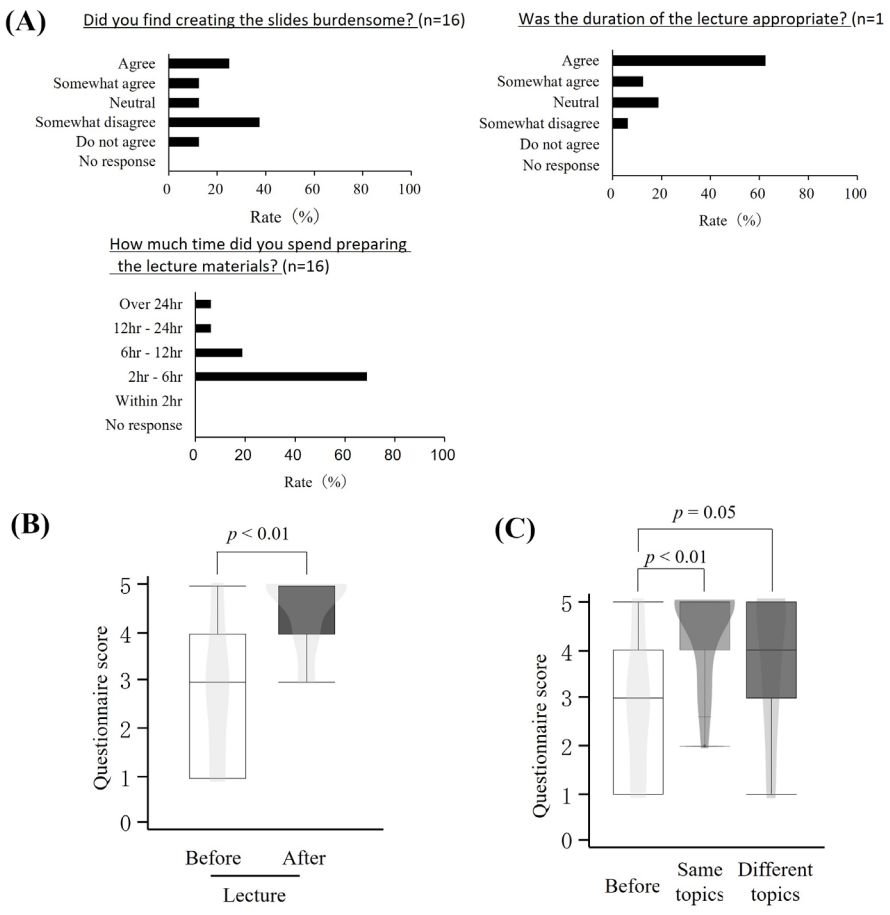


**Figure 1. Lecturers' perceptions and emotional changes related to the LBTP.** (**A**) Lecturer's burden regarding the lecture. (**B**) Changes in lecturers' attitudes towards the lecture before and after the session. (**C**) Changes in lecturers' attitudes when asked to lecture on the same or a different theme in the following year.

follow-up, the sustainability of the observed benefits, such as retained knowledge or behavioral change in clinical settings, remains unknown. Second, the LBTP was developed without benchmarking against standardized or evidence-based models used in other institutions, potentially missing opportunities to adopt best practices. Third, the study relied solely on subjective, self-reported measures. While these provide valuable insights into perceived effectiveness, they cannot fully assess objective learning outcomes or changes in clinical performance. No pre- and post-tests or performance-based assessments were conducted to verify whether actual knowledge or skills improved as a result of the training. Future research should aim to overcome these limitations through multi-institutional, longitudinal studies incorporating objective assessment tools such as knowledge tests, skill-based evaluations, and patient care indicators. This approach would allow for a more comprehensive understanding of the LBTP's real-world impact on pharmacist development and patient safety.

Few previous studies have evaluated educational lectures from both the participant and lecturer perspectives or incorporated design elements that emphasize psychological safety by restricting participation to a specific peer group. The overwhelmingly positive reception of this program from both audiences suggests that such a structure may contribute not only to cognitive learning but also to emotional and professional growth. The dual benefit — to both learners and lecturers — supports the potential for training programs to serve as platforms for mutual development.

In conclusion, the LBTP developed and implemented at our institution proved to be a meaningful educational initiative that benefited participants and lecturers. By combining structured learning with opportunities for teaching and reflection, the program fostered not only knowledge acquisition but also professional growth, confidence, and mindset change. Continued refinement, including the introduction of objective evaluations and broader institutional collaboration, is warranted to further enhance its effectiveness and sustainability.

*Funding*: None.

*Conflict of Interest*: The authors have no conflicts of interest to disclose.

## References

1. Ministry of Health, Labor and Welfare of Japan. *https://www.mhlw.go.jp/content/11120000/000946955.pdf* (accessed November 10, 2024).
2. Mori J. A guide for active and interactive lecture. Shinshu Med J. 2014; 62:25-32.
3. Oyama M, Matsuda T. Current trends and perspectives of ICT utilization in active learning. Japan J Educ Technol. 2018; 42:211-220. (in Japanese)
4. Dent JA, Harden RM. A practical Guide For Medical Teachers. Shinoharashinsha Publishing Inc, 2010, pp. 56-65.
5. Bunce DB, VandenPlas JV, Havanki KL. Comparison of the effectiveness of a student response system versus online WebCT quizzes. J Chem Educ. 2006; 83:488-493.
6. Ishikawa N, Kogo C. Self-regulated learning and problem-solving strategies used by students in online universities. Japan J Educ Technol. 2018; 41:329-343. (in Japanese)
7. Fujimura M. The effects of reflection of success and failure experience on the confidence and effort. Fukoka Jogakuin Daigaku kiyoo. 2014; 15:81-87. (in Japanese?)
8. Inoue H, Uchihashi K, Hirano S, Fujimoto T, Nishikawa Y. Examination of the usefulness of classes using clicker-aided technology on knowledge retention in dental education. J Jap Dent Educ Assoc. 2018; 34:25-32. (in Japanese)
9. Matsushita K. Self-directed learning in university classrooms: from the perspective of learning theories. J Japan Assoc Coll Univ Educ. 2009; 31:14-18. (in Japanese)

Received July 4, 2025; Revised August 18, 2025; Accepted August 23, 2025.

**Address correspondence to:*
Yuma Nonomiya, Division of Pharmaceutical Care Sciences, Center for Social Pharmacy and Pharmaceutical Care Sciences, Keio University Faculty of Pharmacy, 1-5-30 Shibakoen, Minato-ku, Tokyo 105-8512, Japan.
E-mail: nonomiya-ym@keio.jp

Released online in J-STAGE as advance publication August 26, 2025.

Correspondence

DOI: 10.5582/ddt.2025.01068

# A pilot study investigating the efficiency of an Internet of things (IOT)-aided warehouse management system in the management of consumables for the operating room in a Chinese setting

**Guimei Zhang[1], Qi Wang[1], Li Zhao[1], Hao zhang[1], Jie Lin[2,*], Tetsuya Asakawa[3,*]**

[1] Department of Anesthesia, National Clinical Research Center for Infectious Diseases, Shenzhen Third People's Hospital, Shenzhen, Guangdong, China;
[2] Department of Pricing and Medical Insurance Management, National Clinical Research Center for Infectious Diseases, Shenzhen Third People's Hospital, Shenzhen, Guangdong, China;
[3] Institute of Neurology, National Clinical Research Center for Infectious Diseases, Shenzhen Third People's Hospital, Shenzhen, Guangdong, China.

**SUMMARY**: The aim of this study was to investigate the value of an Internet of things (IOT)-aided warehouse management system (IAWMS) to improve the efficiency of consumables management for the operating room (OR). Indices in three domains (error alerts, time taken for work, and level of satisfaction) were selected. Records were compared for two groups, namely the IAWMS group (records after implementation of IAWMS from March 2024 to September 2024) and the control group (manual work before implementation of IAWMS from July 2023 to December 2023). Results revealed that the IAWMS significantly reduced error alerts and the time taken for routine work. The level of satisfaction of the medical staff improved significantly. Noticeably, the time taken to conduct a physical inventory decreased markedly (12.57 ± 1.27 min *vs*. 840.00 ± 120.00 min, $p < 0.0001$). This pilot study confirmed the value of an IAWMS in improving the operational efficiency of consumables management for the OR in a Chinese setting. The IAWMS relieves medical staff from heavy manual work. Thus, the IAWMS is recommended for routine management of consumables for the OR.

***Keywords***: Internet of things (IOT), consumables management, operating room, operational efficiency, level of satisfaction

An operating room (OR) is one of the most important locations in a general hospital. Research has indicated that over 60% of patients are treated in the OR, accounting for 33% of inpatient costs (*1*). The OR markedly affects revenue and costs in a given hospital. Moreover, the OR plays a crucial role in the efficiency and safety of hospitals. Warehouse management plays a vital role in OR management. Warehouse management, and particularly consumables management, significantly influences the surgical process (*2*). Highly efficient and convenient consumable availability help to reduce medical costs and improve the quality of care (*3*). Conversely, disruption of or inefficiency in the OR, such as a disruption of flow, may cause the cessation of surgery or increase the operating time, ultimately influencing surgical efficiency. Accordingly, improving warehouse management, and particularly consumables management, is an urgent task for OR managers. However, conventional management of consumables for the OR in warehouses relies on manual work. There are often scores of consumables for the OR; the demand is high, but the medical staffing is insufficient. Poor management can cause medical errors, loss of consumables, or unnecessary waste. Moreover, a large amount of time may be spent and manpower allocated to perform routine work, such as registering consumables upon receipt/return, conducting a physical inventory, and calculation of costs. Therefore, a more effective OR-related warehouse management system is required. Thanks to the development of computer technology, many computer-based management systems have been developed and used in OR management in Chinese settings.

An Internet of things (IOT)-aided warehouse management system (IAWMS, Figure 1A) was introduced to manage consumables for the OR in March 2024. Thus, this pilot study was designed to investigate the efficiency of the IAWMS. We investigated whether the IAWMS can reduce error alerts and the time taken for work. The level of satisfaction among the medical staff involved was also investigated. This study should help to gain a better understanding of the value of an IAWMS during management of consumables for the OR.

Figure 1A shows the system configuration for the IAWMS. The supply, processing, and distribution (SPD) smart management system serves as the host machine, which is connected to sensors, a face recognition system, user interface, storage system, and alarm system *via* a local area network (Figure 1A). All consumables are categorized and encoded with a label with a quick response (QR) code, with colors representing the attributes of these consumables (Figure 1B). Figure 1C depicts the standard operating procedure (SOP) for different implementation scenarios. First, all qualified medical staff members are registered in the system for face recognition. When receiving consumables, they enter the warehouse and select the required consumables, scan the QR code on the consumable *via* a portable data assistant (PDA) terminal connected to the WIFI network, and obtain the consumable. All information regarding consumables is recorded in the system, including the number of consumables and their costs. When returning consumables, all QR codes on the returned consumables are scanned and recorded in the system. During a physical inventory, consumables are conveniently managed by scanning the QR codes. All procedures are connected to and supervised by hospital management

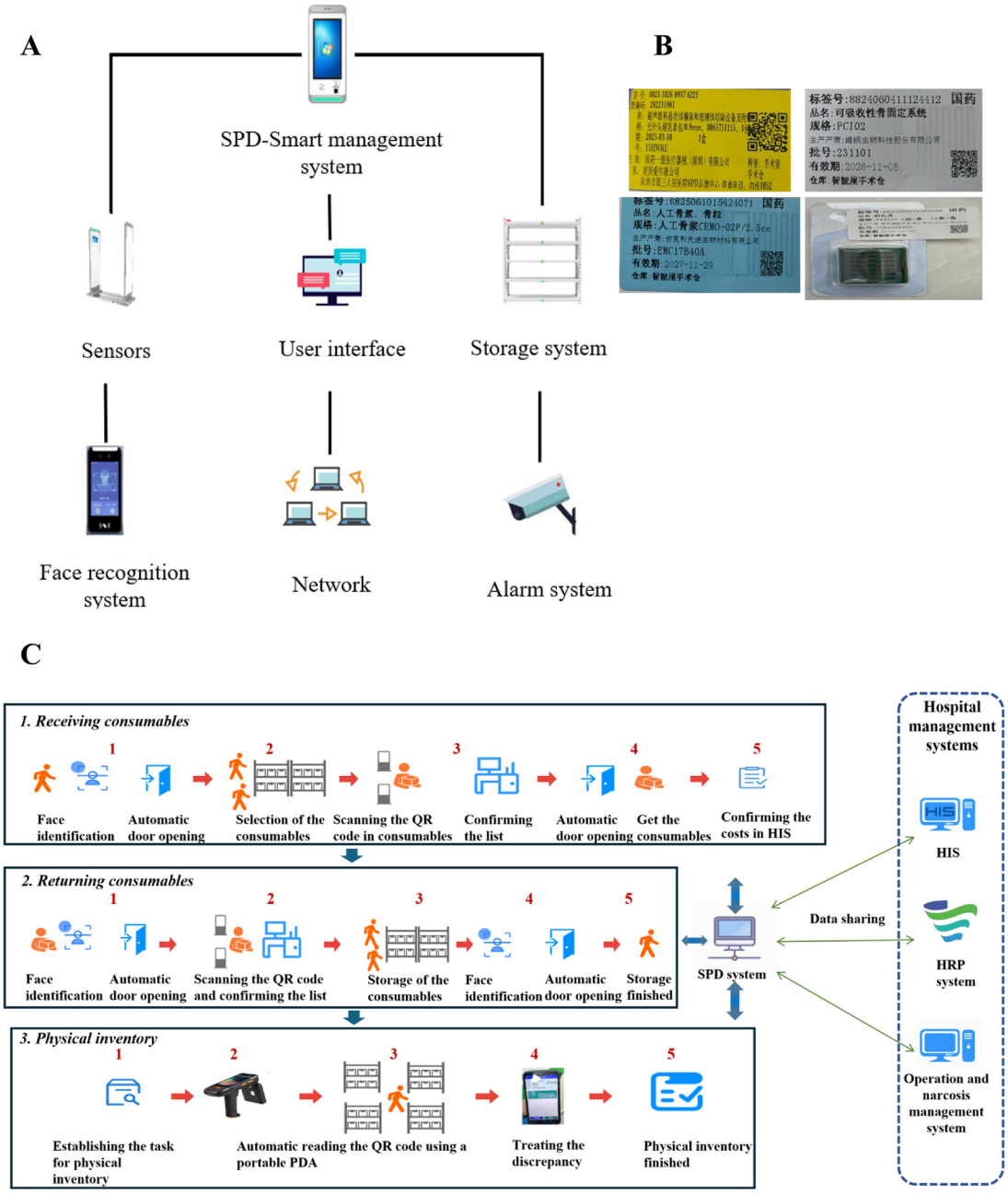


**Figure 1. Diagram of the use of an IOT-aided warehouse management system (IAWMS) in a clinical setting. (A)** Diagram of the IAWMS. **(B)** Labels for consumables with different colors, which represent different categories of consumables. (C) Standard operating procedures for receiving consumables, returning consumables, and physical inventory using the IAWMS. IAWMS, IOT-aided warehouse management system; IOT, Internet of things; HIS, hospital information system; HRP, hospital resource planning; PDA, portable data assistant; QR code, quick response code; SPD, supply, processing, and distribution.

**Table 1. Indices of warehouse management**

| Item | IAWMS group | Control group | *p* |
|---|---|---|---|
| Total number of warehouses exits | 205.7 ± 36.35 | 204.8 ± 35.89 | 0.85 |
| Error alerts | *n* = 90 | *n* = 92 | |
| No QR code scanned during warehouse exit | 0.37 ± 0.68 | 21.96 ± 11.96 | < 0.001 |
| No QR code scanned during invoicing | 0.48 ± 0.71 | 16.83 ± 7.14 | < 0.001 |
| Errors in system login | 0.13 ± 0.34 | 16.4 ± 6.88 | < 0.001 |
| Errors involving items not returned to their original position | 0.28 ± 0.45 | 0.63 ± 5.46 | < 0.001 |
| Time (minutes) taken for work | *n* = 4,075 | *n* = 4,116 | |
| Time taken to conduct a physical inventory | 12.57 ± 1.27 | 840.00 ± 120.00 | < 0.0001 |
| Time taken to receive consumables | 0.16 ± 0.05 | 15.48 ± 2.72 | < 0.001 |
| Time taken to audit expenses | 4.25 ± 0.10 | 29.94 ± 4.56 | < 0.001 |
| Level of satisfaction (%) (*n* = 76) | | | |
| Convenient process | 81.82 | 25.00 | < 0.0001 |
| Trace management | 77.27 | 14.47 | < 0.0001 |
| Sorting and reorganizing | 81.82 | 6.58 | < 0.0001 |

systems, and data are shared (Figure 1).

Records of two groups were compared, namely the IAWMS group (records after implementation of the IAWMS from March 2024 to September 2024) and the control group (manual work before implementation of the IAWMS from July 2023 to December 2023). This study included indices in three domains. The first domain was the "error alerts" generated by the IAWMS and previous manual records, including the indices of "No QR code scanned during warehouse exit", "QR code scanned during invoicing", "errors in system login", and "errors involving items not returned to their original position." We analyzed the errors recorded in the system. The second domain was the "time taken for work", which recorded times including "the time taken to conduct a physical inventory", "the time taken to receive consumables", and "the time taken to audit expenses." The time taken for each index was recorded in a clinical setting. The third domain was the "level of satisfaction", which covered a "convenient process", "trace management", and "sorting and reorganizing." A three-question questionnaire was developed in light of the problems that were identified in a poll before implementation of the IAWMS, that is the top three concerns regarding the manual management of consumables for the OR. It was used to investigate the level of satisfaction with the three aspects above.

The software SPSS (V26.00, IBM, IL, USA) was used for statistical analysis. The Kolmogorov-Smirnov test was used to confirm the normal distribution of the data. Data are expressed as the mean ± standard deviation (SD). The Student's t-test was used to compare the differences in continuous variables between the two groups. The chi-square test was used to compare the differences in rates between the two groups. $p < 0.05$ was considered to indicate a statistically significant difference.

Table 1 shows the improvements resulting from use of the IAWMS. The first domain is the "error alerts" generated by the system. A total of 182 records (90 from the IAWMS group and 92 from the control group) were analyzed. Indices of "No QR code scanned during warehouse exit" (0.37 ± 0.68 *vs*. 21.96 ± 11.96, $p < 0.001$), "No QR code scanned during invoicing" (0.48 ± 0.71 *vs*. 16.83 ± 7.14, $p < 0.001$), "errors in system login" (0.13 ± 0.34 *vs*. 16.4 ± 6.88, $p < 0.001$), and "errors involving items not returned to their original position" (0.28 ± 0.45 *vs*. 0.63 ± 5.46, $p < 0.001$) decreased significantly due to use of the IAWMS (IAWMS group *vs*. control group). In the domain of "time taken for work", a total of 8,191 records (4,075 in the IAWMS group and 4,116 in the control group) were investigated. Using the IAWMS significantly reduced "the time taken to conduct a physical inventory" (12.57 ± 1.27 min *vs*. 840.00 ± 120.00 min, $p < 0.0001$), "the time taken to receive consumables" (0.16 ± 0.05 min *vs*. 15.48 ± 2.72 min, $p < 0.001$), and "the time taken to audit expenses" (4.25 ± 0.10 min *vs*. 29.94 ± 4.56 min, $p < 0.001$) compared to times for the control group. Notably, the time taken to conduct a physical inventory decreased markedly (average 12.57 min for the IAWMS group *vs*. 840.00 min for the control group). A total of 76 valid questionnaires were received with respect to the domain of satisfaction. The IAWMS group had a significantly improved level of satisfaction with the "convenient process" (81.82% *vs*. 25.00%, $p < 0.001$), "trace management" (77.27% *vs*. 14.47%, $p < 0.001$), and "sorting and reorganizing" (81.82% *vs*. 6.58%, $p < 0.001$) compared to the control group (Table 1). Hence, the implementation of an IAWMS significantly improved the operational efficiency of consumables management for the OR.

The present study conducted a pilot study to compare the efficiency of consumables management for the OR of a general hospital in China before and after use of an IAWMS. Results revealed that the implementation of the IAWMS significantly reduced error alerts and the time taken for routine work. The level of satisfaction of the medical staff improved significantly. Findings indicated the value of an IAWMS in improving consumables management for the OR.

The quality of OR management significantly affects

the quality of medical care in a clinical setting. Studies worldwide have confirmed that improved management can indeed enhance operational efficiency in the OR (*2,4-6*). The evidence obtained in this study is that the IAWMS helps to reduce errors. This means that the accuracy improved significantly, which agrees with the results of a previous study conducted in China. Liu *et al*. found that using an intelligent mode reduced the total error rate from 4% to 1% (*6*). The second piece of evidence is that the IAWMS reduced the time taken for routine work, and particularly conducting a physical inventory (average 12.57 min *vs*. 840.00 min). Compared to a previous study in which the inventory time was 12 ± 5 min less, the inventory accuracy increased from 94.6% to 98.6% in Liu's study (*6*), and the improvements noted in the current study are greater. Indeed, the IAWMS was highly capable of reducing the time taken for work. Thus, the operational efficiency improved and manpower was saved. Moreover, the IAWMS helped to improve the level of satisfaction of the medical staff. Before the implementation of the IAWMS, the routine work of consumables management, such as conducting a physical inventory, was a heavy and stressful job because it mainly relied on manual work. Using a simple "scan", the IAWMS relieves the medical staff from heavy manual work. Improvement of the level of satisfaction helps to alleviate workplace stress and improve operational efficiency, which may help to improve the quality of medical care.

Although this study verified the value of an IAWMS in improving the operational efficiency of consumables management, a point that should be borne in mind is that the IAWMS, as a computer-based system, should be optimized in response to the development of surgical technology and novel consumables. Moreover, this "improvement" was based on the machine record and investigation of medical staff. However, once the efficiency of consumables management is improved, it can reduce the time for surgical preparations and the duration of anesthesia, thereby decreasing surgical complications. We believe that improvements provided by an IAWMS may directly improve surgical procedures. Future studies should focus on direct improvement in the quality of surgery and clinical outcomes for patients.

This study had several limitations: *i*) This study used a before-and-after experimental design rather than a randomized or contemporaneous control setting, so the present findings might be influenced by time-related confounders, such as seasonal effects, changes in hospital policy, and staff turnover, thereby potentially inflating the intervention's effect size. *ii*) We did not measure the reliability of these investigations in this pilot study, such as test-retest and internal consistency, which should be addressed in a future study.

In conclusion, this pilot study investigated the value of an IAWMS in improving the operational efficiency of consumables management for the OR in a Chinese setting. The IAWMS relieves medical staff from heavy manual work. Accordingly, it reduced error alerts and the time taken during routine work, and it improved the level of satisfaction among the medical staff. Thus, an IAWMS is recommended for routine consumables management for the OR.

*Funding*: This study was supported by a grant from the Shenzhen Fund for Construction of High-level Hospitals (no. 23274G1001).

*Conflict of Interest*: The authors have no conflicts of interest to disclose.

**References**

1. Hosseinzadeh F, Sepehri MM, Khasha R, Taherkhani N. A framework to find flow disruptions in the operating rooms' consumable supplies. Periop Care OR Mgmt. 2020; 21:100136.
2. Mohan S, Mangal TD, Colbourn T, *et al*. Factors associated with medical consumable availability in level 1 facilities in Malawi: A secondary analysis of a facility census. Lancet Glob Health. 2024; 12:e1027-e1037.
3. Zhao F, Yu M, Zhao Z, Zhou X. Cost control and management of low-value consumables in operating room. 2019.
4. Berry M, Berry-Stolzle T, Schleppers A. Operating room management and operating room productivity: The case of Germany. Health Care Manag Sci. 2008; 11:228-239.
5. Pugliesi PS, Frick H, Guillot S, Ferrare K, Renzullo C, Benoist A, Ribes S, Beltramo G, Maldiney T, Ter Schiphorst R, Abdul Malak C, Bevand A, Marrauld L, Lejeune C. Cost of carbon in the total cost of a healthcare procedure: Example of micro-costing study in a French setting. Appl Health Econ Health Policy. 2025; 23:265-275.
6. Liu J, Xing LM, Shi X. Application of intelligent management mode for drugs and consumables in anesthesiology department. Eur Rev Med Pharmacol Sci. 2022; 26:5053-5062.

Received July 4, 2025; Revised August 8, 2025; Accepted August 24, 2025.

**Address correspondence to:*
Tetsuya Asakawa, Institute of Neurology, National Clinical Research Center for Infectious Diseases, Shenzhen Third People's Hospital, 29 Bulan Road, Shenzhen 518112, Guangdong, China.
E-mail: asakawat1971@gmail.com

Jie Lin, Department of Pricing and Medical Insurance Management, National Clinical Research Center for Infectious Diseases, Shenzhen Third People's Hospital, 29 Bulan Road, Shenzhen 518112, Guangdong, China.
E-mail: 470096676@qq.com

Released online in J-STAGE as advance publication August 26, 2025.

**Correspondence**

DOI: 10.5582/ddt.2025.01058

# Telisotuzumab vedotin: The first-in-class c-Met-targeted antibody-drug conjugate granted FDA accelerated approval for treatment of non-squamous non-small cell lung cancer (NSCLC)

**Chenru Zhao[1], Daoran Lu[2], Jianjun Gao[2,*]**

[1] Department of Pharmacy, Qingdao Central Hospital, University of Health and Rehabilitation Sciences, Qingdao, Shandong, China;
[2] Department of Pharmacology, School of Pharmacy, Qingdao Medical College, Qingdao University, Qingdao, Shandong, China.

**SUMMARY**: Telisotuzumab vedotin represents a clinically important antibody-drug conjugate (ADC) that received accelerated approval from the US Food and Drug Administration in May 2025, establishing it as the first-in-class targeted therapy for adult patients with immunohistochemistry (IHC)-confirmed high-c-Met, EGFR wild-type, locally advanced or metastatic non-squamous non-small cell lung cancer (NSCLC). Its mechanism of action relies on precise targeting of the c-Met protein receptor, followed by internalization and release of the potent cytotoxic payload monomethyl auristatin E (MMAE) to eradicate tumor cells. The pivotal phase II LUMINOSITY trial demonstrated that the high c-Met overexpressing group had an overall response rate (ORR) of 34.6%. This therapeutic agent addresses a critical unmet need within a molecularly defined NSCLC subpopulation, marking a substantial advancement in c-Met-targeted oncology. The regulatory authorization and clinical use of telisotuzumab vedotin may significantly advance precision medicine for NSCLC, though an ongoing phase III trial will further confirm its efficacy and safety and determine its eligibility for full regulatory approval in the future.

***Keywords***: MET, lung cancer, NSCLC, Teliso-V

Non-small cell lung cancer (NSCLC) accounts for approximately 85% of all lung cancer cases and represents one of the leading causes of cancer-related mortality worldwide (*1*). Based on its histopathological characteristics, NSCLC is primarily classified into three major subtypes: adenocarcinoma, squamous cell carcinoma, and large cell carcinoma. Adenocarcinoma constitutes the most prevalent subtype, representing approximately 40% of NSCLC cases, followed by squamous cell carcinoma (25-30%), and large cell carcinoma (10-15%) (*2*). The development of targeted therapies for NSCLC stands as a paradigm of precision oncology in solid tumors. From epidermal growth factor receptor (EGFR) tyrosine kinase inhibitors to breakthrough agents against emerging targets such as human epidermal growth factor receptor 2 (HER2) and Kirsten rat sarcoma viral oncogene homologue (KRAS), NSCLC treatment has entered an era of molecularly guided precision therapy (*3,4*). While significant advances have been made in targeted therapies for NSCLC, acquired resistance to targeted agents remains a critical challenge in clinical practice, substantially hampering further improvements in therapeutic efficacy. The development of novel-targeting agents holds promise for enhancing patient outcomes.

On May 14, 2025, the US Food and Drug Administration (FDA) granted accelerated approval to telisotuzumab vedotin (Emrelis) for the treatment of patients with locally advanced or metastatic non-squamous NSCLC exhibiting high c-Met protein expression (defined as strong staining in ≥ 50% of tumor cells) who have experienced disease progression following a prior systemic therapy (*5*). Concurrently, the FDA approved the VENTANA MET (SP44) RxDx assay as a companion diagnostic tool to identify patients with high c-Met tumors eligible for this therapy. Telisotuzumab vedotin is a tripartite antibody-drug conjugate consisting of: (*i*) A humanized immunoglobulin G1 kappa (IgG1κ) monoclonal antibody that specifically binds to the c-Met receptor on tumor cell surfaces; (*ii*) A protease-cleavable valine-citrulline linker tethering the antibody to the cytotoxic payload; and (*iii*) The microtubule-inhibiting agent monomethyl auristatin E (MMAE), which induces tumor cell apoptosis through inhibition of microtubule polymerization (*6*). Following binding to c-Met-overexpressing tumor cells and subsequent internalization, telisotuzumab vedotin releases MMAE,

enabling targeted cytotoxicity against actively dividing cancer cells while minimizing toxicity to normal tissues. As the first and currently only FDA-approved antibody-drug conjugate specifically indicated for high c-Met NSCLC, this agent addresses a significant therapeutic gap in this molecularly defined patient population.

The accelerated approval of telisotuzumab vedotin was based on findings from the LUMINOSITY trial (NCT03539536) (*7*). This multicenter, open-label, multi-cohort phase 2 clinical trial evaluated the therapeutic efficacy of telisotuzumab vedotin in the treatment of non-squamous EGFR wild-type NSCLC with c-Met overexpression (≥ 25% of tumor cells with 3+ staining, with high expression defined as ≥ 50% of tumor cells with 3+ staining and moderate expression defined as 25-50% of tumor cells with 3+ staining). Participants received telisotuzumab vedotin at a dose of 1.9 mg/kg *via* intravenous infusion every two weeks until disease progression or unacceptable toxicity. A total of 78 patients in the high c-Met expressing group were included in the efficacy analysis. The primary endpoint, the overall response rate (ORR), was 34.6%, and the secondary endpoints were as follows: the disease control rate (DCR) was 60.3%, the median duration of response (DOR) was 9.0 months, median progression-free survival (PFS) was 5.5 months, and median overall survival (OS) was 14.6 months (*7*). In the moderate c-Met expression group, 83 patients were included in the efficacy analysis. The primary endpoint, the ORR, was 22.9%, and the secondary clinical endpoints were as follows: the DCR was 57.8%, median DOR was 7.2 months, median PFS was 6.0 months, and median OS was 14.2 months (*7*). In terms of treatment-related adverse events (AEs), the most common all-grade AEs were peripheral sensory neuropathy (30%), peripheral edema (16%), and fatigue (14%); the most common grade ≥ 3 AE was peripheral sensory neuropathy (7%) (*7*).

Previously, small-molecule inhibitors targeting c-Met, such as capmatinib, tepotinib, and savolitinib, have been approved for the treatment of advanced NSCLC patients with tumors harboring *MET* exon 14 (METex14) skipping mutations. Telisotuzumab vedotin represents a first-in-class antibody-drug conjugate directed against the biomarker of c-Met protein overexpression. This agent provides a critical second-line and beyond treatment option for EGFR wild-type, high c-Met non-squamous NSCLC patients who previously lacked effective targeted therapies. As an agent with accelerated approval, its confirmatory phase III trial (TeliMET NSCLC-01, NCT04928846) is currently underway, directly comparing telisotuzumab vedotin versus docetaxel in the treatment of non-squamous, c-Met-overexpression, EGFR wild-type advanced/metastatic NSCLC, with OS and PFS as primary endpoints (*8*). The trial outcomes will determine its eligibility for full regulatory approval in the future.

*Funding*: None.

*Conflict of Interest*: The authors have no conflicts of interest to disclose.

## References

1. Stravopodis DJ, Papavassiliou KA, Papavassiliou AG. Vistas in non-small cell lung cancer (NSCLC) treatment: of kinome and signaling networks. Int J Biol Sci. 2023; 19:2002-2005.
2. Khodabakhshi Z, Mostafaei S, Arabi H, Oveisi M, Shiri I, Zaidi H. Non-small cell lung carcinoma histopathological subtype phenotyping using high-dimensional multinomial multiclass CT radiomics signature. Comput Biol Med. 2021; 136:104752.
3. Tang Y, Pu X, Yuan X, Pang Z, Li F, Wang X. Targeting KRASG12D mutation in non-small cell lung cancer: Molecular mechanisms and therapeutic potential. Cancer Gene Ther. 2024; 31:961-969.
4. Yu Y, Yang Y, Li H, Fan Y. Targeting HER2 alterations in non-small cell lung cancer: Therapeutic breakthrough and challenges. Cancer Treat Rev. 2023; 114:102520.
5. US Food and Drug Administration. FDA grants accelerated approval to telisotuzumab vedotin-tllv for NSCLC with high c-Met protein overexpression. *https://www.fda.gov/drugs/resources-information-approved-drugs/fda-grants-accelerated-approval-telisotuzumab-vedotin-tllv-nsclc-high-c-met-protein-overexpression* (accessed June 21, 2025).
6. EMRELISTM (telisotuzumab vedotin-tllv) for injection, for intravenous use. *https://www.accessdata.fda.gov/drugsatfda_docs/label/2025/761384s000lbl.pdf* (accessed June 21, 2025).
7. Camidge DR, Bar J, Horinouchi H, Goldman J, *et al*. Telisotuzumab vedotin monotherapy in patients with previously treated c-Met protein-overexpressing advanced nonsquamous EGFR-wildtype non-small cell lung cancer in the phase II LUMINOSITY trial. J Clin Oncol. 2024; 42:3000-3011.
8. Lu S, Goldman JW, Tanizaki J, *et al*. A phase 3 global study of telisotuzumab vedotin versus docetaxel in previously treated patients with c-Met overexpressing, EGFR wildtype, locally advanced/metastatic nonsquamous NSCLC (TeliMET NSCLC-01). J Clin Oncol. 2024; 42 (Suppl):TPS8656.

Received June 24, 2025; Revised July 6, 2025; Accepted July 7, 2025.

**Address correspondence to:*
Jianjun Gao, Department of Pharmacology, School of Pharmacy, Qingdao Medical College, Qingdao University, Qingdao, Shandong, China.
E-mail: gaojj@qdu.edu.cn

Released online in J-STAGE as advance publication July 11, 2025.

DD&T
Drug Discoveries & Therapeutics

# Guide for Authors

**1. Scope of Articles**

***Drug Discoveries & Therapeutics*** (Print ISSN 1881-7831, Online ISSN 1881-784X) welcomes contributions in all fields of pharmaceutical and therapeutic research such as medicinal chemistry, pharmacology, pharmaceutical analysis, pharmaceutics, pharmaceutical administration, and experimental and clinical studies of effects, mechanisms, or uses of various treatments. Studies in drug-related fields such as biology, biochemistry, physiology, microbiology, and immunology are also within the scope of this journal.

**2. Submission Types**

**Original Articles** should be well-documented, novel, and significant to the field as a whole. An Original Article should be arranged into the following sections: Title page, Abstract, Introduction, Materials and Methods, Results, Discussion, Acknowledgments, and References. Original articles should not exceed 5,000 words in length (excluding references) and should be limited to a maximum of 50 references. Articles may contain a maximum of 10 figures and/or tables. Supplementary Data are permitted but should be limited to information that is not essential to the general understanding of the research presented in the main text, such as unaltered blots and source data as well as other file types.

**Brief Reports** definitively documenting either experimental results or informative clinical observations will be considered for publication in this category. Brief Reports are not intended for publication of incomplete or preliminary findings. Brief Reports should not exceed 3,000 words in length (excluding references) and should be limited to a maximum of 4 figures and/or tables and 30 references. A Brief Report contains the same sections as an Original Article, but the Results and Discussion sections should be combined.

**Reviews** should present a full and up-to-date account of recent developments within an area of research. Normally, reviews should not exceed 8,000 words in length (excluding references) and should be limited to a maximum of 10 figures and/or tables and 100 references. Mini reviews are also accepted, which should not exceed 4,000 words in length (excluding references) and should be limited to a maximum of 5 figures and/or tables and 50 references.

**Policy Forum** articles discuss research and policy issues in areas related to life science such as public health, the medical care system, and social science and may address governmental issues at district, national, and international levels of discourse. Policy Forum articles should not exceed 3,000 words in length (excluding references) and should be limited to a maximum of 5 figures and/or tables and 30 references.

**Case Reports** should be detailed reports of the symptoms, signs, diagnosis, treatment, and follow-up of an individual patient. Case reports may contain a demographic profile of the patient but usually describe an unusual or novel occurrence. Unreported or unusual side effects or adverse interactions involving medications will also be considered. Case Reports should not exceed 3,000 words in length (excluding references).

**Communications** are short, timely pieces that spotlight new research findings or policy issues of interest to the field of global health and medical practice that are of immediate importance. Depending on their content, Communications will be published as "Comments" or "Correspondence". Communications should not exceed 1,500 words in length (excluding references) and should be limited to a maximum of 2 figures and/or tables and 20 references.

**Editorials** are short, invited opinion pieces that discuss an issue of immediate importance to the fields of global health, medical practice, and basic science oriented for clinical application. Editorials should not exceed 1,000 words in length (excluding references) and should be limited to a maximum of 10 references. Editorials may contain one figure or table.

**News** articles should report the latest events in health sciences and medical research from around the world. News should not exceed 500 words in length.

**Letters** should present considered opinions in response to articles published in *Drug Discoveries & Therapeutics* in the last 6 months or issues of general interest. Letters should not exceed 800 words in length and may contain a maximum of 10 references. Letters may contain one figure or table.

**3. Editorial Policies**

For publishing and ethical standards, *Drug Discoveries & Therapeutics* follows the Recommendations for the Conduct, Reporting, Editing, and Publication of Scholarly Work in Medical Journals issued by the International Committee of Medical Journal Editors (ICMJE, *https://icmje.org/recommendations*), and the Principles of Transparency and Best Practice in Scholarly Publishing jointly issued by the Committee on Publication Ethics (COPE, *https://publicationethics.org/resources/guidelines-new/principles-transparency-and-best-practice-scholarly-publishing*), the Directory of Open Access Journals (DOAJ, *https://doaj.org/apply/transparency*), the Open Access Scholarly Publishers Association (OASPA, *https://oaspa.org/principles-of-transparency-and-best-practice-in-scholarly-publishing-4*), and the World Association of Medical Editors (WAME, *https://wame.org/principles-of-transparency-and-best-practice-in-scholarly-publishing*).

*Drug Discoveries & Therapeutics* will perform an especially prompt review to encourage innovative work. All original research will be subjected to a rigorous standard of peer review and will be edited by experienced copy editors to the highest standards.

**Ethical Approval of Studies and Informed Consent:** For all manuscripts reporting data from studies involving human participants or animals, formal review and approval, or formal review and waiver, by an appropriate institutional review board or ethics committee is required and should be described in the Methods section. When your manuscript contains any case details, personal information and/or images of patients or other individuals, authors must obtain appropriate written consent, permission and release in order to comply with all applicable laws and regulations concerning privacy and/or security of personal information. The consent form needs to comply with the relevant legal requirements of your particular jurisdiction, and please do not send signed consent form to *Drug Discoveries & Therapeutics* to respect your patient's and any other individual's privacy. Please instead describe the information clearly in the Methods (patient consent) section of your manuscript while retaining copies of the signed forms in the event they should be needed. Authors should also state that the study conformed to the provisions of the Declaration of Helsinki (as revised in 2013, *https://wma.net/what-we-do/medical-ethics/declaration-of-helsinki*). When reporting experiments on animals, authors should indicate whether the institutional and national guide for the care and use of laboratory animals was followed.

**Reporting Clinical Trials:** The ICMJE (*https:// icmje.org/recommendations/browse/publishing-and-editorial-issues/clinical-trial-registration.html*) defines a clinical trial as any research project that prospectively assigns people or a group of people to an intervention, with or without concurrent comparison or control groups, to study the relationship between a health-related intervention and a health outcome. Registration of clinical trials in a public trial registry

at or before the time of first patient enrollment is a condition of consideration for publication in *Drug Discoveries & Therapeutics*, and the trial registration number will be published at the end of the Abstract. The registry must be independent of for-profit interest and publicly accessible. Reports of trials must conform to CONSORT 2010 guidelines (*https://consort-statement.org/consort-2010*). Articles reporting the results of randomized trials must include the CONSORT flow diagram showing the progress of patients throughout the trial.

**Conflict of Interest:** All authors are required to disclose any actual or potential conflict of interest including financial interests or relationships with other people or organizations that might raise questions of bias in the work reported. If no conflict of interest exists for each author, please state "There is no conflict of interest to disclose".

**Submission Declaration:** When a manuscript is considered for submission to *Drug Discoveries & Therapeutics*, the authors should confirm that 1) no part of this manuscript is currently under consideration for publication elsewhere; 2) this manuscript does not contain the same information in whole or in part as manuscripts that have been published, accepted, or are under review elsewhere, except in the form of an abstract, a letter to the editor, or part of a published lecture or academic thesis; 3) authorization for publication has been obtained from the authors' employer or institution; and 4) all contributing authors have agreed to submit this manuscript.

**Initial Editorial Check:** Immediately after submission, the journal's managing editor will perform an initial check of the manuscript. A suitable academic editor will be notified of the submission and invited to check the manuscript and recommend reviewers. Academic editors will check for plagiarism and duplicate publication at this stage. The journal has a formal recusal process in place to help manage potential conflicts of interest of editors. In the event that an editor has a conflict of interest with a submitted manuscript or with the authors, the manuscript, review, and editorial decisions are managed by another designated editor without a conflict of interest related to the manuscript.

**Peer Review:** *Drug Discoveries & Therapeutics* operates a single-anonymized review process, which means that reviewers know the names of the authors, but the authors do not know who reviewed their manuscript. All articles are evaluated objectively based on academic content. External peer review of research articles is performed by at least two reviewers, and sometimes the opinions of more reviewers are sought. Peer reviewers are selected based on their expertise and ability to provide quality, constructive, and fair reviews. For research manuscripts, the editors may, in addition, seek the opinion of a statistical reviewer. Every reviewer is expected to evaluate the manuscript in a timely, transparent, and ethical manner, following the COPE guidelines (*https://publicationethics.org/files/cope-ethical-guidelines-peer-reviewers-v2_0.pdf*). We ask authors for sufficient revisions (with a second round of peer review, when necessary) before a final decision is made. Consideration for publication is based on the article's originality, novelty, and scientific soundness, and the appropriateness of its analysis.

**Suggested Reviewers:** A list of up to 3 reviewers who are qualified to assess the scientific merit of the study is welcomed. Reviewer information including names, affiliations, addresses, and e-mail should be provided at the same time the manuscript is submitted online. Please do not suggest reviewers with known conflicts of interest, including participants or anyone with a stake in the proposed research; anyone from the same institution; former students, advisors, or research collaborators (within the last three years); or close personal contacts. Please note that the Editor-in-Chief may accept one or more of the proposed reviewers or may request a review by other qualified persons.

**Language Editing:** Manuscripts prepared by authors whose native language is not English should have their work proofread by a native English speaker before submission. If not, this might delay the publication of your manuscript in *Drug Discoveries & Therapeutics*.

The Editing Support Organization can provide English proofreading, Japanese-English translation, and Chinese-English translation services to authors who want to publish in *Drug Discoveries & Therapeutics* and need assistance before submitting a manuscript. Authors can visit this organization directly at *https://www.iacmhr.com/iac-eso/support.php?lang=en. IAC-ESO* was established to facilitate manuscript preparation by researchers whose native language is not English and to help edit works intended for international academic journals.

**Copyright and Reuse:** Before a manuscript is accepted for publication in *Drug Discoveries & Therapeutics*, authors will be asked to sign a transfer of copyright agreement, which recognizes the common interest that both the journal and author(s) have in the protection of copyright. We accept that some authors (*e.g.*, government employees in some countries) are unable to transfer copyright. A JOURNAL PUBLISHING AGREEMENT (JPA) form will be e-mailed to the authors by the Editorial Office and must be returned by the authors by mail, fax, or as a scan. Only forms with a hand-written signature from the corresponding author are accepted. This copyright will ensure the widest possible dissemination of information. Please note that the manuscript will not proceed to the next step in publication until the JPA Form is received. In addition, if excerpts from other copyrighted works are included, the author(s) must obtain written permission from the copyright owners and credit the source(s) in the article.

**4. Cover Letter**

The manuscript must be accompanied by a cover letter prepared by the corresponding author on behalf of all authors. The letter should indicate the basic findings of the work and their significance. The letter should also include a statement affirming that all authors concur with the submission and that the material submitted for publication has not been published previously or is not under consideration for publication elsewhere. The cover letter should be submitted in PDF format. For an example of Cover Letter, please visit: Download Centre (*https://www.ddtjournal.com/downcentre)*.

**5. Submission Checklist**

The Submission Checklist should be submitted when submitting a manuscript through the Online Submission System. Please visit Download Centre (*https://www.ddtjournal.com/downcentre)* and download the Submission Checklist file. We recommend that authors use this checklist when preparing your manuscript to check that all the necessary information is included in your article (if applicable), especially with regard to Ethics Statements.

**6. Manuscript Preparation**

Manuscripts are suggested to be prepared in accordance with the "Recommendations for the Conduct, Reporting, Editing, and Publication of Scholarly Work in Medical Journals", as presented at *http://www.ICMJE.org*.

Manuscripts should be written in clear, grammatically correct English and submitted as a Microsoft Word file in a single-column format. Manuscripts must be paginated and typed in 12-point Times New Roman font with 24-point line spacing. Please do not embed figures in the text. Abbreviations should be used as little as possible and should be explained at first mention unless the term is a well-known abbreviation (*e.g.* DNA). Single words should not be abbreviated.

**Title page:** The title page must include 1) the title of the paper (Please note the title should be short, informative, and contain the major key words); 2) full name(s) and affiliation(s) of the author(s), 3) abbreviated names of the author(s), 4) full name, mailing address, telephone/fax numbers, and e-mail address of the corresponding author; 5) author contribution statements to specify the individual contributions of all authors to this manuscript, and 6) conflicts of interest (if you have an actual or potential conflict of interest to disclose, it must be included as a footnote on the title page of the manuscript; if no conflict of interest

exists for each author, please state "There is no conflict of interest to disclose").

**Abstract:** The abstract should briefly state the purpose of the study, methods, main findings, and conclusions. For article types including Original Article, Brief Report, Review, Policy Forum, and Case Report, a one-paragraph abstract consisting of no more than 250 words must be included in the manuscript. For Communications, Editorials, News, or Letters, a brief summary of main content in 150 words or fewer should be included in the manuscript. For articles reporting clinical trials, the trial registration number should be stated at the end of the Abstract. Abbreviations must be kept to a minimum and non-standard abbreviations explained in brackets at first mention. References should be avoided in the abstract. Three to six key words or phrases that do not occur in the title should be included in the Abstract page.

**Introduction:** The introduction should provide sufficient background information to make the article intelligible to readers in other disciplines and sufficient context clarifying the significance of the experimental findings.

**Materials/Patients and Methods:** The description should be brief but with sufficient detail to enable others to reproduce the experiments. Procedures that have been published previously should not be described in detail but appropriate references should simply be cited. Only new and significant modifications of previously published procedures require complete description. Names of products and manufacturers with their locations (city and state/country) should be given and sources of animals and cell lines should always be indicated. All clinical investigations must have been conducted in accordance with the Declaration of Helsinki (as revised in 2013, *https://wma.net/what-we-do/medical-ethics/declaration-of-helsinki*). All human and animal studies must have been approved by the appropriate institutional review board(s) and a specific declaration of approval must be made within this section.

**Results:** The description of the experimental results should be succinct but in sufficient detail to allow the experiments to be analyzed and interpreted by an independent reader. If necessary, subheadings may be used for an orderly presentation. All Figures and Tables should be referred to in the text in order, including those in the Supplementary Data.

**Discussion:** The data should be interpreted concisely without repeating material already presented in the Results section. Speculation is permissible, but it must be well-founded, and discussion of the wider implications of the findings is encouraged. Conclusions derived from the study should be included in this section.

**Acknowledgments:** All funding sources (including grant identification) should be credited in the Acknowledgments section. Authors should also describe the role of the study sponsor(s), if any, in study design; in the collection, analysis, and interpretation of data; in the writing of the report; and in the decision to submit the paper for publication. If the funding source had no such involvement, the authors should so state.

In addition, people who contributed to the work but who do not meet the criteria for authors should be listed along with their contributions.

**References:** References should be numbered in the order in which they appear in the text. Citing of unpublished results, personal communications, conference abstracts, and theses in the reference list is not recommended but these sources may be mentioned in the text. In the reference list, cite the names of all authors when there are fifteen or fewer authors; if there are sixteen or more authors, list the first three followed by *et al*. Names of journals should be abbreviated in the style used in PubMed. Authors are responsible for the accuracy of the references. The EndNote Style of *Drug Discoveries & Therapeutics* could be downloaded at **EndNote** (*https://www.ddtjournal.com/examples/Drug_Discoveries_Therapeutics.ens*).

Examples are given below:

*Example 1 (Sample journal reference):*

Nakata M, Tang W. Japan-China Joint Medical Workshop on Drug Discoveries and Therapeutics 2008: The need of Asian pharmaceutical researchers' cooperation. Drug Discov Ther. 2008; 2:262-263.

*Example 2 (Sample journal reference with more than 15 authors):*

Darby S, Hill D, Auvinen A, *et al*. Radon in homes and risk of lung cancer: Collaborative analysis of individual data from 13 European case-control studies. BMJ. 2005; 330:223.

*Example 3 (Sample book reference):*

Shalev AY. Post-traumatic stress disorder: Diagnosis, history and life course. In: Post-traumatic Stress Disorder, Diagnosis, Management and Treatment (Nutt DJ, Davidson JR, Zohar J, eds.). Martin Dunitz, London, UK, 2000; pp. 1-15.

*Example 4 (Sample web page reference):*

World Health Organization. The World Health Report 2008 – primary health care: Now more than ever. *https://apps.who.int/iris/handle/10665/43949* (accessed September 23, 2022).

**Tables:** All tables should be prepared in Microsoft Word or Excel and should be arranged at the end of the manuscript after the References section. Please note that tables should not in image format. All tables should have a concise title and should be numbered consecutively with Arabic numerals. If necessary, additional information should be given below the table.

**Figure Legend:** The figure legend should be typed on a separate page of the main manuscript and should include a short title and explanation. The legend should be concise but comprehensive and should be understood without referring to the text. Symbols used in figures must be explained. Any individually labeled figure parts or panels (A, B, *etc*.) should be specifically described by part name within the legend.

**Figure Preparation:** All figures should be clear and cited in numerical order in the text. Figures must fit a one- or two-column format on the journal page: 8.3 cm (3.3 in.) wide for a single column, 17.3 cm (6.8 in.) wide for a double column; maximum height: 24.0 cm (9.5 in.). Please make sure that artwork files are in an acceptable format (TIFF or JPEG) at minimum resolution (600 dpi for illustrations, graphs, and annotated artwork, and 300 dpi for micrographs and photographs). Please provide all figures as separate files. Please note that low-resolution images are one of the leading causes of article resubmission and schedule delays.

**Units and Symbols:** Units and symbols conforming to the International System of Units (SI) should be used for physicochemical quantities. Solidus notation (*e.g*. mg/kg, mg/mL, mol/mm$^2$/min) should be used. Please refer to the SI Guide *www.bipm.org/en/si/* for standard units.

**Supplemental data:** Supplemental data might be useful for supporting and enhancing your scientific research and *Drug Discoveries & Therapeutics* accepts the submission of these materials which will be only published online alongside the electronic version of your article. Supplemental files (figures, tables, and other text materials) should be prepared according to the above guidelines, numbered in Arabic numerals (*e.g*., Figure S1, Figure S2, and Table S1, Table S2) and referred to in the text. All figures and tables should have titles and legends. All figure legends, tables and supplemental text materials should be placed at the end of the paper. Please note all of these supplemental data should be provided at the time of initial submission and note that the editors reserve the right to limit the size

and length of Supplemental Data.

**7. Online Submission**

Manuscripts should be submitted to *Drug Discoveries & Therapeutics* online at *https://www.ddtjournal.com/login*. Receipt of your manuscripts submitted online will be acknowledged by an e-mail from Editorial Office containing a reference number, which should be used in all future communications. If for any reason you are unable to submit a file online, please contact the Editorial Office by e-mail at *office@ddtjournal.com*

**8. Accepted Manuscripts**

**Page Charge:** Page charges will be levied on all manuscripts accepted for publication in *Drug Discoveries & Therapeutics* (Original Articles / Brief Reports / Reviews / Policy Forum / Communications: $140 per page for black white pages, $340 per page for color pages; News / Letters: a total cost of $600). Under exceptional circumstances, the author(s) may apply to the editorial office for a waiver of the publication charges by stating the reason in the Cover Letter when the manuscript online.

**Misconduct:** *Drug Discoveries & Therapeutics* takes seriously all allegations of potential misconduct and adhere to the ICMJE Guideline (*https://icmje.org/recommendations*) and COPE Guideline (*https://publicationethics.org/files/Code_of_conduct_for_journal_editors.pdf*). In cases of suspected research or publication misconduct, it may be necessary for the Editor or Publisher to contact and share submission details with third parties including authors' institutions and ethics committees. The corrections, retractions, or editorial expressions of concern will be performed in line with above guidelines.

(As of December 2022)

**Drug Discoveries & Therapeutics**
Editorial and Head Office
Pearl City Koishikawa 603,
2-4-5 Kasuga, Bunkyo-ku,
Tokyo 112-0003, Japan.
E-mail: office@ddtjournal.com